Multi-bioactive Peptide Coatings for Dental Implants

A Dissertation
SUBMITTED TO THE FACULTY OF
UNIVERSITY OF MINNESOTA
BY

Xi Chen

IN PARTIAL FULFILLMENT OF THE REQUIREMENTS
FOR THE DEGREE OF
DOCTOR OF PHILOSOPHY

Supervisor: Conrado Aparicio

May 2014

Acknowledgements

My time at UMN has been an incredible experience. For that I owe thanks to a great many people for their guidance, advice, support, and friendship.

First of all I would like to express my deepest appreciation to my supervisor: Professor Conrado Aparicio. He transformed me from a person with no experience into a researcher. He trained me on not only bench top techniques but most importantly, the thinking method and the ability to solve problems. He believes in me, encourages me to be creative and gives me freedom to pursue my research interest. His vision and enthusiasm have been most inspiring to me.

There are many members in the Minnesota Dental Research Center for Biomaterials and Biomechanics and members in our collaborator's lab who have been a source of great support along the way and I thank them all. Special thanks go to Dr. Alex Fok, Dr. Ralph Delong, Dr. Maria Pintado, Dr. Sven Gorr and Dr. Joel Rudney for offering me the amazing and enlightening opportunity to work and learn in their labs. I am also grateful to Dr. Helmut Hirt, Dr. Yuping Li, Dr. Pablo Sevilla, Dr. Kyle Holmberg, Mr. Young Heo, Mr. Michael Weston, Mrs. Ruoqiong Chen and Mrs. Renee Jenson for their help from their great experience and skill. It has been a great time working with you all.

In addition, thanks are also due to my committee members, for their valuable suggestions and constructive advises to improve my project and my dissertation.

Last, but certainly not least, I cannot express enough appreciation to my parents and my husband. Their constant support and unconditional love has truly enabled me to get through this entire journey. They share my happiness and get me through the most difficult period. I am so lucky to have you around.

Abstract

Functionalization of implants with multiple bioactivities is desired to obtain surfaces with improved biological and clinical performance. The outcome of dental implants depends on the process of "racing for the surface". To assist bone cells to win the race, bacterial colonization of the surface and tissue healing promotion around it need to be accomplished soon after implantation. Therefore, functionalizing titanium (Ti) surfaces with bioactive coatings which can either enhance cellular adhesion and differentiation or inhibit bacteria adhesion, or both, is desired.

To enhance cellular performance on Ti surface, we developed a simple route to covalently co-immobilize two different oligopeptides on Ti surfaces. Appropriately designed oligopeptides containing either RGD or PHSRN bioactive sequences were mixed and covalently-bonded on CPTES-silanized surfaces. The obtained peptide coatings showed strong mechanical stability as well as enhanced osteoblast adhesion.

To prevent bacteria adhesion on Ti surfaces, we tethered using silanes on Ti surface an antimicrobial peptide, GL13K which is derived from human parotid secretory protein. Our previous work demonstrated that, after immobilization, GL13K displayed antimicrobial effect against *Porphyromonas gingivalis*, a pathogen closely associated with dental peri-implantitis. In addition, GL13K coating showed adequate cyto-compatibility with osteoblasts and human gingival fibroblasts. This work showed that the covalently bonded GL13K coating resisted mechanical, hydrolytic and proteolytic challenges and displayed sustained bioactivity after cycles of body fluid incubation and

autoclaving. GL13K coating prevented biofilm formation by killing *S.gordonii* at their early developmental stage and the antimicrobial effect of GL13K coating was highly dependent on the secondary structure of the tethered peptides. When we investigated the activity of GL13K coating in simulated dynamic conditions with a drip flow bioreactor, unique cell wall damage was observed.

The simple and reliable methodology to tether peptides on Ti surface that was developed in this work can be used to establish a multifunctional coating with both bone-regenerative and bacteria inhibitive bioactivities.

Table of Contents

List of Tables

List of Figures

Chapter 1

Introduction

1.1 Need for Improving Surface Properties of Dental Implants

Commercially pure titanium (c.p. Ti) is the dominant material for making dental implants because it is biocompatible by combining very high corrosion resistance in contact with biological fluid and appropriate mechanical properties, namely high strength, high fracture toughness and relatively low modulus of elasticity[1, 2].

According to the National Institute of Dental and Craniofacial Research (NIDCR), 90% of Americans will have lost at least 3 functioning teeth in their dentition before 50 yrs of age and require replacement to restore form and function [3]. Dental implants have become a well-accepted treatment for replacing missing teeth, with over 400,000 implants being placed every year and an anticipated growth of 9.1% annually [4].

Generally, more than 90 % of implant success rates are achieved after 10–15 years of implantation [5, 6]. However, considering the huge amount of titanium dental implants being placed each year, the 10% failure rate translates into a large number of failure cases. Also, the rate of success for dental implants reported in literature varied from paper to paper mainly because the definition of success for the clinical outcome has not been yet consensuated by researchers and clinicians in the field. Dental implants face two major problems. Firstly, the inert nature of titanium is unfavorable to bone cells growth and differentiation, which is an obstacle to a rapid and reliable new bone formation on implant surfaces and leads to the potential of implant failure under long-term loading. The biocompatibility of titanium implants is based on the stable oxide layer with a thickness of 3–10 nm that spontaneously forms when titanium is exposed to body fluid

[7]. Therefore, Titanium is a bioinert material with passive interactions with the biological environment. Titanium does not trigger any specific positive reactions in the surrounding biological environment to improve the process of bone healing [8]. The process of osseointegration on titanium surfaces starts with wetting of surface and adsorption of biological active molecules, and follows with recruitment of osseoprogenitor cells that finally orchestrate the regeneration of the tissue [9] and facilitate the reduction of foreign body reaction [10, 11]. Considering the inert nature of titanium, there are several limitations on the dental implant performances. Even under healthy conditions the process of bone regeneration is very slow and is far from allowing early or immediate loading of implants [12]. That has significantly increased the patient morbidity and health care costs [13]. Moreover, placing these implants in patients that present compromised clinical scenarios (elderly patients, smokers, traumatic damage, systemic diseases…) is counter-indicated because of the delayed bone healing. Therefore, patients with the aforementioned symptoms do not usually receive dental implant treatment. Thus, dental implants still have room for improvement to enhance their osseointegration and peri-implant bone regeneration.

Secondly, the main reason for failure of dental implants is peri-implant infection. The past three decades have seen the emergence of two new oral diseases: peri-implantitis and peri-implant mucositis [14]. Evidence indicates that peri-implant mucositis occurs in 50% to 90% of implants, while 20% of implants with an average function time of 5 to 11 yrs develop peri-implantitis [14]. The implant surface has a higher risk of infection compared with natural tooth surface because it accumulates serum proteins which promote bacterial

adherence and colonization. This is even more prone to happen on the current devices as they all incorporate microroughness surfaces that further facilitate bacteria attachment. Many implant related infections occur not only as a consequence of the initial exposure during the surgery but also after a long time of implantation, from months to years, as the bacteria invade peri-implant environment, destruct peri-implant tissue and colonize the implant surfaces.

The outcome of dental implants depends on the process called “race for the surface”, which was suggested by Gristina to describe the competition between bacterial adhesion and tissue integration[15] (Figure 1.1). The general idea is that if the bacteria first land on a surface and form a biofilm, they will win the race because biofilm are difficult to eradicate, and bacteria in biofilm tend to resist antimicrobial agents. As a consequence, tissue cells were not able to displace bacteria colonies, leading to decreased tissue integration and occurrence of infection. On the other hand, if bone cells win the battle and occupy the surfaces, tissue regeneration and osseointegration can be achieved. Therefore, the inhibition of bacterial adhesion and promotion of cell adhesion on a surface is regarded to be crucial in facilitating that tissue cells to win the first battle[16]. A post implantation period of 6 hr has been identified as the “decisive period” when the implant is particularly susceptible to bacteria colonization[17].

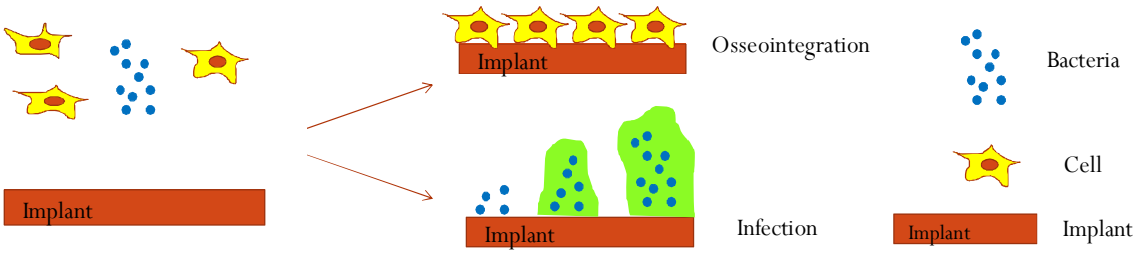

Figure 1.1 Bacteria and cell race for implant surfaces.

Bacterial adhesion to biomaterials usually consists of two steps [18]. Physicochemical forces such as hydrophobic interactions, electrostatic interactions and Van der Waals forces facilitate bacteria attachment. In the following step, the bacteria cell uses nanofibers such as pili and flagella for bridging between the cell and surface. After implantation, serum proteins will immediately adsorb on Ti surface, which transform the bacteria-material interaction into bacteria-protein interaction. Most proteins, such as fibronectin, fibrinogen and thrombin, increase bacteria attachment through ligand receptor interactions [19, 20]. Cellular adhesion mechanism on materials follows an analogous process. On uncoated Ti surfaces, physicochemical forces drive cellular attachment, while on protein-adsorbed surfaces, cells strongly adhere to extracellular matrix (ECM) molecules including fibronectin, vitronectin and type I collagen which contain integrin interactive aminoacid sequences such as RGD, GFOGER and FRHRNRKGY. To improve osteointegration and antimicrobial activity, bacterial adhesion prevention and cellular adhesion promotion need to be performed immediately after implantation.

Functionalization of titanium surfaces with coatings made of biological molecules with known biological activity has been used during recent years for this purpose. To improve

bone formation, bioactive proteins (BMPs, …) or peptides (RGD, …) have been immobilized on Ti surfaces through physical adsorption, electrostatic attraction or covalent bonding [21]. To prevent implant-related infections, antimicrobial agents such as antibiotics or antimicrobial peptides have been attached on titanium surfaces [22]. Those are introduced in chapter 1.2.2.

1.2 Functionalization of Dental Implants with Bioactive Coatings

The traditional approaches to modify dental implant surfaces include 1) to modify surface topography like surface roughness and hydrophobicity. Implant surface topography is nowadays modified in commercially available products [23, 24] by chemical etching [25], grit-blasting [26], plasma-spraying titanium coatings[27], electrochemical processes with different solutions [28], or by a combination of some of them [29]. However, none of those surface treatments change the intrinsic bioinert chemical characteristics of the titanium surfaces and are limited in their ability to accelerate and improve osseointegration. 2) Another focus on traditional surface treatments for dental implants is to coat the surface of titanium with a layer of calcium-phosphates [24, 30]. The deposition of bioactive calcium-phosphate minerals, such as apatite, can enhance implant performance at an early stage after implantation by an osseoinductive process of regeneration around the implant [31]. This is because the biological nature of apatites, which represent the mineral phase in bone, have the potential to actively signal the cells that interrogate the surface after implantation [32]. However, neither of those two traditional methods induces specific cell and tissue responses, and neither of them

showed very promising results in reducing bacteria activity on titanium surfaces. Currently, surface modification of dental implants using biochemical methods bring an attractive new approach to promote implant success as it aims to induce specific cell and tissue responses using critical biological components [33]. The regeneration of bone highly depends on the communication between cells and extracellular matrix components. Thus, the extracellular matrix proteins and its components, growth factors and bone morphogenetic proteins govern various key biological events, including cell adhesion, proliferation and differentiation. Immobilization of these bioactive molecules on the surface of the implant potentially provides control over the tissue implant interface with further improvement of cell communication. In addition, antimicrobial molecules like antibiotics and antimicrobial peptides are also widely immobilized on titanium surfaces to prevent peri-implant infections [34, 35].

1.2.1 Methods for Immobilizing Biomolecules on Ti Surfaces

There are two main methods for surface immobilization of biomolecules [36] for surfaces coatings for dental implant applications. The simplest one is by physical adsorption of the organic molecules onto the surface, which can be achieved by immersing the substrate into a solution of the bioactive molecule. However, the physical adsorption method provides little strength for the long-term stability of the coatings. As the attachment of the molecules depends on secondary weak bonds –hydrogen bonds, electrostatic attraction, etc.—, the adsorbed molecules on the implant surface can be easily detached from the surface by desorption or displacement by other molecules. Thus, the surface can rapidly

lose their bioactive properties. Others have proved that titanium surfaces coated with physically-adsorbed bone morphogenic protein lost 96% of their bioactivity after the first hours in contact with biological fluids [37]. Moreover, this method can not precisely control the surface density and/or orientation of the molecules, which are vital for regulating the interactions of the coatings with the cells. The conformation of the biomolecules can also change during time and, thus, lose their bioactivity [38].

Alternatively, covalently bonding biomolecules to implant surfaces provides coatings that are more stable and more resistant to disruption not only under harsh physiological conditions but also during fabrication of the coating and implantation at the time of the surgery. Overall, this can help preserve the biological activity of the bound biomolecules [39]. The covalent bonding of the biomolecules also provides the potential to control their density and orientation, e.g. aligning and/or exposing the appropriate active sites at the interface, and thus provoking a more specific and rapid host reaction [40, 41]. The passive titanium oxide that naturally covers the surface provides plenty of hydroxyl groups under adequate fabrication conditions. Functional groups such as amino, carboxyl, and thiol can be deposited on metallic surfaces after the surface activation treatments such as plasma treatment [42], photo-initiated polymerization, chemical etching [40], or ion beam etching [43], which could be further used to attach biomolecules.

The most widely used way to couple biomolecules on Ti surfaces are through silane agents. Covalent anchoring of biomolecules by silane chemistry is a simple and versatile method to modify surface properties. To graft silane agents to Ti surfaces, surfaces are

first activated to form hydroxyl groups by etching or plasma treatment. Silane coupling agents with different end functional groups are attached via reaction with the activated hydroxyl groups. The functional groups of the silane molecule at the opposite end are used to couple the bioactive molecules, either directly or via a cross-linker molecule. Generally, the process of silanization with biomolecules can be grouped into four types of directed reactions, namely thiol-, amino-, carboxyl-, and chloro-, according to the functional end group in the silane molecule. The selection of the chemical group is based on the active residues of the biomolecules that are aimed to be used in the immobilization process. The ductile alkyl spacers on silane agents can partially absorb the biomaterial-tissue interfacial stresses and may be also used to appropriately orientate and expose the bioactive molecules at the biomaterial interface in an arrangement to induce the desired tissue responses. Conventional, well established, and commercially-exploited techniques for immobilization of biomolecules on substrates use a silane agent like aminopropyl triethoxysilane (APTES) to crosslink the biomolecules to different inorganic substrates [44, 45]. However, in this case, the use of additional coupling agents, such as HBTU or EDC are needed to esterify carboxylic groups in the biomolecule [46] and thus enable the nucleophilic reaction with amines present at the organosilane molecule. Otherwise, linkers like carbodiimades and glutaraldehydes should be used to anchor terminal amino groups of biomolecules to the silane agents [40, 47].

1.2.2 Biomolecules Immobilized on Ti Surface to Improve its Bioactivity

As discussed before, bacterial adhesion prevention and cellular adhesion promotion need to be performed immediately after implantation. Functionalizing Ti surface with bioactive coatings which can either enhance cellular adhesion or inhibit bacteria adhesion, or both, would be the solution to the aforementioned problems.

To enhance cellular performance on Ti surface, both long-chain extracellular matrix (ECM) proteins [48-50] and short peptides, which are the functional motifs in ECM proteins with specific bioactivities [51-53] have been immobilized on Ti surfaces. The ECM of bone, which is synthesized, deposited and mineralized by osteoblasts, consists of 90% collagenous proteins (type I collagen 97% and type V collagen 3%) and 10% non-collagenous proteins (osteocalcin, osteonectin, bone sialoproteins, proteoglycans, osteopontin, fibronectin, growth factors, etc) [54]. ECM proteins mediate cell responses, such as adhesion, proliferation and differentiation. Collagen [55], fibronectin [56, 57], and growth factors such as bone morphogenetic proteins (BMP) [58] were immobilized on Ti surfaces and proved to be effective in enhancing cellular performance. However, ECM proteins are difficult to be reconstructed, synthesized, and modified. On the contrary, short peptides are small and chemically defined [59], which implies that they can be easily synthesized, modified or reconstructed. By using techniques such as solid phase peptide synthesis (SPPS), peptides of up to 30-50 aminoacids can be routinely prepared with good yields [60]. In addition, peptides can be precisely conjugated to biomaterial surfaces compared with large molecules proteins. Also, non-native

chemistries and functional groups can be conveniently incorporated in the peptide sequence with not much difficulty [59]. However, the short length of peptides limits their ability to selectively acquire the most desired conformation to achieve their bio-function. The most well known short peptide sequence with the ability of enhancing cellular performances as a coating on a substrate is the RGD (Arginine-Glycine-Aspartate) amino acid sequence. RGD is a key mediator of cellular adhesion through interaction with integrins at the cell membrane [61]. RGD peptide is found in many ECM molecules, including fibronectin, vitronectin, type I collagen, osteopontin and bone sialoprotein [62]. Covalently immobilized peptides with RGD sequences to implant surfaces has been recognized as a strategy for enhancing cell interaction with implants [21]

More recently, a Proline-Histidine-Serine-Arginine-Asparagine (PHSRN) sequence in the 9th type III repeating unit of fibronectin, was found to have synergistic effect with RGD on improving cell adhesion. Many authors have demonstrated that multi-component peptide systems containing both RGD (the primary recognition site for α5β1 integrin) and PHSRN (the synergistic site for α5β1 integrin) were more efficient in increasing cell adhesion, spreading, proliferation, and differentiation than the RGD peptide alone [63-68]. In the native conformation of fibronectin, RGD and PHSRN are spaced by approximately 40 aminoacids [65]. Therefore, the distance between PHSRN and RGD are important for the synergistic interaction of the two peptides. In addition, structure, conformation, orientation and spatial distribution of RGD and PHSRN peptides are all important parameters in affecting the bioactivity of the modified surface.

To inhibit bacteria formation on dental implant surfaces, antimicrobial agents such as antibiotics and antimicrobial peptides have been anchored on Ti surfaces. Gentamicin have been loaded into nanotubes [69], poly (D,L-lactide) coating [70] or porous hydroxyapatite coatings [34] on titanium implants. The antibiotic-hydroxyapatite-coatings exhibited significant improvement in infection prevention [71]. Antibiotics have been normally physically adsorbed on titanium surfaces for the ease of processing. The physical adsorption process, however, limits the loaded amount and release characteristics of the drugs. Loading antibiotics in hydroxyapatite coatings, for example, led to 80-90% of the total loaded drug being released during the first 60 min in contact with fluids [72, 73] and drugs loaded into nanotubes were fully released in 50-150min [69]. Surfaces incorporating chlorhexidine [74], sliver [75], poly lysine [76] and chitosan [77] have all been developed. Recently, vancomycin has been successfully covalently-bonded to titanium and its antibacterial activity is retained even after incubation in PBS for at least 11 months [78-81]. Compared with the non covalent coatings that quickly release antibiotics, covalently-bonded antibiotics remained active for notably longer periods. Although antibiotics coated on titanium proved to be effective, their use is controversial because of their potential host cytotoxicity and bacterial resistance. For instance, Weber and Lautenbach [82] noted that 41% of bacteria isolated postoperatively were resistant to gentamicin following the application of gentamicin-impregnated bone cement. Other investigations also showed drug resistant bacteria isolated from orthopedic implants [83]. In addition, although antibiotics are normally thought to be biocompatible, their potentials in inducing host cytotoxicity have been widely reported [84-88].

The use of antimicrobial peptides (AMPs) has recently emerged as an alternative antimicrobial approach with strong potential to improve dental implants performance. Naturally, the bacterial flora in the oral cavity is mediated by the human innate immune system, which is rich in antimicrobial proteins and peptides [89, 90]. These AMPs can kill bacteria directly through membrane disruption, or act as immune modulators by enhancing bacteria clearance using our innate defense system [91]. The advantages of using AMPs over antibiotics are 1) they are of human origin; hence, with potential low host cytotoxicity. 2) The long existing antimicrobial effect of AMPs against bacteria in hundreds of years suggested low bacterial resistance of AMPs. 3) The exceptionally broad activity of AMPs indicates that a single peptide can have activity against gram-negative and gram positive bacteria, fungi, and even viruses and parasites [91]. However, the disadvantage of AMPs involves the potential liability to proteases, which indicates the possibility of being proteolytically degraded by enzymes secreted by the microbial flora. Over 45 AMPs with different antimicrobial mechanisms have already been identified from the human immune system, ranging from small cationic peptides to enzymes and large agglutinating proteins [89]. They may act as metal ion chelators, protease inhibitors, or promoters of enhanced bacterial agglutination [89].

There are several reports regarding the application of AMPs on titanium surfaces to prevent peri-implant infection. Kazemzadeh-Narbat et al. [35] used physically-adsorbed AMPs on micro-porous calcium-phosphate coated titanium surfaces and showed it had efficient antimicrobial activity and acceptable biocompatibility. However, physical adsorption of AMPs resulted in a rapid burst out of the agent from the surface. Recently,

the same research group built up a covalently anchored antimicrobial coating on titanium surfaces based on hydrophilic polymer brushes conjugated with the AMPs [92]. The hydrophilic polymer brushes were tethered on titanium using atom-transfer radical polymerization (ATRP). The surfaces were maleimide functionalized, and cysteine modified AMPs were conjugated to the coatings. These tethered AMPs demonstrated excellent in vitro and in vivo antimicrobial activity with no toxicity to osteoblasts. We have also immobilized AMPs derived from the parotid secretory protein using silane chemistry. Our results showed sustained antimicrobial activity of the AMPs, resistance to form bacteria biofilm, and appropriate cytocompatibility [93].

1.3 Need for the Improvement of Bioactive Coatings

Surface modification of titanium to improve osseointegration of dental implants by improving cell recruitment and differentiation, biomineral formation, or antimicrobial activity has been widely investigated. However, the fabrication of advanced multifunctional coatings that bear the combined bioactivities, such as combined bone regenerative and antimicrobial activities, is an desired goal that has been seldom pursued. It is a challenging task, though, as it requires original designs for the bioactive molecules as well as the methodological steps to obtain a robust and active coating. In addition, the immobilization conditions need to be optimized to balance the distribution of both of the biomolecules during the co-immobilization process. To maximize the affinity of surfaces to both of the two molecules, reaction conditions should be adjusted to hinder the competitive immobilization between the two molecules. In chapter 2, we will introduce a

simple and reliable method to obtain multi-bioactive peptide coatings with combination of RGD and PHSRN peptides. The well known RGD and PHSRN peptides were selected as a model to validate the co-immobilization method.

Different cationic antimicrobial peptides derived from human original proteins have been coated [35, 94] on implant surfaces and displayed excellent antimicrobial activity. However, there are two major obstacles that hinder clinical application of the antimicrobial peptide coatings and need further investigation. The first severe problem that antimicrobial peptide coatings encountered is the finite functional life time of the coating [95]. Dental implant coatings face numerous challenges like autoclaving before implantation, notable mechanical shearing forces during implantation, and exposure to hydrolytic and proteolytic degradative agents in body fluids after implantation. Since long-term peri-implantitis raises increasing notable concern, the resistance of the coatings to these multiple challenges and their retained bioactivity under "harsh" environment conditions become a major consideration to be addressed. Also, although plenty of antimicrobial peptide coatings showed very promising antimicrobial activity, the distinct properties of them that determine their specific antimicrobial activity deserve further research. It is well accepted that the antimicrobial effect of AMPs relies on their cationic and amphiphilic properties. Those properties enable interaction of the peptides with the bacteria membrane through electrostatic attraction and hydrophobic interactions, leading to bacteria membrane disturbance [96]. Abundant literature reports the roles that the hydrophobicity and cationic property of antimicrobial peptides played in the disturbance of cell membranes, especially when the peptides are tethered and spatially confined on a

surface. However, conflicting conclusions were drawn on the contribution of either hydrophobicity or charge on the antimicrobial effect of the coatings, which leads to investigate alternative physical and chemical properties of the peptides influencing their effective prevention of bacteria colonization. In chapter 3, a robust and stable antimicrobial peptide coating due to its super hydrophobicity will be introduced to overcome the multiple challenges that the implants will face when exposed to the harsh biological environment. The key properties contributing to its antimicrobial action were investigated and presented here in chapter 4. Finally, the performance and effectiveness of the antimicrobial coatings under dynamic conditions simulating the oral environment in a drip-flow bioreactor are presented in chapter 5.

Chapter 2

A Simple and Reliable Method to Obtain Robust Multi-bioactive Peptide Coatings with Enhanced Cellular Performance

2.1 Objectives

The main objective of the present chapter is to design and develop a simple and reliable method to build a multifunctional coating with co-immobilization of two different oligopeptides with combined bioactivities. The multifunctional coating can be accomplished by covalent bonding of two different peptides using silane as covalent linker, thus, the obtained peptide coatings should be mechanically stable due to the strong covalent linking force between peptide coatings and surfaces. In addition, the immobilized oligopeptides should retain their respective bioactivities on surfaces. Oligopeptides containing RGD and PHSRN sequences were co-immobilized on Ti surface and the synergistic effect of the two peptides on enhancing osteoblast performance was shown. This method for co-immobilizing biomolecules can easily be transferred to fabricate other multi-functional surfaces by changing RGD and PHSRN sequences into oligopeptides with other targeted bioactivities.

2.2 Introduction

Functionalization of surfaces of biomedical materials is a challenging task in biomaterials. It has the objective of providing specific bioactivities to materials used to repair and/or regenerate specific tissues. The possibility of obtaining a multi-functional surface by immobilizing biomolecules --proteins, polysaccharides, oligopeptides, recombinant biopolymers, …-- on synthetic substrates is still a challenging task that needs to be tailored, notably when covalent co-anchoring of different biomolecules –with different physical and chemical properties—is desired .

Titanium (Ti) is widely used for dental and orthopedic implants due to its excellent mechanical properties, chemical stability and biocompatibility [1, 2]. However, the bioinert nature of titanium is unfavorable to bone cells growth and differentiation, which hinders new bone formation and compromises clinical implant success [97]. Infection is the other main cause for short- and long-term implant failures after implantation [95, 98].

Functionalization of titanium surfaces with coatings made of biological molecules with known biological activities has been used during recent years to overcome the aforementioned clinical problems [23, 99]. Bioactive proteins (bone morphogenetic proteins, collagen…)[44, 100-102], nucleotides[103, 104] or peptides (RGD, FN_{III}(7-10), …)[21, 105-108] and antimicrobial agents[70-72, 76, 109] have been immobilized separately to display a functional property on the modified Ti surface. However, to better improve the biological performance of Ti implants, coatings with multiple bioactivities – cell recruitment and differentiation, mineral formation, antimicrobial activity, induction of osseointegration— on the same surface are desired. To that purpose others have explored electrostatic attraction or physical adsorption of two different biomolecules to build coatings on metallic substrates to obtain multifunctional surfaces [110]. Chua et al. developed a hyaluronic acid/chitosan polyelectrolyte multilayer coating to functionalize Ti surfaces incorporating the well-known cell-adhesive argynine-glycine-aspartate (RGD) peptides [77]. The hyaluronic acid/chitosan polyelectrolyte multilayered surface inhibited bacterial adhesion and the immobilized RGD motif promoted osteoblast functions, thus facilitating the development of a multifunctional Ti surface. Lee et al. developed a gentamicin and bone morphogenetic protein-2 (BMP-2) delivering Ti

surfaces with enhanced antibacterial activity and promotion of osseointegration [111]. Positively charged gentamicin and BMP-2 were adsorbed on negatively charged, heparinized-Ti surface to also get multifunctional surfaces.

Neither physical adsorption nor electrostatic attraction are appropriate to produce coatings that are mechanically stable in the surgical scenario and thermochemically stable in the biological environment, which is of great importance in the case of dental and orthopedic Ti implants. A strong covalent bond between the metal and the biomolecules should provide a strong and stable coating that will be able to withstand forces exerted at the surface during surgical implantation and the flow of fluids *in vivo*. Biochemical immobilization methods, including coupling with silane agents [21, 40] and thiols [112, 113], have been studied to provide strong mechanical and biochemical stability of coatings made of proteins or other biomolecules. Aminopropyl triethoxysilane (APTES) chemistry has been previously used to crosslink the biomolecules to different inorganic substrates and thus, to decorate them with bioactive motifs [44, 45]. However, the use of additional coupling agents, such as HBTU or EDC should be used to esterify carboxylic groups in the biomolecule [46] and enable the nucleophilic reaction with amines present at the organosilane molecule.

Our objective is developing a simple and reliable method to obtain stable multifunctional coatings made of oligopeptides. Here, we present a simple and effective covalent conjugation method to co-immobilize on titanium surfaces two different oligopeptides with known cooperative bioactivities. PHSRN peptide is not biologically active by itself.

However, a synergistic effect with RGD peptide on cell adhesion has been identified as PHSRN is adjacent to RGD in the type III repeating unit of fibronectin [53, 114]. Recombinant peptides including both PHSRN and RGD motifs [63-65, 115, 116] and multi- peptide systems with both RGD and PHSRN[114] have been proved more efficient in increasing cell adhesion, spreading and proliferation in comparison with systems that incorporate the RGD sequence alone. Polyethylene glycol hydrogels have been the most widely used substrates to incorporate both RGD and PHSRN peptides for studying their effect on cell response [66, 67, 117].

We appropriately designed oligopeptides that incorporated one of either RGD or PHSRN bioactive sequences and successfully co-immobilized them on Ti surfaces using organosilanes as covalent linkers. Both RGD and PHSRN-containing oligopeptides incorporated three lysines (K3) and four glycines (G4) at the peptide N-terminus for enabling covalent anchoring through direct reaction with the organosilane molecules, (3-chloropropyl)triethoxysilane (CPTES); and spacing the bioactive motifs for easier interaction with the surface-colonizing cells, respectively. The synergistic effect of these two peptides on cell response was *in vitro* tested on our model surfaces to examine the ability of the modified Ti surfaces to retain the multi-bioactive response conferred by the immobilized oligopeptides.

2.3 Material and Methods

Materials

Anhydrous pentane, (3-chloropropyl)triethoxysilane (CPTES), diisopropylethylamine (DIEA), 2-(N-Morpholino)ethanesulfonic acid (MES), 2-Amino-2-methyl-1-propanol (AMP), 4-Nitrophenyl phosphate disodium salt hexahydrate (p-Npp), and antivinculin primary antibody were purchased from Sigma-Aldrich (St. Louis, MO). 1-Ethyl-3-[3-dimethylaminopropyl]carbodiimide hydrochloride (EDC), N-hydroxysulfosuccinimide (Sulfo-NHS), and Halt™ protease inhibitor cocktail were purchased from Thermo Scientific (Rockford, IL). Alpha minimum essential medium (α-MEM), fetal bovine serum (FBS), trypsin-EDTA (0.5%), Alexa Fluor 488 secondary antibody, DAPI and Rhodamine Phalloidin were purchased from Invitrogen (Grand Island, NY). 5-FAM cadaverine and 5-TAMRA cadaverine were purchased from Anaspec (Fremont, CA). Float-A-Lyzer® dialysis tubes were purchased from Spectrum (Rancho Dominguez, CA). Bio-Rad DC™ protein assay was purchased from BioRad (Hercules, CA). NH_2-K3G4RGDS and NH_2-K3G4PHSRN oligopeptides (purity>98%) were synthesized by solid-phase peptide synthesis and purchased from AAPPTec (Louisville, KY).

Immobilization of Oligopeptides on Ti Surfaces

The oligopeptide-containing coatings on Ti surfaces were prepared through a method in three preparation steps. The surface was first activated by O_2-plasma cleaning and then

silanized using (3-chloropropyl)triethoxysilane (CPTES). Then, immobilization of mono or multi-oligopeptides coatings on CPTES-modified Ti surfaces was performed.

Commercially pure Titanium Grade II discs (1mm thick, 7.5mm in diameter) were grinded with papers with decreasing SiC-particle size, and finally polished with a suspension of alumina particles (1.0μm and 0.5μm of mean size) on cotton clothes. Samples were soaked in acetone overnight and ultrasonicated in cyclohexane for 10 minutes, rinsed with distilled water and acetone, followed by drying with N_2 gas (Ti group). The polished surfaces were activated by O_2 plasma cleaning (PDC-32G, Harrick plasma, US) for 5 minutes (Ti/O_2 group) to form reactive $–OH^-$ groups on the plasma-cleaned Ti surfaces. After activation the samples were introduced in a N_2-saturated glass chamber and 7ml anhydrous pentane, 1.2ml (3-chloropropyl)triethoxysilane (CPTES) and 0.6ml diisopropylethylamine (DIEA) were sequentially added to submerge the Ti samples. Samples were in the CPTES solution for 1h and periodic 2-minute ultrasonication cycles were applied. Then silanized samples were rinsed with ethanol, isopropanol, deionized water, and acetone, and dried with N_2 gas (Ti/CPTES group). Covalent conjugation of oligopeptides on Ti surfaces was accomplished by immersing overnight silanized Ti discs into a mixed 1:1 molar ratio solution of K3G4RGDS and K3G4PHSRN with 0.5mg/ml Na_2CO_3 under argon atmosphere. Ti discs were rinsed with deionized water and acetone (Ti/CPTES/Mix group). Ti surfaces functionalized with only one of the two oligopeptides, K3G4RGDS (Ti/CPTES/RGD group) or K3G4PHSRN (Ti/CPTES/PHSRN group), were prepared following the same protocols and tested as controls. Ti discs coated with a mixture of physically-adsorbed K3G4RGDS and

K3G4PHSRN were obtained by immersing overnight O_2-plasma cleaned surfaces in a 1:1 molar ratio solution of the two oligopeptides (Ti/Physi/Mix group).

Water Contact Angle Goniometry

Sessile drop contact angle measurements on modified Ti discs were performed using a contact angle analyzer (DM-CE1, Kyowa Interface Science, Japan) with appropriate software (FAMAS, Kyowa Interface Science, Japan). Deionized water was used as the wetting liquid with a drop volume of 2µl.

X-ray Photoelectron Spectroscopy (XPS)

Samples were ultrasonicated for 5 minutes and rinsed in DI-water and acetone, and dried with N_2 prior to measurements. XPS was performed (SSX-100, Al Kα x-ray, 1mm spot size, 35° take-off angle) to characterize the atomic composition of the surface. Survey scans (0-1100 binding energy, 4scans/sample) were done at 1eV step-size. High resolution scans (20scans/sample) of C1s, N1s, and O1s were taken at 0.1eV step-size. The peak fittings and semi-quantification of surface chemical composition were conducted using ESCA 2005 software provided with the XPS system.

Fluorescence Labeling of Peptides

K3G4RGDS and K3G4PHSRN were conjugated with fluorescence probes to directly visualize the coatings on the treated surfaces and assess the co-immobilization of the two oligopeptides. 1mM K3G4RGDS, 10mM EDC and 25mM Sulfo-NHS were added into

1mL MES buffer (0.1M MES, 0.5M NaCl, 0.04M NaOH, pH=5.95) for 15 min at room temperature. 1.5mM 5-FAM cadaverine in 1mL PBS was subsequently added into K3G4RGDS/EDC/NHS solution (2h, pH=7.5, room temperature). K3G4PHSRN was conjugated with 5-TAMRA cadaverine using the same methodology. A 1.5-fold molar excess of oligopeptides was used to ensure complete labeling of the oligopetides. The labeled K3G4RGDS and K3G4PHSRN peptides were dialyzed in PBS buffer for 20h (MWCO: 500-1000 Dalton) to remove excess of non-reacted probe molecules. The buffer solution was changed twice after 2h and 6h of dialysis treatment. After dialysis, K3G4RGDS and K3G4PHSRN were frozen at -80^{o}C overnight and lyophilized (Freeze Dryer 4.5, Labconco, US) for 24h. The lyophilized labeled-peptides were re-dissolved in 0.5 mg/ml Na_2CO_3 solution and reacted with silanized Ti surfaces as previously described for non-labeled peptides. Ti discs modified with fluorescence-labeled peptides were finally rinsed with deionized water and acetone and fluorescence images on the coated surfaces were recorded using a fluorescence microscope (Eclipse E800, Nikon, Japan).

Mechanical Stability of the Coatings

All differently-treated Ti surfaces were mechanically challenged by ultrasonication in deionized water for 2h. Water contact angles, XPS and fluorescence visualization of the surfaces were performed and compared with results before ultrasonication.

Cell Culture

Murine osteoblasts of the MC3T3-E1 cell line were cultured in α-MEM supplemented with 10% fetal bovine serum (FBS) and 1 % penicillin/streptomycin (P/S) at 37°C in a humidified atmosphere of 5% CO_2. Media was changed every 48 h. Cultured cells were trypsinized (0.05% trypsin-EDTA) and further seeded on Ti, Ti/CPTES/RGD, Ti/CPTES/PHSRN and Ti/CPTES/Mix surfaces. Before cell seeding, the modified Ti discs were sterilized under UV light overnight, soaked in 70% ethanol for 1 hour, washed with PBS buffer three times, and finally transferred into 48-well plates.

Cell Adhesion

MC3T3-E1 cells were seeded on tested surfaces at a density of 2,000cells/well and cultured for 2h and 4h for triple-staining immunofluorescence analysis. Cells were fixed on the surfaces with 4% paraformaldehyde in PBS for 20min. After fixing, cells were lysed and permeablized in PBS+0.3% TritonX-100 for 5min, followed by blocking with 3% BSA to enhance the specific conjugation between antigen and primary antibody. Samples were immersed in antivinculin primary antibody (1:500 in 3% BSA) and incubated at 37°C for 3h. After washing with PBS+0.1%Triton-X three times, samples were immersed in 3% BSA with Alexa Fluor 488 secondary antibody (1:500), DAPI (1:1500) and Rhodamine Phalloidin(1:5000) , then incubated in dark at 37°C for 1 h. Subsequently, the morphology and spreading of cells were observed by fluorescence microscopy (Eclipse E800, Nikon, Japan). The number of adhered cells was assessed by counting nuclei per image field using image analysis software (Image J, NIH, Bethesda,

MD). Three fields were selected for each sample and four samples were analyzed and averaged for each group.

Cell Proliferation

MC3T3-E1 cells were seeded on tested surfaces at a density of 2,000cells/well and cultured for 3 and 5 days. Cells were then fixed, permeabilized and incubated in DAPI (1:1500) for 15min. Cell proliferation was assessed by counting at each period of culture the number of cell nuclei per image field. Three fields per sample and four samples per group were analyzed.

Cell Differentiation

MC3T3-E1 cells were cultured on tested surfaces at a density of 20,000cells/well. After reaching confluency, cells were cultured in osteogenic media (α-MEM supplemented with 10% FBS, 1% P/S, 50μg/ml L-ascorbic acid, and 10mM β-glycerophospate). Media was changed every 2 days. After 7 and 14 days of cell culture in osteogenic media, cells were collected for determining alkaline phosphatase activity (ALP) as a marker of early differentiation into the osteoblastic lineage. Cells were washed twice with PBS and lysed in 200μL ALP lysis buffer (1% Triton X-100, 0.1m M $MgCl_2$ and 150mM Tris-base, pH=10.5) for 10min with 1% protease inhibitors to prevent ALP degradation . The lysates were centrifuged at 3000 rpm for 10 min and supernatants were collected. 2μl supernatant and 100μl freshly prepared AMP reaction buffer (11.25μl 1:4 diluted AMP, 6μl 2M-$MgCl_2$, one 20mg tablet of p-nitrophenyl phosphate, and water to 5mL) were

added into a 96-well plate and incubated at 37 °C for 1 h. The absorbance for each sample was read at 405nm wavelength and subtracted from blank. The absorbance was normalized with total protein concentration using Bio-Rad DC^{TM} protein assay using BSA as standard.

Statistical Analysis

Statistically significant differences among groups were assessed using one-way ANOVA Tables with post-hoc tests ($p<0.05$). Multiple comparison LSD and Dunnett's T3 tests were performed when equality of variances between compared groups was or was not assumed, respectively.

2.4 Results and Discussion

Fabrication and Characterization of Surfaces Coated With Coatings Containing Oligopeptides

Multi-oligopeptide biofunctionalized Ti surfaces were obtained through a three-step method using CPTES as coupling agent. O_2-plasma cleaning was conducted to activate the Ti surfaces. The high polarity conferred by the hydroxyl groups that formed on the activated surface was responsible for the significant decrease in water contact angles measured for Ti/O_2 surfaces (Figure 2.1). Following standard conditions, attachment of CPTES on Ti was achieved by hydrolysis of the ethoxy groups and reaction with the hydroxyl groups present on the activated surface leading to polycondensation reaction to form Si-O-Si and Ti–O-Si bonds. The final covalent binding of the oligopeptides to the

silanized surface is achieved by a direct nucleophilic substitution. Free amine groups of the oligopeptides are the nucleophilic groups and chlorine atoms from the organofunctional groups of CPTES are the leaving groups and electrophilic center of the reaction. This prevents the use of additional coupling molecules to accomplish the final reaction, as it is the case when APTES is used. To favor this reaction and thus, mechanical and chemical stability of the coatings, we designed our peptides with a series of three lysines –each one provides with a potentially reacting free amine-- at their N-terminus.

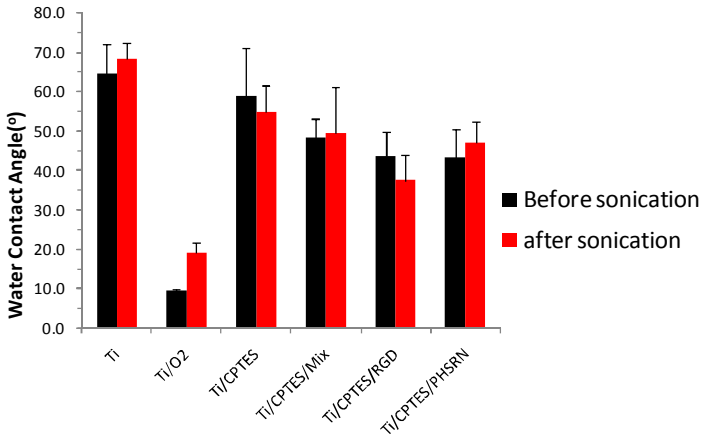

Figure 2.1 Wettability. Water contact angle values (mean ± standard deviation), before and after ultrasonication in water for 2h, on Ti surfaces after each fabrication step for obtaining the coatings and for each of the three coatings studied containing different oligopeptides. Error bars are the standard deviation of at least three samples in each group.

The immobilization of the mixed oligopeptides was conducted in Na_2CO_3 buffer solution at pH=9.5 even though a higher pH would have enhanced the nucleophilic reaction between the free amines and the organosilanes. This pH was selected to equal the net charge of the two peptides in solution, which in turn hindered competitive electrostatic

attraction between the two oligopeptides to the CPTES-silanized surface. The iso-electric point of K3G4RGDS and K3G4PHSRN are pH=10.8 and pH=11.7, respectively. Thus, when in solution at pH =9.5 the two oligopeptides carried similar positive charge. The resulting similar fluorescent intensity for the green and red signals on the surfaces with co-immobilized peptides (Figure 2.5) suggested that close amounts of the two oligopeptides were anchored. In fact, our preliminary results showed that solutions with a mixture of the two peptides at pH=11 notably favored K3G4PHSRN binding with almost no K3G4RGDS attached to the CPTES treated surface.

Water contact angle measurements on the progressively modified Ti surfaces suggested the successful attachment of the peptide coatings (Figure 2.1). The average water contact angle on polished untreated Ti discs was 65±7°. After O_2-plasma the surfaces were highly hydrophilic and further attachment of CPTES increased water contact angles near to the initial values. The presence of all types of oligopeptides increased surface hydrophilicity compared to silanized surfaces. According to the Hopp and Woods scale for aminoacid hydrophilicity [118], K3G4RGDS and K3G4PHSRN have average hydrophilicity values of 15.3 and 12.0, respectively. Therefore, Ti/CPTES/RGD surface had a notably higher hydrophicility than Ti/CPTES/PHSRN and Ti/CPTES/Mix surfaces. The value of water contact angles for each tested surface before and after 2 hours of ultrasonication in water was very similar with no statistically significant differences.

Images obtained with SEM revealed topographical and chemical features of the modified Ti surfaces (Figure 2.2). After silanization with CPTES the surfaces showed a darker

appearance than the original Ti surfaces. The darker appearance was attributed to the presence of the organosilane on the metallic surfaces. The topography of silanized surfaces as well as the one of all surfaces with oligopeptide coatings was similar, suggesting that the peptides were retained on areas previously coated with CPTES.

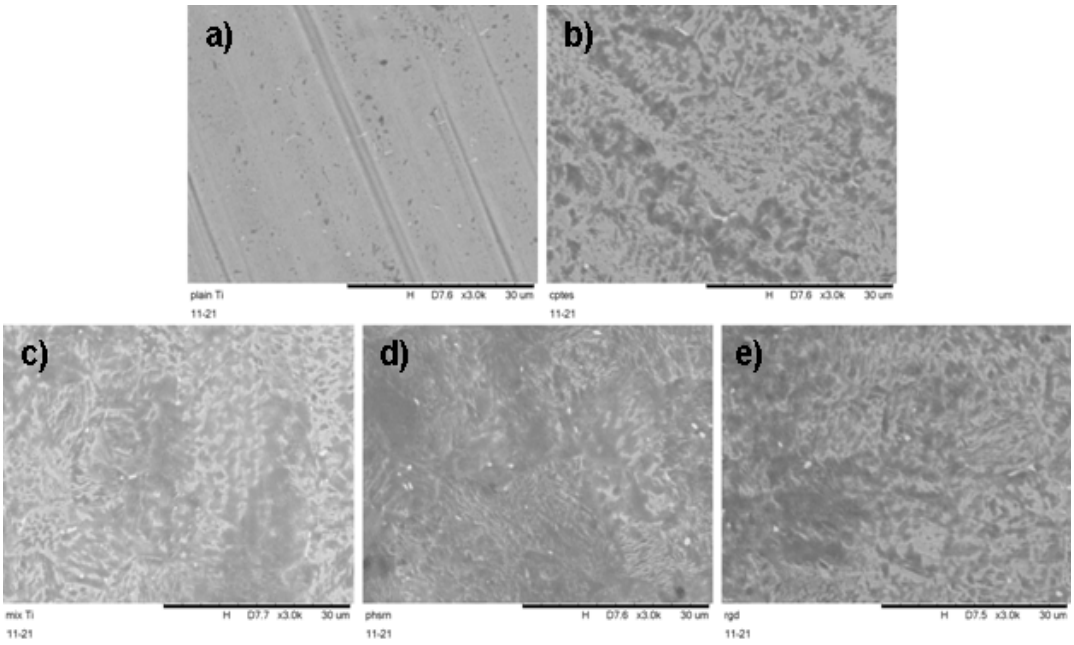

Figure 2.2 Scanning Electron Microscopy images of treated Ti surfaces. (a) untreated Ti; (b) CPTES-silanized Ti; and Ti silanized and functionalized surfaces with (c) a mixture of K3G4RGDS and K3G4PHSRN, (d) K3G4RGDS; and (e) K3G4PHSRN.

XPS results further confirmed the covalent immobilization of the peptide coatings on the silanized surfaces. Table 2.1 displays the quantitative elemental composition of the XPS survey spectra (Figure 2.3) of treated surfaces before and after ultrasonication for 2 hours in water. Untreated Ti surfaces showed characteristic C1s (285 eV), Ti 2p (460 eV) and O1s (530 eV) peaks [119]. A high percentage of Si on untreated surfaces was detected from remnants of SiC particles that are embedded in the grinding discs used to flatten and

polish the surfaces. The percentages of Si on these surfaces were dramatically reduced after ultrasonication of the samples in water. The emergence of Cl2p (2.4%) and Si2s (5.1%) peaks was detected on Ti/CPTES surfaces confirming the presence of CPTES and thus, successful silanization of titanium surfaces. All of the surfaces with covalently-immobilized oligopeptides ---Ti/CPTES/Mix; Ti/CPTES/RGD and Ti/CPTES/PHSRN showed strong Nitrogen (5.2%-8.6%) signal. The reduction to almost undetectable levels of Si and Cl signals on the oligopeptide-coated surfaces was attributed to a) the achievement of a thick layer of oligopeptides with full coverage of the underlying layer of organosilanes; and b) to the release of Chlorine ions during the nucleophilic reaction with free amines of the peptides. After ultrasonication in water for 2 hours N1s signals of all surfaces with covalently-immobilized oligopeptides remained almost unaltered. However, surfaces coated with physically adsorbed oligopeptides (Ti/Physi/Mix) showed a dramatic reduction in N1s signal after ultrasonication (6.8% before and 0.9% after ultrasonication). This was further confirmation of the mechanical stability of the coatings obtained.

Figure 2.4 shows high resolution C1s, O1s and N1s XPS peaks for Ti, Ti/CPTES, and Ti/CPTES/mix surfaces. The C1s high resolution spectrum of untreated Ti surfaces was deconvoluted in three components with binding energies at 285.1, 286.7 and 289 eV, and attributed to C-C/C-H, C-O/C-Cl and O=C-O groups, respectively[120-122]. Ti/CPTES surfaces revealed similar components but with different relative intensities compared to Ti surfaces. The notable increase of C-O/C-Cl can be attributed to the presence of those groups in CPTES molecules. The deconvolution of the C1s spectrum of Ti/CPTES/Mix

surfaces showed a more complex combination of groups with the relevant emergence of the peptide/protein characteristic C-N (binding energy at 286 eV) and O=C-N(binding energy at 288.1 eV) groups. The deconvolution of O1s-peaks showed that the relative intensity of O=C-O/O=C-N/Si-O signal gradually incremented from Ti to Ti/CPTES to Ti/CPTES/Mix surfaces in agreement with the increasing presence of organomolecules on the silanized and biofunctionalized surfaces. Finally, the deconvolution of the N1s peak for Ti/CPTES/Mix surfaces showed three separate components with binding energies at 399.6, 400.4 and 401.5 eV, corresponding to NH_2, amide-N/imide-N and NH_3^+[122], respectively.

Table 2.1 Quantification of chemical composition of treated surfaces at each fabrication steps and final oligopeptides coatings before and after ultrasonication for 2 hours in water.

	Composition							
	C (%)	O (%)	Ti (%)	Cl(%)	Si (%)	N (%)	Bal. (%)	N/Ti
Ti	50.3	33.8	5.5	0	8.5	0	1.9	0
Ti/CPTES-B	45.8	36.7	9.9	2.4	5.1	0	0.1	0
Ti/CPTES-A	49.3	34.9	8.1	1.8	1.9	1.7	2.3	0.2
Ti/CPTES/Mix-B[a]	46.6	35.7	5.8	0.2	0.2	7.0	4.5	1.2
Ti/CPTES/Mix-A[b]	44.6	35.8	7.9	0.2	0.5	7.1	3.9	0.9
Ti/CPTES/RGD-B	41.5	40.3	7.5	0.5	0.4	5.2	4.6	0.7
Ti/CPTES/RGD-A	38.5	40.7	8.7	0.3	1.1	4.7	6.1	0.5
Ti/CPTES/PHSRN-B	45.0	36.7	7.5	0.1	0.8	8.4	1.5	1.1
Ti/CPTES/PHSRN-A	44.6	36.0	8.2	0.3	0.3	8.6	2.0	1.0
Ti/Physi/Mix-B	46.4	36.9	9.3	0	0	6.8	0.8	0.7
Ti/Physi/Mix-A	33.1	53.0	12.1	0	0	0.9	0.9	0.1

[a] B – before sonication.
[b] A – after sonication.

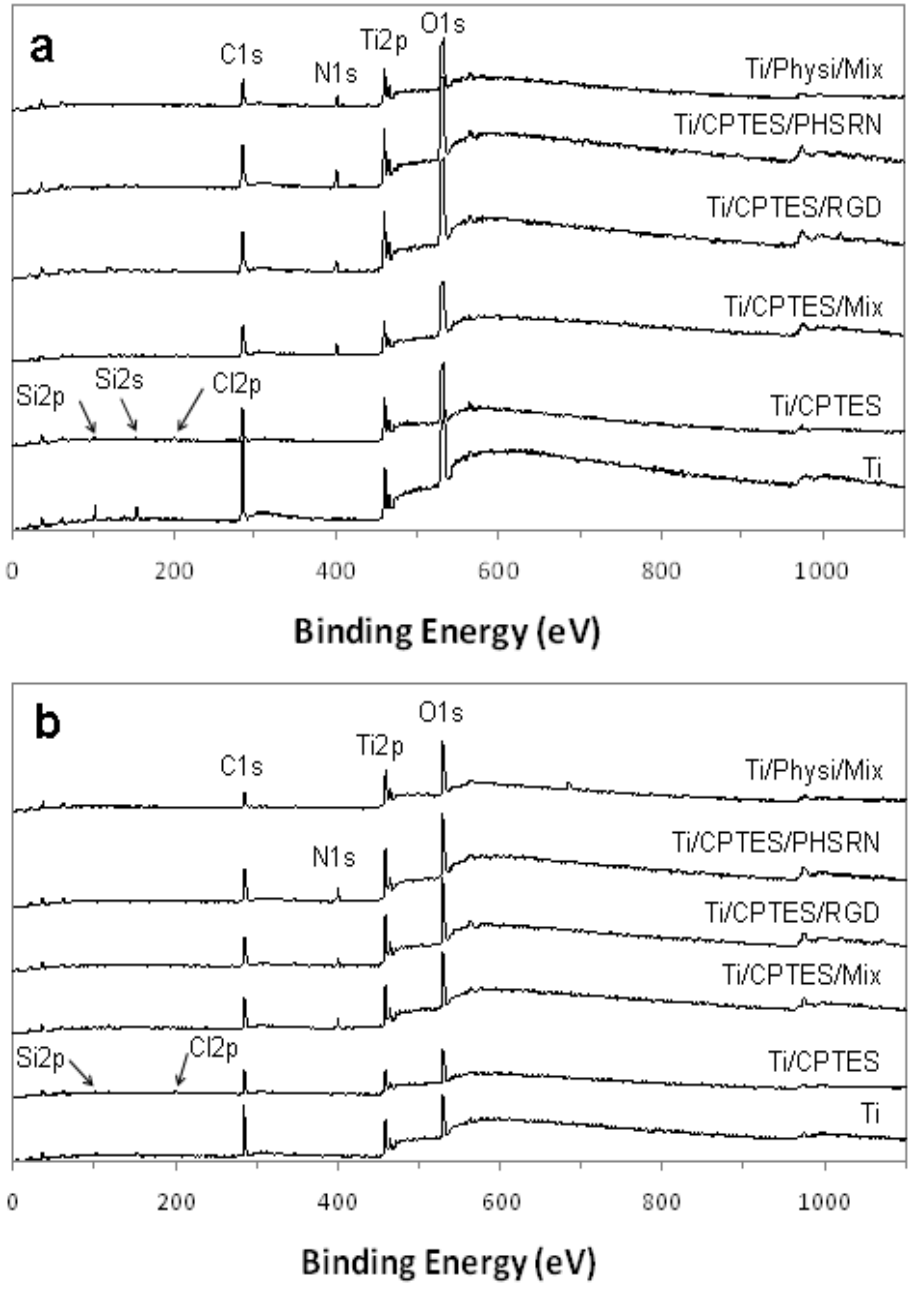

Figure 2.3 XPS survey spectra of treated Ti surfaces before (a) and after (b) ultrasonication in water for 2 hours. Surfaces after each of the steps of fabrication of the coatings and for each of the three coatings studied containing different oligopeptides were evaluated. An additional group of surfaces with a mixture of physically adsorbed oligopeptides (Ti/Physi/Mix) was tested as negative control for the stability test.

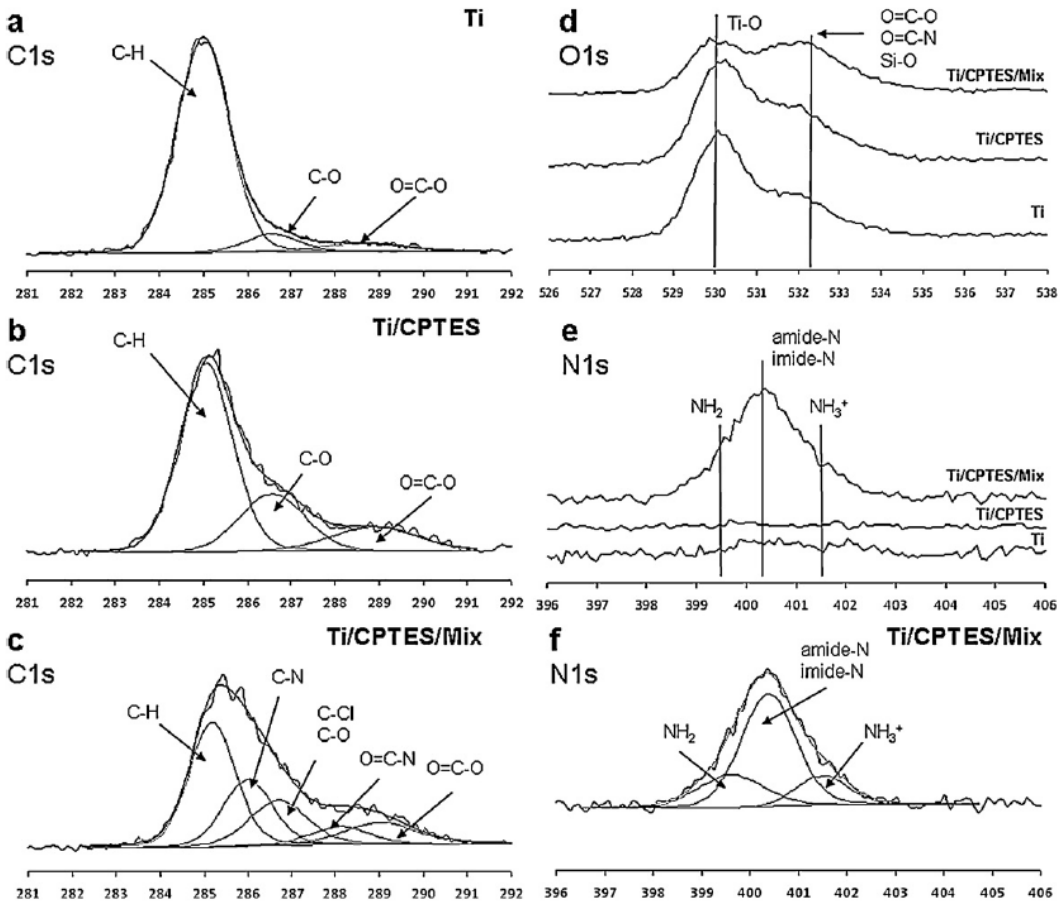

Figure 2.4 Surface chemical composition. Deconvolution of high resolution XPS peaks: C1s(a-c), O1s(d), and N1s(e,f) peaks for Ti (a,d-e), Ti/CPTES(b,d-e), and Ti/CPTES/Mix(c,d-f) surfaces.

All those results combined suggested that we successfully covalently-immobilized oligopeptides on titanium surfaces by a simple method that uses organosilane molecules to obtain mechanically-stable coatings.

Verification of the Co-immobilization of Oligopeptides on Titanium Surfaces

To verify covalent co-immobilization of the two oligopeptides, K3G4RGDS and K3G4PHSRN, on Ti surfaces we conjugated each peptide with a fluorescence probe with

distinctive but different color and surfaces coated with the fluorescently-labeled oligopeptides were visualized under a fluorescent microscope. K3G4RGDS and K3G4PHSRN were labeled with 5-FAM cadaverine (green) and 5-TAMRA cadaverine (red), respectively. Cadaverine fluorescent probes react with carboxylic groups of the oligopeptides and thus, the free amine groups in the peptides are still fully available to subsequently react with CPTES-silanized Ti surfaces.

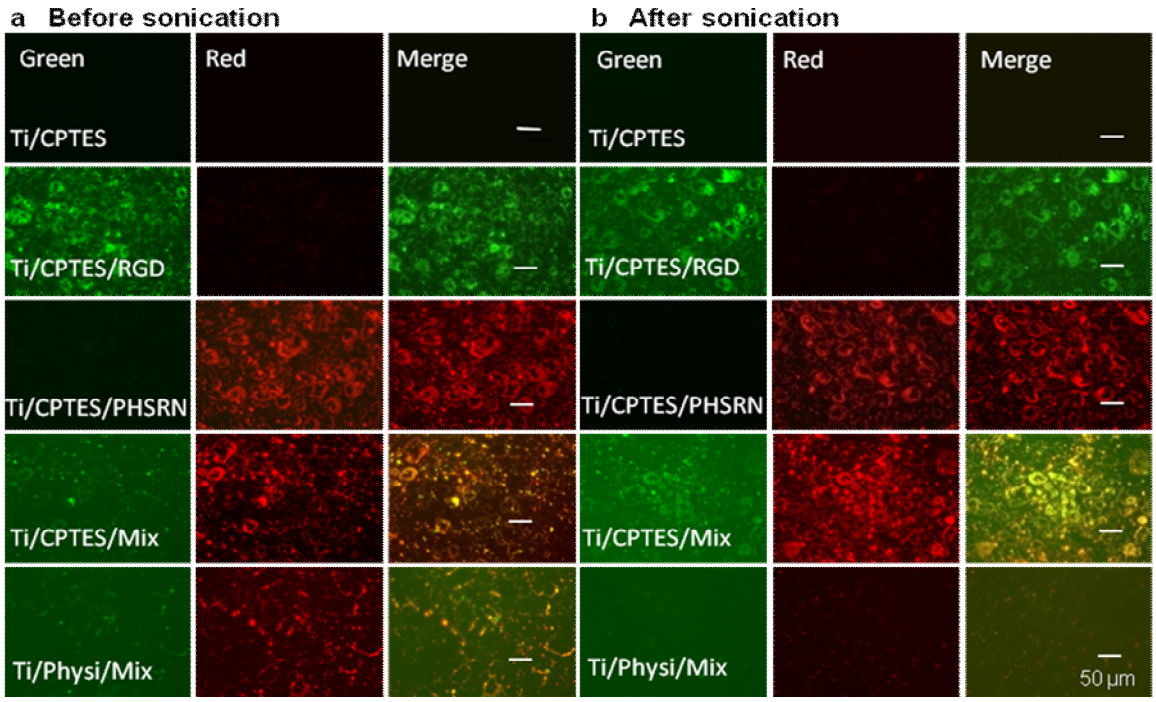

Figure 2.5 Co-immobilization of RGD and PHSRN-containing oligopeptides. Fluorescence microscopy images of all surfaces coated with oligopeptides before(a, left) and after(b, right) ultrasonication for 2h in water. RGD-containing oligopeptides were conjugated to a green fluorescence probe and PHSN-containing peptides were conjugated to a red fluorescence probe. Co-immobilization of the two oligopepties in the same surface was assessed by merging red and green images which produced a yellowish fluorescence signal.

Figure 2.5 shows that control Ti/CPTES surfaces had undetectable fluorescence signal. Ti/CPTES/RGD and Ti/CPTES/PHSRN surfaces produced only green or only red signals, respectively. Ti/CPTES/Mix and Ti/Physis/Mix surfaces before ultrasonication produced both green and red signals and the merging of those two produced yellowish images. Thus, we were successful in co-immobilizing K3G4RGDS and K3G4PHSRN peptides on Ti surfaces. The covalently co-immobilized peptide coatings produced brighter yellow images than surfaces with physically adsorbed peptides.

After 2 hours of ultrasonication in water the Ti/CPTES/Mix surfaces retained strong yellow signal, but Ti/Physi/Mix surfaces lost most of their fluorescence intensity. This was evidence of effective immobilization of both oligopeptides in the coatings through covalent binding to CPTES molecules. This is relevant for the potential stability of the coatings during surgery placement of the implant and to bear fluid flow forces. Labeling the two peptides with fluorescence probes of different colors enabled direct visualization and relative assessment of co-immobilized peptides on the treated surface and allowed the characterization of surfaces with multi-functional motifs.

Bioactivity of Surfaces Coated with Oligopeptides

We assessed adhesion, proliferation and differentiation of the osteoblastic lineage of MC3T3-E1 murine osteoblasts on titanium surfaces coated with co-immobilized oligopeptides incorporating RGD and PHSRN bioactive sequences.

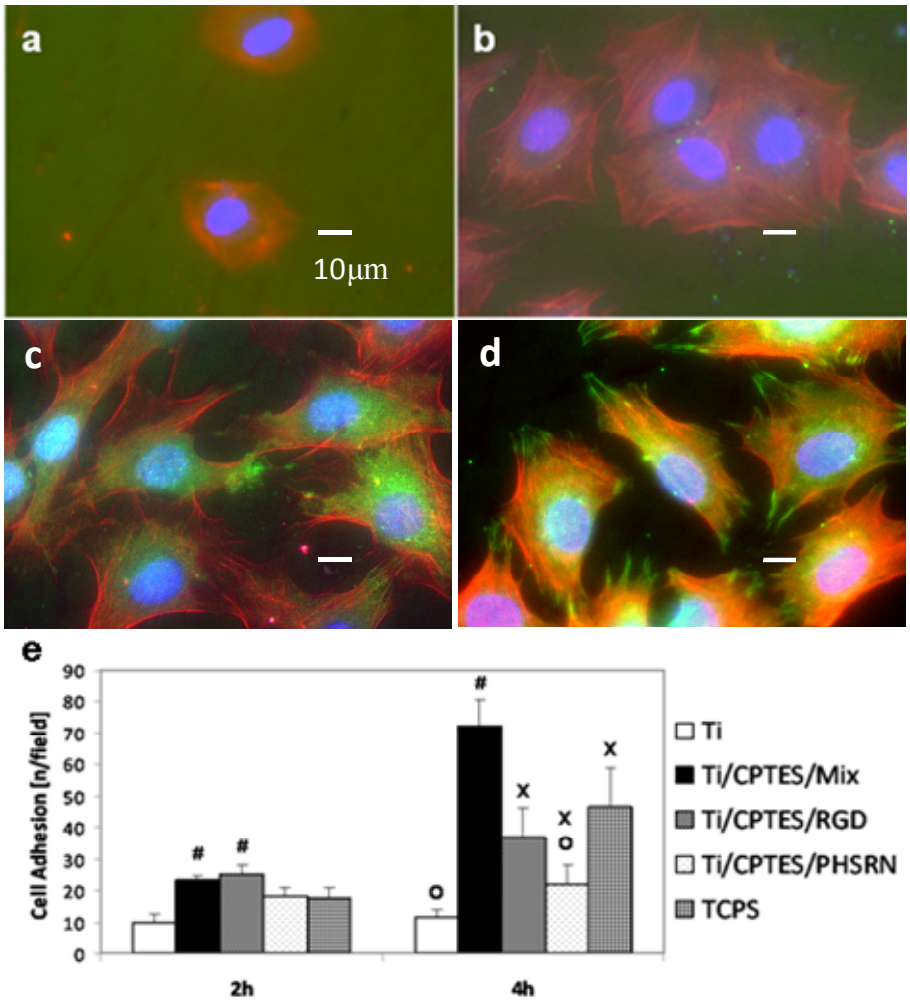

Figure 2.6 Adhesion of MC3T3 osteoblasts. Fluorescence images of cells cultured on untreated Ti (a), Ti/CPTES/PHSRN (b), Ti/CPTES/RGD (c), and Ti/CPTES/Mix (d). Red: actin filaments (cytoskeleton); green: vinculin (focal adhesion points); blue: nuclei. (e) Mean ± standard deviation of adhered MC3T3-E1 cells on the tested surfaces after 2 and 4 h in culture. Error bars are the standard deviation of at least three samples in each group. Bars with different symbols (#, O, X) are from surfaces with statistically significant differences (p-value < 0.05) at the same time point.

Immunofluorescence triple-staining revealed the morphology of MC3T3 osteoblasts cultured on treated Ti surfaces (Figure 2.6 a-d). Cells cultured on Ti/CPTES/Mix and

Tissue culture plates---TCPS (not shown) displayed well-defined cytoskeletons and large areas with focal adhesion points in comparison to cells cultured on untreated Ti, Ti/CPTES/PHSRN, and even Ti/CPTES/RGD surfaces. This indicated that the presence of the two peptides had a cooperative effect by further inducing osteoblast adhesion. This was further confirmed as higher number of cells adhered on Ti/CPTES/Mix and Ti/CPTES/RGD surfaces than on all other type of surfaces, with values that were statistically higher on Ti/CPTES/Mix surfaces after 4 hours of cell culture (Figure 2.6 e).

Figure 2.7 shows results for cell proliferation on coated surfaces after 3 and 5 days in culture. Although all of the modified surfaces sustained cell proliferation, Ti/CPTES/Mix and positive control TCPS surfaces significantly enhanced osteoblast proliferation in comparison to all the rest of surfaces tested.

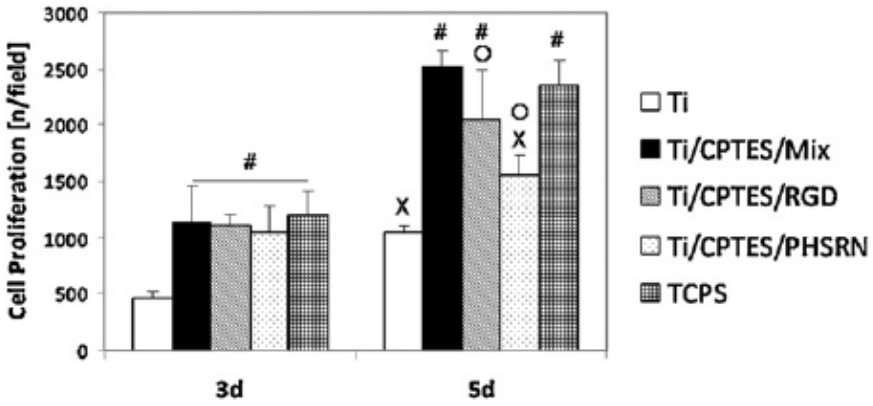

Figure 2.7 Proliferation of MC3T3 osteoblasts. Mean ± standard deviation of proliferated MC3T3-E1 cells on the tested surfaces after 3 and 5 days in culture. Error bars are the standard deviation of at least three samples in each group. Bars with different symbols (#, O, X) are from surfaces with statistically significant differences (p-value < 0.05) at the same time point.

Alkaline phosphatase (ALP) activity was determined for MC3T3 cells cultured for 7 and 14 days on the tested surfaces (Figure 2.8). Thus, the surfaces with coatings incorporating a combination of RGD and PHSRN containing oligopeptides enabled differentiation of osteoblasts as ALP activity for cells on Ti/CPTES/Mix surfaces were higher than for all the other titanium surfaces. Those differences in ALP activity among the coated samples were not statistically significant, though.

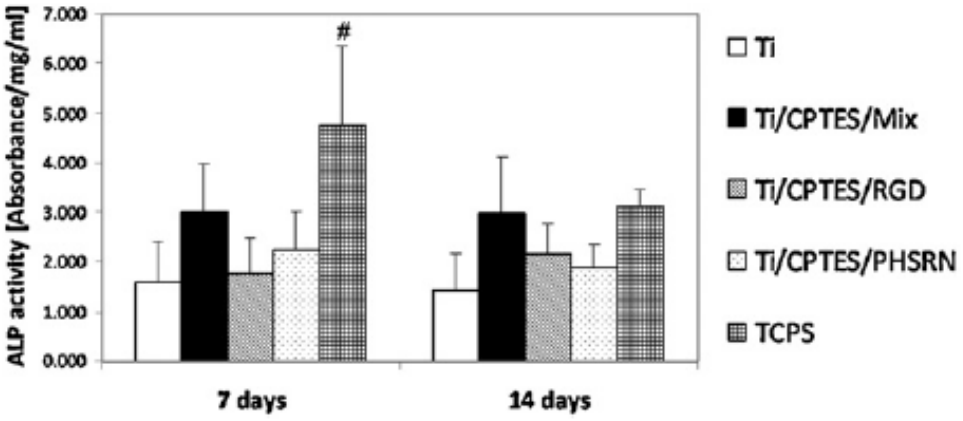

Figure 2.8 Differentiation of MC3T3 osteoblasts. ALP activity (mean ± standard deviation) by MC3T3-E1 cells differentiated on tested surfaces after 7 and 14 days in culture. Error bars are the standard deviation of at least three samples each groups. Bars with different symbols (#, O, X) are from surfaces with statistically significant differences (p-value < 0.05) at the same time point.

All these results combined showed that the surfaces of titanium with covalently-anchored coatings that contain a combination of K3G4RGD and K3G4PHSRN peptides were bioactive as cooperatively enhanced cell adhesion and proliferation of osteoblasts and sustain their differentiation into the osteoblastic lineage. The retained bioactivities on the

coated surfaces are pivotal for the appropriate biological performance of implants with multifunctional properties.

It is worth noting that many bone-replacing implants fail because 1) the inert nature of titanium is unfavorable to bone cells growth and differentiation, which inhibits new bone formation, and 2) infections lead to early- and late-life implant failures after implantation. Monofunctional coatings are not well suited to simultaneously address these two problems [123]. In fact, surfaces that are functionalized with RGD oligopeptides and other ECM proteins have been widely investigated for implant applications to improve cellular adhesion and bone formation around implant surface. However, the bioactive molecules facilitating cellular adhesion and growth also mediate and facilitate adhesion of bacteria. One example is ECM protein fibronectin, which is recognized also by Staphylococci having Fn-binding proteins [124]. Moreover, as introduced previously, the fate of implant has been described as a race between microbial colonization of the implant surface vs. tissue integration [125]. Thus, methodologies as the one presented here are in need and represent a potential successful alternative to simultaneously addressing bone integration and inhibition of biofilm formation.

2.5 Conclusion

We have successfully produced covalently co-immobilized oligopeptides that retained their bioactivities on titanium surfaces. The obtained peptide coatings were mechanically stable. The coatings with mixed RGD and PHSRN peptides significantly improved osteoblast response in comparison to their response on surfaces with only one of the

peptides. This suggests that a synergistic effect on cell response can be obtained following the co-immobilization of the two peptides.

This reliable method for co-immobilizing biomolecules can be used to obtain other multi-functional surfaces by combining oligopeptides with different targeted bioactivities --cell recruitment and differentiation, biomineral nucleation, antimicrobial activity-- and thus, further improving clinical performance of implants.

Chapter 3

A Robust Antimicrobial Peptide GL13K Coating on Ti Surfaces with Sustained Activity

3.1 Objective

The objective of chapter 3 is to investigate the robustness of antimicrobial GL13K-peptide coating on Ti surfaces with the covalent linking chemistry we established in chapter 2. The obtained coating should show high stability on surfaces with strong resistance to mechanical, hydrolytic and proteolytic challenges. The robustness of the antimicrobial peptide coating is required for its long-term effectiveness. The stability of the coating also contributes to its sustained bioactivity after autoclaving, and repeated cycles of bacteria challenge. These repeated cycles simulate the repeated periodical infection that might occur during the functional life time of dental implants.

3.2 Introduction

Dental implants have rapidly become the treatment of choice for patients in need of replacing missing teeth. According to data from the American Academy of Implant Dentistry, the annual dental implant market reaches $1.3 billion in US, $8.1 billion globally, and the numbers keep growing rapidly. Despite significant progress in clinical success rates in recent years, the 8% implant failure rate translates into more than one million failed implants per year worldwide [126]. The outcomes for patients with failed implants are often persistent pain during failure and additional surgical procedures, including grafting, to prepare for a second implant attempt. Infection is one of the most prevalent causes for implant failure. Recent evidence suggests that besides the short-term occurrence as a consequence of the initial exposure during the surgery, the long-term peri-implantitis tends to increase over long-term follow-up [127, 128]. The prevalence of

peri-implantitis varies between 2% and 44% depending on the population studied and the case definition used [129]. However, the repeated reports of above 30% incidence of peri-implantitis in various clinical studies [130-132] indicated that it is not a marginal problem.

Functionalization of titanium surfaces with coatings made of antimicrobial agents has been used during recent years to inhibit peri-implantitis. Various antibiotics, i.e. Gentamicin [34, 69, 70] and Vancomycin [78-81] have been immobilized on Ti surfaces to display their functions. Although antibiotic coatings on titanium proved to be effective, their use is controversial because of their potential host cytotoxicity and bacterial resistance. E.g. Vancomycin is not suitable for long-term use because of the potential severe bacterial resistance. The use of antimicrobial peptides (AMPs) has recently been raised as an alternative antimicrobial approach with strong potential to improve dental implants performance[110]. Compared with antibiotics, the advantages of AMPs include broad-spectrum antimicrobial activity against bacteria, fungi and virus [133], low host cytotoxicity and low bacteria resistance [96]. Different cationic antimicrobial peptides derived from human proteins have been either physically adsorbed [35, 94], or covalently attached [92] on implant surfaces. These implants displayed excellent antimicrobial activity.

Antimicrobial peptide coatings are currently widely investigated and show promising results. However, there are several obstacles that antimicrobial peptide coatings encountered, which hinder the clinical application of the coatings. The most important of

which is the finite functional life time of the coating [95]. Dental implant coatings face numerous challenges like autoclaving before implantation, mechanical friction during implantation, as well as hydrolytic and proteolytic degradation in body fluids after implantation. In addition, layers of adsorbed proteins from plasma, saliva or other body fluids may rapidly cover the surface and block the effectiveness of the coating [123]. Since long-term peri-implantitis is more of a concern, the resistance of the coatings to these multiple challenges and their retained bioactivity under "harsh" environment has become a major consideration. The systematic investigation of the long-term effectiveness of antimicrobial coatings under multiple aggressive challenges has not been widely conducted.

Here we immobilized on Ti surface an antimicrobial peptide GL13K. It features a 13 amino acid sequence, modified from peptide sequence GL13NH2, which is derived from parotid secretory protein (PSP). GL13K shows both anti-inflammatory and bactericidal activity [134]. GL13K is bactericidal in solution against multiple species including *Pseudomonas aeruginosa* and *Escherichia coli* [134]. Our previous work on tethering GL13K on Ti surface for antimicrobial purposes demonstrated that [135] after immobilization, GL13K displayed antimicrobial effect against *Porphyromonas gingivalis*, a pathogen closely associated with dental peri-implantitis. In addition, GL13K coating showed adequate cyto-compatibility with osteoblasts and human gingival fibroblasts. Here we tested the robustness of our coating under mechanical, hydrolytic and proteolytic challenges, and the retained activity of the coating after consecutive cycles of proteolytic/bacteria dual challenges as well as sterilization. Our results showed

GL13K coating was strongly retained on the surface after multiple challenges with robustly sustained antimicrobial activity. The robustness of the coating is attributed to the strong covalent bonding, which tethered the coating to the surface. The super hydrophobicity of the coating protects it from hydrolysis and enzyme degradation.

We also tethered on surface two control peptides: GL13KR1---the randomized/scrambled sequence of GL13K; and GK7NH2---the truncated sequence for GL13NH2 [134]. Peptide sequences for GL13K, GL13KR1 and GK7NH2 are listed in Table 3.1. The rationale for choosing these two control peptides is based on their different physicochemical properties, e.g. hydrophobicity and electrostatic charge. The randomized sequence, GL13KR1 has equal hydrophobicity and charge as GL13K. But GK7NH2 has higher hydrophobicity (lower hydrophobicity value according to Hopp-Woods hydrophobicity scale [118]), and lower charge compared to GL13K. By investigating the stability and antimicrobial effects of these 3 coatings we will assess the contribution of their physicochemical properties to the robustness of the coatings as well as their antimicrobial effects.

Table 3.1 Peptide sequences. Positively charged amino acids are underlined and hydrophobic amino acids are bold. Hydrophobicity is calculated according to Hopp-Woods hydrophobicity scale.

Peptide	Sequence	Theoretical Net Charge at PH7	Hydrophobicity
GL13K	G**K**I**I**K**L**K**A**S**L**K**LL**-NH_2	+5	+1
GL13KR1	**I**G**I**K**LL**K**S**K**L**K**AL**-NH_2	+5	+1
GK7NH2	GQ**II**N**L**K-**N**H_2	+2	-2

3.3 Materials and Methods

Immobilization of GL13K Peptide Coatings on Ti Surfaces

Antimicrobial peptide GL13K, and control peptides GL13KR1 and GK7NH2 were immobilized on Ti surface through a three-step method (schematic demonstration in Figure 3.1A): 1) NaOH etching to activate Ti surfaces (eTi); 2) silanization using (3-chloropropyl)triethoxysilane (CPTES) as coupling agent (eTi-Sil); 3) covalent peptide attachment (cov-GL13K, cov-GL13KR1 and cov-GK7NH2).

Commercially pure Titanium Grade II discs (1mm thick, 7.5mm in diameter) were grinded with papers with decreasing SiC-particle size, and polished with a suspension of alumina particles (1.0μm and 0.5μm of mean size) on cotton clothes. Samples were ultrasonicated in cyclohexane for 10 minutes, rinsed with distilled water and acetone. The polished surfaces were immersed in 5M NaOH solution overnight at 60^{o}C to form reactive $–OH^{-}$ groups. After activation the samples were introduced in a N_2-saturated glass chamber, 7ml anhydrous pentane, 1.2ml (3-chloropropyl)triethoxysilane (CPTES), and 0.6ml diisopropylethylamine (DIEA) (the chemicals are from the same sources detailed in chapter 2) were sequentially added to submerge the Ti samples. Samples remained in CPTES solution for 1h, and periodic 2-minute ultrasonication cycles were applied after every 10 minutes reaction. Silanized samples were rinsed with ethanol, isopropanol, deionized water, and acetone.

Covalent conjugation of peptides was accomplished by immersing silanized Ti discs into 0.1mM GL13K, GL13KR1 or GK7NH2 peptides (Peptides International, US) with 0.5mg/ml Na_2CO_3 overnight. Phys-GL13K surface was obtained by immersing NaOH etched Ti in 0.1mM GL13K solution overnight, to detect the stability of GL13K coating when physically adsorbed on Ti surfaces with electrostatic attraction.

Water Contact Angle Goniometry

Sessile drop contact angle measurements on modified Ti discs were performed using a contact angle analyzer (DM-CE1, Kyowa Interface Science, Japan) with appropriate software (FAMAS, Kyowa Interface Science, Japan) after each step of the coating method. Deionized water was used as the wetting liquid with a drop volume of 2μL. To test the stability of the coatings, surfaces were first mechanically-challenged by ultrasonication in deionized water for 3h then hydrolytically challenged by incubation with PBS at 37^{o}C for 7 days. Water contact angle was tested before and after ultrasonication and PBS incubation.

X-ray Photoelectron Spectroscopy (XPS)

XPS was performed (SSX-100, Al Kα x-ray, 1mm spot size, 35° take-off angle) to characterize the atomic composition of the surface after each step of the coating method. Survey scans (0-1100 binding energy, 4scans/sample) were done at 1eV step-size. The peak fittings and semi-quantification of surface chemical composition were conducted using ESCA 2005 software provided with the XPS system.

To further test the stability of the coatings, surfaces were first mechanically-challenged by ultrasonication in deionized water for 3h then hydrolytically challenged by incubation with PBS at 37^{o}C for 7days. XPS was performed before and after ultrasonication and PBS incubation.

Resistance of GL13K Peptide Coatings to Hydrolytic Degradation

Fluorescent labeled GL13K-ED-FAM by solid peptide synthesis (purchased from AAPPTec, US) was covalently immobilized on Ti surface (cov-GL13K). In control group, fluorescent labeled GL13K was physical adsorbed on non-treated plain Ti surface (pTi-phys-GL13K). Samples were ultrasonicated in de-ionized water for 3h then incubated in PBS at 37^{o}C for 28 days. At selected time points (3h, day1, day2, day7, day21 and day28), samples were taken out and rinsed with distilled water and acetone. The retained fluorescence signals on surfaces were read with a synergy TM 2 multi-mode microplate reader (BioTek, US) at a wavelength of 485/528 nm. Surface fluorescence intensities were also observed under fluorescence microscope (Eclipse E800, Nikon, Japan). Solutions in which samples were submerged were collected at each time point and the releasing fluorescence intensity in solution was measured using the synergy TM 2 multi-mode microplate reader. The fluorescence intensity was transferred into peptide concentration by referring to the standard curve (from 10μg/ml to 0.1μg/ml).

Resistance of GL13K Peptide Coatings to Proteolytic Degradation

Fluorescent labeled GL13K was covalently bonded (cov-GL13K) or physical adsorbed (pTi-phys-GL13K) on Ti surfaces followed by incubating with saliva or serum at 37^{o}C for 11 days. Saliva was freshly collected from healthy volunteers and filtered with 0.22μm filters (Argos Technologies, US). Fetal bovine serum was purchased from Thermo Scientific (US). Saliva and serum were renewed every 2 days. Peptide releasing amount in saliva or serum were measured using the synergy TM 2 multi-mode microplate reader by referring to the standard curve. The intensity of the retained peptide on the surface on day 0, 1, 4 and 7 was assessed by fluorescence optical density (OD) on the surface measured with the microplate reader. Then, the OD values of samples at day1, 4 and 7 were converted into the concentration of the peptide on the surface by referring to the surface peptide concentration at time = 0 min as determined with the Bradford assay (see below). The Bradford assay cannot be used to determine the surface peptide concentration after the surface was immersed in body fluid as unspecific protein adsorption on the peptide-coated surface will interfere with the measurements of these test. The percentage of released peptide was calculated by dividing the amount of released peptide in saliva or serum by the amount of the retained peptide on the surface. Homogeneity of the surface fluorescence intensities was also visualized using a fluorescence microscope (Eclipse E800, Nikon, Japan).

Peptide Concentration on Ti Surfaces Coated with GL13K peptides

Quantification of peptide concentration on modified Ti surfaces was conducted by a direct dye-binding Bradford assay [136, 137]. Standard curve was prepared by mixing 100µl of serial dilutions of GL13K (1/2; 1/4; 1/8… in PBS) with 100µl Bradford reagent (Biorad, US) in 96-well plate and shaken for 15 min at 37^{o}C. Optical Density value was read at 465 nm (unreacted) instead of 595nm (reacted) in order to determine the amount of unbound dye remaining in solution at each concentration. Test samples were immersed in 100µl PBS plus 100µl Bradford reagent and shaken for 15 min at 37^{o}C. The supernatant was collected and the absorbance was measured at 465nm. Measurements were made in triplicate.

Mechanical Resistance to Removal of GL13K Peptide Coatings on Dental Implants

In vitro implantation of GL13K-coated commercial dental implants under simulated clinical conditions was performed by placing the implants inside of a rigid polyurethane foam block of 0.32 g/cm^3 (Pacific Research Laboratories, Inc., USA)[138]. The implant was coated with fluorescence-labeled GL13K peptides and the implant placement was initiated in the block utilizing a 2mm pilot drill. The osteotomy was sequentially enlarged following the drilling sequence recommended by the implant system manufacturer for the placement of 3.75mm in diameter and 13 mm in length implants (MG-InHex, Mozo-grau, Spain) following routine clinical protocols. Implants were placed at the level of the block utilizing an implant handpiece working at 20rpm, 35N/cm^2 settings. Subsequently, the implants were retrieved applying reverse torque, rinsed with distilled water followed by 1

hour water ultrasonication to remove loosely bond peptide and debris. The integrity of the GL13K coating was assessed by taking fluorescence microscopy images of the implants before and right after insertion as well as after further implant ultrasonication.

Antimicrobial Activity of GL13K Peptide Coatings

The antimicrobial effects of GL13K coating against *S.gordonii*, a primary colonizer for *P.gingivalis* in peri-implantitis were evaluated. *Streptococcus gordonii* (*S.gordonii*) ML-5 was inoculated in 2ml Bacto Todd-Hewitt broth (BD Biosciences, US) and this overnight culture was diluted 10 folds with 0.9% NaCl then 50 folds with Todd-Hewitt broth. Titanium discs were UV for 10min then placed into 48 well plate and 1ml of the diluted culture was added to each well and incubated at 37^0C with mild shaking for 24 hours. After incubation period, the discs were taken out and carefully rinsed with 1ml NaCl for 3 times. The discs were transferred to a new 48well plate and incubated for additional 2 hours. The additional incubation aimed to increase the metabolic activity of the bacteria; thus improving the sensitivity of adenosine triphosphate (ATP) assay. After incubation, Ti discs were thoroughly rinsed with 0.9% NaCl to remove loosely bonded bacteria; then sonicated in 300µl NaCl for 10 min to collect the adhered bacteria on surface. 100µl of the collected solution was mixed with 100µl of the BacTiter-Glo™ Microbial Cell Viability kit (Promega, US) into opaque wall 96 well plate. After 5 minutes of incubation at 37^0C, the luminescence was measured using a microplate luminometer (BioTek, US). Another 100µl of collected solution was used for Colony Forming Units (CFU) test following standard protocols. 100µl of the obtained solution

was diluted serially for 10, 100, 1000 and 10000 folds. Then, 10µl of solutions at each concentration were plated on Todd-Hewitt Agar plates and incubated overnight at 37^0C in a humidified atmosphere of 5% CO_2. The number of CFU was counted after the incubation period.

Retained Antimicrobial Activity of GL13K under Sustained Challenges

Samples were treated with cycles of dual challenge (saliva or serum incubation + *S.gordonii* culture) to simulate the repeated periodic infection which might occur at the functional life time of dental implants. Etched Ti discs (eTi) and GL13K covalently tethered Ti discs (cov-GL13K) were immersed in filtered saliva or serum for 7 days and then cultured with *S.gordonii* overnight (cycle 1). After that, samples were rinsed thoroughly and sonicated with 0.9% NaCl for 10min to collect the bacteria on surface. ATP activity assay and CFU were performed to test the bacteria adherence on surfaces following the aforementioned protocol. Once the cycle was finished, samples were cleaned with PBS and UV for 10min for being re-tested in the next cycle. Cycles 2 and 3 included saliva or serum incubation for 2 days and overnight *S.gordonii* culture. ATP activity and CFU assays were carried out after each cycle.

Retained Antimicrobial Activity of GL13K after Autoclaving

GL13K coated and etched Ti discs were exposed to autoclaving under 121^{o}C for 20 min. The two groups were labeled as GL13K-AC and eTi-AC. After that, ATP activity and CFU assays were carried out to evaluate the retained antimicrobial effects of the coatings

after autoclaving. Non autoclaved eTi (eTi-Non AC) and non autoclaved GL13K coating (GL13K-Non AC) were used as controls to test the antimicrobial effects of the coatings before autoclaving.

Statistical Analysis

Statistically significant differences among groups were assessed using one-way ANOVA Tables with post-hoc tests ($p<0.05$). Multiple comparison LSD and Dunnett's T3 tests were performed when equality of variances between compared groups was or was not assumed, respectively. All groups have at least 3 samples in order to conduct statistical analysis.

3.4 Results and Discussion

Characterization of GL13K Peptide Coatings. Stability of the Coatings under Mechanical and Hydrolytic Challenges

Water contact angle test was conducted on different surfaces to evaluate the hydrophobicity of the peptide coatings, and the stability of the coatings under both mechanical and hydrolytic challenges (Figure 3.1 A). The high polarity of the surface after etching due to the formation of hydroxyl groups resulted in notably low water contact angles on the eTi surfaces. Following silanization, water contact angle on the eTi-Sil surface increased due to the attachment of the silane CPTES layer. Attachment of CPTES on Ti was achieved by the hydrolysis of ethoxy groups and the reaction with hydroxyl groups present on the activated surface. This reaction leads to polycondensation

reaction to form Si-O-Si, and Ti–O-Si bonds. The final covalent binding of peptides to silanized surface is achieved by a direct nucleophilic substitution. Free amine groups of the peptides are the nucleophilic groups. Chlorine atoms from the organo-functional groups of CPTES are the leaving groups as well as the electrophilic center of the reaction. After covalent peptide bonding, surface hydrophobicity varied according to the different peptide sequences attached. Both cov-GL13K and cov-GL13KR1 surfaces displayed "super hydrophobicity" with a water contact angle above 100^{o}, while cov-GK7NH2 surface is relatively hydrophilic with a value around 50^{o}. According to the Hopp-Woods hydrophobicity scale, charged amino acids have positive value and hydrophobic amino acids have negative value. Table 3.1 shows that GL13K and GL13KR1 sequences have net positive value due to the high number of hydrophilic lysines in their aminoacid sequence. Therefore, overall they are hydrophilic but the fact that they also include a large number of hydrophobic aminoacids make these two peptides with amphiphilic properties, as many of the known antimicrobial peptides. However, after these peptides are immobilized on the silanized titanium surfaces, both of the two coatings showed very high hydrophobicity. We propose this is because the spatial arrangement of the peptide sequences on these surfaces is guided by electrostatic attractions between the negatively-charged chlorine groups of the silanes and the positively-charged amine groups in the lysines. Thus, the peptides get their amphiphilic structures by orienting most of the hydrophilic groups towards the titanium surface whereas exposing the hydrophobic aminoacids at the air/liquid-coating interface. The amphiphilic structures with GK7NH2 should be much less favorable to form than in the case of GL13K because GK7NH2 has

only one hydrophilic group. Therefore, the coatings with GK7NH2 have lower water contact angle; i.e., they are notably more hydrophilic. The large differences in surface hydrophobicity followed by peptide bonding indicated the successful immobilization of the different sequences on Ti surfaces.

To investigate the stability of the coatings under mechanical and hydrolytic challenges, we evaluated the change of water contact angle on various surfaces after 3h of ultrasonication (simulation of sustained mechanical challenge by contacting with fluids), which was followed by 7 days PBS incubation at 37^{o}C (simulation of hydrolytic challenge). The results showed that both cov-GL13K and cov-GL13KR1 surfaces maintained high hydrophobicity, indicating the stability of the coatings under mechanical and hydrolytic challenges. However, cov-GK7NH2 surface showed notable decrease in the water contact angle, suggesting the removal of peptide following the challenges. We proposed that the strong stabilities of GL13K and GL13KR1 surfaces are due to high hydrophobicity of the coatings, which hindered hydrolysis of the underlying silane layer. The silane layers is susceptible to hydrolysis [139]. Thus, the GL13K and GL13KR1 coatings provided with a hydrophobic shield to the coated surface that protected the silane layer from being hydrolyzed, thereby stabilizing the whole coating when submitted to these challenges.

GL13K peptide was physically adsorbed on the etched Ti surfaces, and the properties of the coating (phys-GL13K) were tested. The results showed that phys-GL13K was also hydrophobic and showed reasonable stability after the different challenges. The strong

electrostatic attraction between the positively charged GL13K peptides and the negatively charged etched Ti surface may be responsible for the stability of the physically adsorbed GL13K-coating. However, further evaluation of the robustness of the coatings by X-ray Photoelectron Spectroscopy (XPS) indicated that a stronger bond strength for cov-GL13K than phys-GL13K was achieved. Figure 3.1 B shows the nitrogen percentage on

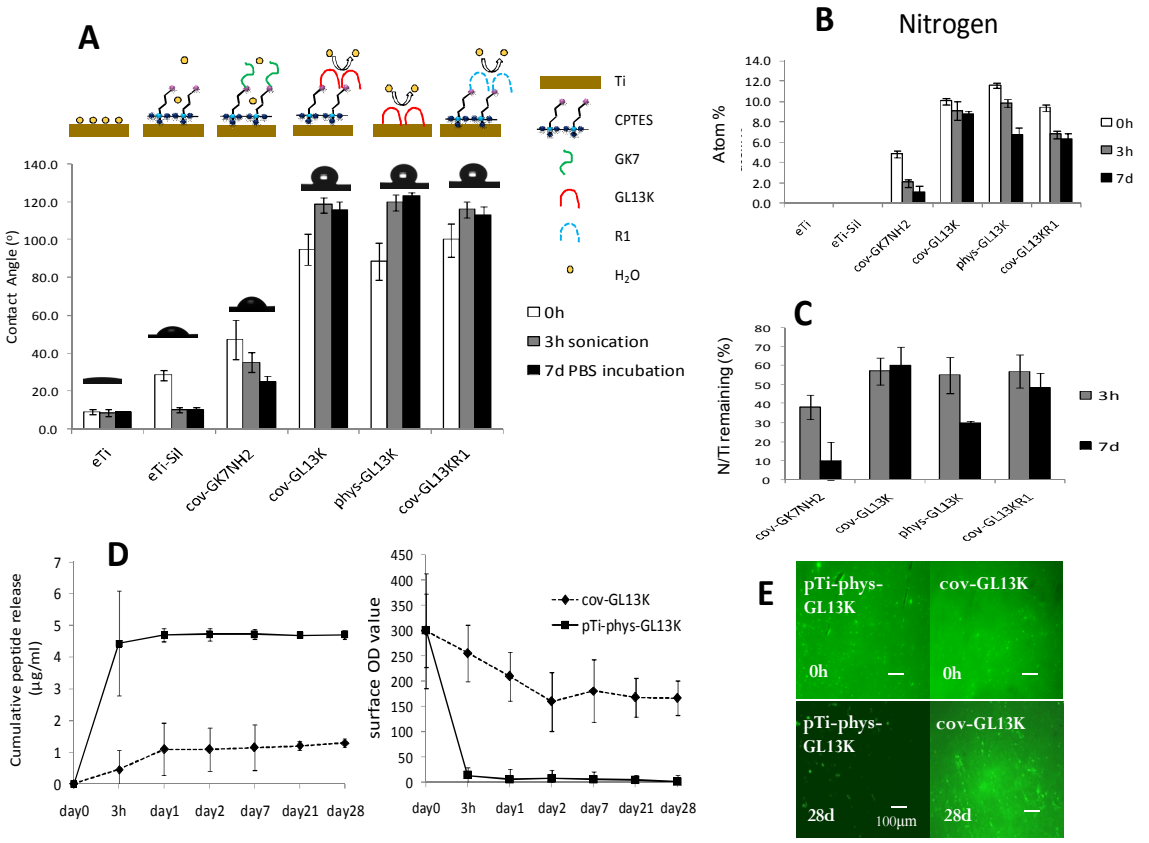

Figure 3.1 The successful immobilization of peptide coatings on Ti surfaces and the stability of the coatings after mechanical and hydrolytic challenges were tested by Water contact angle (A), XPS (B,C) and fluorimeter quantification and microscopy visualization of fluorescence-labeled peptides (D,E). Error bars are the standard deviation of three samples in each group.

different surfaces. The emergence of the Nitrogen peak is solely due to the presence of the bonded peptides on the surfaces. The Nitrogen percentage for cov-GK7NH2, cov-

GL13K, phys-GL13K and cov-GL13KR1 before mechanical and hydrolytic challenges were 4.9±0.3%; 10.1±0.3%; 11.6±0.3% and 9.4±0.3%, respectively. The remaining peptide amount after the mechanical and hydrolytic challenges were calculated by ratio between Ni/Ti values at time = 3h or time = 7d and Ni/Ti values at time = 0h (Figure 3.1C). A high percentage of peptide retained on the cov-GL13K and cov-GL13KR1 surfaces was detected both after 3h of ultrasonication and 7d in PBS. However, only 10% of peptide was retained on the cov-GK7NH2 surfaces; further suggesting that GL13K and GL13KR1 coatings had a protective role by a hydrophobic shielding effect. Phys-GL13K coatings showed much higher release of peptides than cov-GL13K coating after 7days in PBS. This suggested that the strong electrostatic attraction was less effective to stabilize the coatings than the use of the covalent bonding obtained with CPTES silanes. Figure 3.1D and E show results for the release profile and images of immobilized fluorescence labeled GL13K-peptides on coated titanium surfaces before and after incubation in PBS at 37^{o}C for 28 days. The amount of peptide released from the cov-GL13K surfaces was 1μg/ml after 28 days PBS incubation (Figure 3.1D, left). The surfaces in the control pTi-phys-GL13K group released notable higher amounts of peptide (5μg/ml) as they lack covalent bonding between the coating and the substrate. Also, the control surface was not NaOH etch, therefore, the surface lacked electronegative charge which provide electrostatic attraction to retain GL13K peptides to the surface. Fluorescent signal of the peptides that were retained on the challenged surfaces was evaluated by using a fluorimeter and assessing the surface fluorescence intensity (Figure 3.1D, right). Results of this evaluation demonstrated that the peptides were retained on cov-GL13K surfaces in

significantly higher amounts than on the control group, which hardly retained any peptide on the surface after 28 days in PBS. Visualization of the surfaces with fluorescence peptides retained (Figure 3.1E) corroborated the findings of the fluorimetry quantification. Cov-GL13K surfaces retained significant amounts of peptides as they showed strong and homogeneous fluorescence green signals after 28 days in PBS (right column). However, surfaces in the control group physisorbed-peptides coatings showed a significant reduction of the fluorescence signal (left column). Based on all these evidence, we concluded that the covalently-bonded GL13K-peptide coating was resistant to mechanical and hydrolytic challenges due to the strong covalent bonding, and the high hydrophobicity of the coating.

Resistance of GL13K Peptide Coatings to Proteolytic Degradation

Proteolytic degradation is a crucial problem especially for peptide coatings, which are extremely vulnerable to enzymes and protease in saliva, serum and other body fluids. To test the resistance of our coatings to enzyme degradation, we immobilized fluorescence labeled GL13K peptides onto the surface, followed by immersing the coating in saliva/ serum for 11 days. Samples were thoroughly ultrasonicated before being exposed to the biofluids to remove all loosely-bonded peptides from the tested surfaces. We then investigated the percentage of peptide cleaved from the surface to the surrounding media. The control group was physically-adsorbed GL13K on plain Ti surface. After 11 days of incubation with saliva or serum, cov-GL13K showed around 2% peptide released from the surface to either saliva or serum, while the control showed around 9% peptide

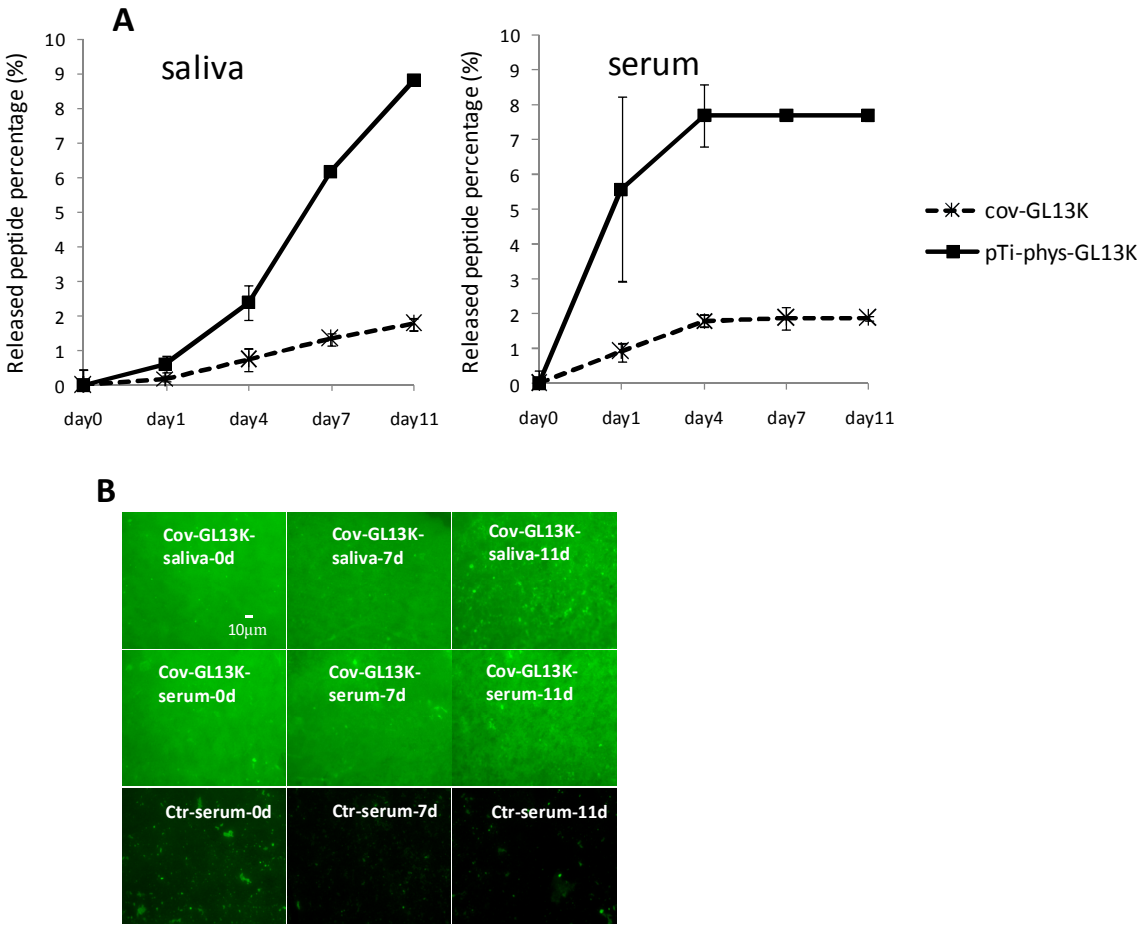

Figure 3.2 The resistance of GL13K-peptide coating to proteolytic degradation in saliva or serum was assessed by fluorimetry(A) and fluorescence microscopy(B). A) Percentage of peptide released from the coated surfaces after 11days of incubation in saliva (left) or serum (right). The intensity of the retained peptides on those surfaces were observed by fluorescence microscope(B) to demonstrate that the peptides were not either degraded or removed from the surface after being exposed to enzyme-containing biological solutions. Error bars are the standard deviation of three samples in each group.

released to saliva and 8% to serum (Figure 3.2 A). Figure 3.2 B shows images of the surfaces degraded by saliva or serum incubation for 11 days. Most of the peptides were retained on coatings of cov-GL13K surfaces after incubation in either saliva or serum after 11 days. Thus, a mild degradation of those coatings was assessed. The control

surfaces showed notable degradation after incubation in both serum and saliva. We proposed that the arranged orientation for GL13K coating in cov-GL13K surfaces and the densely exposed hydrophobic groups improved the resistance of the coatings to enzymatic degradation by reducing the accessibility of their cleavable sites to enzymes.

Resistance to Mechanical Removal of GL13K Peptide Coatings on Dental Implants

The implant placement experiment conducted in polyurethane foam blocks simulated the true mechanical challenges dental implants encountered in clinical settings. Polyurethane foam block is a widely used artificial bone model to test the properties of dental implants, including the integrity of implant surface coatings after insertion [140]. Compared with the aforementioned method of using ultrasonication as a simulation of mechanical challenge, the implant placement experiment is more clinically related, and thus sheds light on the genuine mechanical stability of GL13K coating in clinical applications. Figure 3.3A shows the fluorescence labeled GL13K coating before implant insertion. Bright green signal was observed on both the implant apical area (flat apex) and the implant body area (threads). The dental implant appeared not to be fully covered by green peptide, due to the limited depth of focus of the fluorescence microscope. After insertion, implants were retrieved by reverse torque, and rinsed with distilled water. The consequent microscopy observation in Figure 3.3B shows the moderately reduced fluorescent intensity on the implant surface. The integrity of the coating was not compromised. No exposure of dental implant surface by scratching or delamination was observed. We sonicated the retrieved implant in water for 1 hr to remove loosely-bonded

peptides and debris from the dental implant surface. Figure 3.3C shows the strongly retained peptide coating after this cleaning process. Importantly, we doubled (insertion/screw and retrieval/unscrew) the mechanical challenge of the coating with respect to the one that a dental implant would face in a clinical scenario. The observation that the coating was vastly retained on the dental implant surface suggested it would be stable and thus active in a potential clinical application after surgical implantation.

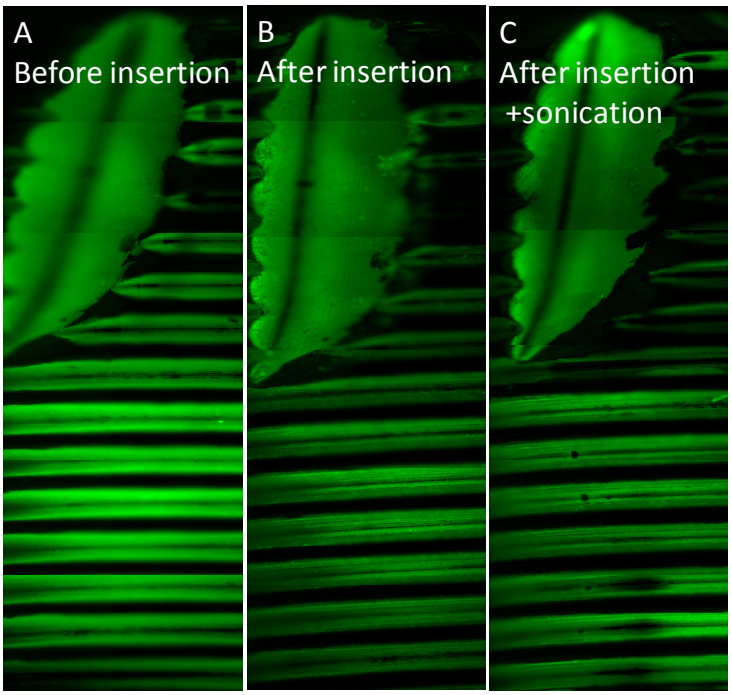

Figure 3.3 Fluorescence-labeled GL13K peptide coating on a dental implant surface A) before implant insertion in simulated clinical conditions; B) after implant insertion; and C) after implant insertion followed by surface cleaning by water sonication.

Sustained Antimicrobial Activity of GL13K after Three Consecutive Cycles of Dual Proteolytic/bacteria Challenges

Body fluids are a harsh environment for bioactive coatings. Body fluids lead to enzymatic degradation or protein adsorption, which diminishes the bioactivity of coatings overtime. Moreover, repeated periodical bacterial challenges during the lifetime of the coating would markedly compromise the stability and activity of the coatings. Therefore, a strong coating with long-term effectiveness should be able to withstand 1) challenges of periodical bacterial attack and 2) challenges of degradation by body fluid in periods between bacterial attacks. To mimic this situation, we designed tests for cycling dual challenges characterized by saliva or serum incubation + *S.gordonii* culture. Then we assessed the retained antimicrobial activity of GL13K peptide coatings after each cycle. Saliva/ serum incubation period was 7 days for cycle 1 and 2 days for cycles 2 and 3. *S.gordonii* culture period was 24 h for each cycle. Figure 3.4 shows that for samples incubated in saliva (left), GL13K-peptide coating had gradual reduction in its antimicrobial effectiveness, but still statistically significant antimicrobial effect against *S. gordonii* after 3 cycles (dashed arrow) was assessed when compared to control non-coated surfaces. This result is consistent with other in literature. V. Antoci et al. [78] and M. Kazemzadeh-Narbat et al. [35] reported that vancomycin or antimicrobial-peptide Tet213 coatings on Ti surfaces showed gradually decreased but efficient antimicrobial effect after 4 and 7 cycles of bacterial challenge, respectively. However, in those previous works, repeated bacterial challenges were conducted consecutively without additional interval of body fluids incubation. The incubation interval mimics the period between

bacterial attacks in the natural infection process, in which body fluids may further enzymatically digest the peptide coatings. For samples incubated with serum (right), bacteria activity on GL13K-peptide coatings was not significantly different than control etched Ti surfaces (solid arrow). However, it is worth noting that both GL13K coated and non-coated control surfaces induced notable inhibition of bacterial activity when compared with same surfaces but exposed to saliva. The number, type, and concentration of proteins in saliva and serum are different and therefore, the layer of proteins that naturally adsorbs on the tested surfaces from serum can be different from the one from saliva and might block adhesion of *S. gordonii* bacteria. Notably, the *S. gordonii* is a bacteria species found in saliva that contain integrin protein on their membrane known to be highly responsive to saliva proteins [141]. On the contrary, no serum proteins are specifically recognized by *S. gordonii* bacteria, which in turn can prevent *S.gordonii* adhesion on the serum protein adsorbed surfaces. A similar result was reported on the significantly reduced adhesion of *S.epidermidis* on blood plasma and saliva coated surfaces [142].

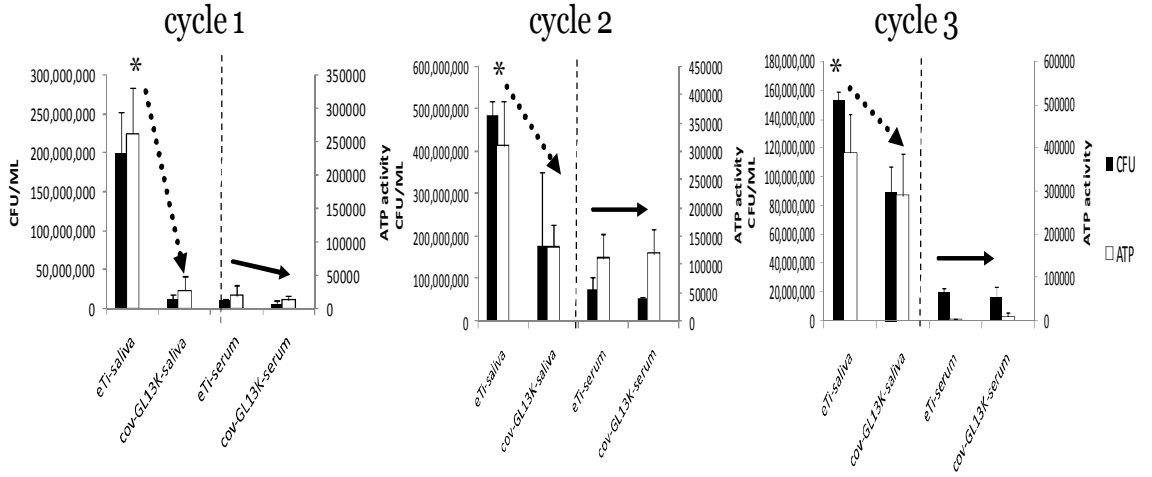

Figure 3.4 Sustained antimicrobial effect of GL13K coating after 3 cycles of saliva/serum incubation + *S.gordonii* culture. When incubated with saliva (left, dashed arrow), the antimicrobial effect of the GL13K peptide coating was gradually reduced. However, the antimicrobial effect of the GL13K coating against *S.gordonii* remained statistically higher than control surfaces after 3 cycles. Surfaces incubated in serum (right, solid arrow) showed reduced bacterial activity on both GL13K and control surfaces.

Sustained Antimicrobial Activity of GL13K Peptide Coatings after Sterilization

Sterilization of dental implants is mandatory before dental implants are placed in bone during surgery. Commonly used sterilization methods include gamma-rays, autoclaving and ethylene oxide atmosphere. Among them, autoclaving is the most widely used one. Many coatings lose their bioactivities after autoclaving because of their heat and water labile properties. Most antibiotics are heat labile [143], and large molecule proteins are easily denatured after autoclaving. D. Zheng et al. showed that immobilized chitosan on silanized Ti surfaces lost their antimicrobial efficiency after autoclaving [144]. However, small molecule peptides showed higher heat resistance [145]. M. Willcox et al reported the heat stability of antimicrobial peptide coating melimine after exposure to autoclaving

[146]. Our GL13K coated and control etched Ti discs were exposed to autoclaving under 121^{o}C for 20 min. Figure 3.5 revealed that after autoclaving (right), GL13K surface had greatly sustained antimicrobial effect, which was comparable to its antimicrobial effect before autoclaving (left). Besides the heat resistance of peptide coatings which enable them to withstand autoclaving, the high hydrophobicity of GL13K coating may protect the coating from being hydrolytically degraded during autoclaving, which is a process under a water vapor atmosphere at high pressure and temperature.

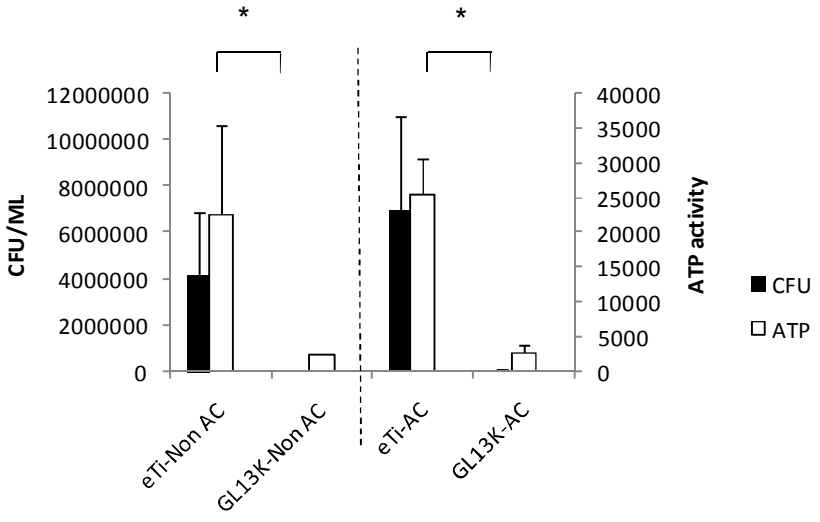

Figure 3.5 Sustained antimicrobial effect of GL13K peptide coating after sterilization by autoclaving (AC, right) is comparable to its antimicrobial effect before autoclaving (Non AC, left). Error bars are the standard deviation of three samples in each group.

3.5 Conclusion

A robust antimicrobial GL13K peptide coating was immobilized on Ti surfaces through covalent bonding with CPTES. The obtained coating showed stability on surfaces with strong resistance to multiple challenges, which included: mechanical force, hydrolytic

degradation and proteolytic degradation. The robustness of the antimicrobial peptide coating was attributed to the strong covalent bonds provided by the silane chemistry, and its high hydrophobicity provided by the GL13K amino acid sequence. The stability of the coating also contributed to its sustained bioactivity after autoclaving and repeated cycles of dual proteolytic and bacterial challenges.

Chapter 4

Antimicrobial Effects of GL13K Coating and the Key Factors of its Action

4.1 Objective

The objectives of this chapter are:

1) Evaluating the antimicrobial effects of GL13K coating. The bacterial adhesion and viability on the coated surfaces will be assessed and analysed to elucidate the anti adhesion and/or bactericidal effects of the coating. Biofilm accumulation on GL13K-coated surfaces and control surfaces will be investigated to determine the effects of GL13K coating on biofilm formation.

2) Investigating the key factors for the assessed antimicrobial activity of the GL13K-peptide coating. Besides the commonly accepted properties of antimicrobial peptides that have effect on their activity; namely hydrophobicity and surface charge, we will also innovatively investigate the effect of the secondary structure of the peptides on their activities.

4.2 Introduction

As discussed in chapter 3, antimicrobial peptide coatings are currently widely investigated with promising results, but there are still obstacles to overcome that hinder their clinical application and lack of fundamental knowledge regarding the effectiveness to prevent infections. Thus, understanding and identifying the key properties that mediate the antimicrobial effects of the antimicrobial peptide coatings will further aid in addressing the problem of losing their long-term stability and sustained activity when exposed to multiple biological and surgical challenges.

It is well accepted that the antimicrobial effect of antimicrobial peptides relies on their cationic amphiphilic property which enables their interaction with the bacteria membrane through electrostatic and hydrophobic interactions. This results in the disturbance of the bacteria membrane [96]. Thus, hydrophobicity and charge are commonly suggested to be the most important factors contributing to the bioactivity of antimicrobial peptides and coatings made with them. There are many works in the literature investigating the effects of hydrophobicity and the cationic nature of antimicrobial peptides on bacteria membrane disturbance. A few of them focused on studying those effects when the peptides are tethered and confined on the surface. M. Bagheri et al reported that higher antimicrobial effects were observed when the charged amino acids were tethered close to the surface, and hydrophobic domains of peptides were immobilized away from the surface [147]. K. Hilpert et al also showed similar results, indicating that hydrophobic residues should be optimally exposed to form direct contacts with bacteria [148]. However, R. Chen et al concluded the opposite as they assessed that the optimal antimicrobial activity is obtained when the cationic portion is away from the surface and more available to interact with bacteria [136]. The conflicting conclusions imply that the separate influence of neither hydrophobicity nor electrostatic charge univocally defines the antimicrobial effect of the antimicrobial peptide coatings. We hypothesized that a more important factor for defining the antimicrobial activity of our peptide coatings is the acquired secondary structure of the peptide on the coating. The spatial arrangement of the hydrophobic and charged groups is as important as, if not more than, the intensity of the charge and hydrophobicity themselves. To investigate the contribution of hydrophobicity, charge and secondary

structure of the tethered-peptide coatings to their bioactivities, we tested Ti surfaces coated with antimicrobial GL13K peptides and control GL13KR1 peptides. To discern the key factors for the antimicrobial activity of the GL13K coating, the antimicrobial effect of these peptide coatings against *S.gordonii*, a primary colonizer for *P.gingivalis* in peri-implantitis was evaluated and the hydrophobicity, charge and secondary structure of the two tethered-peptide coatings were compared.

4.3 Materials and Methods

Immobilization of Peptide Coatings on Ti Surfaces

See chapter 3.3

Evaluation of Antimicrobial Activity of Peptide Coatings

Streptococcus gordonii ML-5 was inoculated in 2ml Bacto Todd-Hewitt broth (BD Biosciences, US). This overnight culture was diluted 10 folds with 0.9% NaCl then 50 folds with Todd-Hewitt broth. Titanium discs were placed under UV for 10min then placed into 48-well plate. 1mL of the diluted culture was added to each well, and incubated at 37^0C with mild shaking for 24 hrs. After incubation, the discs were taken out and carefully rinsed with 1mL NaCl for 3 times. The discs were transferred to a new 48-well plate and incubated for an additional 2 hrs. The goal of additional incubation was to increase the metabolic activity of the bacteria, thus improving the sensitivity of the adenosine triphosphate (ATP) assay. After incubation, Ti discs were thoroughly rinsed with 0.9% NaCl to remove loosely bonded bacteria then sonicated in 300µl NaCl for 10

min to collect adhered bacteria on the surface. 100µl of the collected solution was mixed with 100µl of the BacTiter-Glo™ Microbial Cell Viability kit (Promega, US) into opaque wall 96 well plate. After 5 minutes of incubation at 37^0C, the luminescence was measured by microplate luminometer (BioTek, US). Another 100µl of collected solution was used for the Colony Forming Units (CFU) test. Briefly, 100µl of the obtained solution was diluted serially for 10, 100, 1000 and 10000 fold. Then, 10µl of solutions at each concentration were plated on Todd-Hewitt Agar plates and incubated overnight at 37^0C in a humidified atmosphere of 5% CO_2. The number of CFU was counted after incubation period. LIVE/DEAD® BacLight™ Bacterial Viability Kits (Invitrogen, US) was used for live and dead cell staining. Briefly, Ti discs cultured overnight with *S.gordonii* were rinsed with 0.9% NaCl for 3 times. Equal volumes of green and red dyes in the kit were mixed and diluted at concentration 0.3% in H_2O. 10µl of diluted dye was dropped and spread on tested surfaces and incubated at room temperature in the dark for 15 minutes. Samples were transferred to fluorescence microscope for visualization.

Scanning Electron Microscope

The morphologies of the bacteria on the discs were analyzed using field-emission gun Scanning Electron Microscopy (JEOL 6500 FE-SEM, Japan) at 5 kV. The bacteria were primarily fixed with 2% glutaraldehyde and 0.15% alcian blue in 0.1M sodium cacodylate buffer (pH 7.4) for 1hr, then washed with 0.1M sodium cacodylate buffer for 5 min. They were secondarily fixed with 1% OsO_4 in 0.1M sodium cacodylate buffer for 1 hr and washed with sodium cacodylate buffer. After fixation, samples were dehydrated

with ethanol (50%, 70%, 80%, 95% and 100%, 5 min in each). All samples were critical-point dried using a Critical Point Dryer (Tousimis Samdi-780, US). Samples were then mounted on aluminum stubs with double-sided copper tape and sputter coated with 5 nm Pt. In order to identify the morphologies of live and dead cells, some samples were examined by both fluorescent microscopy and SEM in the same field. The fluorescent microscopy image was rotated to match with the SEM picture and a black background was added.

Zeta Potential Measurements

The surface charge of the different titanium surfaces was determined by means of ζ potential measurements (SurPASS Electro-kinetic Analyzer for solid surface analysis, Anton Paar, Austria).The ζ potential measurements were carried out with 1mM KCl solution as the electrolyte adding KOH 0.1M until the electrolyte pH was adjusted to 7.4. The experimental set up was performed using the SurPASS symmetric adjustable clamping cell, fixing two similar samples in front of each other. Streaming potential measurements with the symmetric cell were taken eight times at pH 7.4. After the measurements, surface conductivity correction was performed measuring the specific electrical conductivity and cell resistance using 0.1M KCl solution. The ζ potential was then calculated using the Smoluchowsky equation:

$$\zeta = \frac{\partial U}{\partial p} \times \frac{\eta}{\varepsilon \times \varepsilon_0} \times \frac{R_{0.1M\ KCl} \times K_{0.1M\ KCl}}{R_{0.001M\ KCl}}$$

where dU/dp is the slope of streaming potential versus pressure, η is the viscosity of the electrolyte solution, ε is the dielectric constant of the electrolyte solution, ε0 is the vacuum permittivity. $K_{0.1M\ KCl}$ and $R_{0.1M\ KCl}$ are the specific electrical conductivity and cell resistance using 0.1 M KCl solution. $R_{0.001M\ KCl}$ is the cell resistance using 1 mM KCl solution.

Circular Dichroism Spectroscopy

For obtaining the circular dichroism (CD) spectrum of GL13K and GL13KR1 peptides in solution, they were dissolved in different buffers at 0.1 mM concentration: pH 7.4 sodium phosphate buffer; pH 10.5 sodium carbonate buffer; and a serial sodium borate buffers at pH 8.5; 9; 9.2; 9.4; 9.6; 9.8; 10; 10.2; 10.4;10.6. CD spectra were recorded using a JASCO J-815 spectropolarimeter and quartz cell with 1.0mm path length. CD spectra were acquired with solvent subtraction from 190 to 260nm. For testing CD spectrum of peptide coatings, the peptides were immobilized on 8x25x0.5 mm quartz slides (SPI, US) using CPTES silane chemistry, and then inserted into a quartz cell with 1.0mm path length. To test the stability of the secondary structure of the peptide coatings, peptide-conjugated quartz slides were immersed in PBS at 37^{o}C for up to 7 d. After that, the quartz slides were cleaned, dried, and re-tested to evaluate the secondary structure of the peptides in the remaining coatings. The acquired CD spectra were converted to mean residue ellipticity. To examine the percentage of secondary structure of peptides, all spectra were fitted using three different programs (CDSSTR, CONTINLL and SELCON3) in CD Pro and the averaged percentage was used in this report.

Statistical Analysis

Statistically significant differences among groups were assessed using one-way ANOVA Tables with post-hoc tests ($p<0.05$). Multiple comparison LSD and Dunnett's T3 tests were performed when equality of variances between compared groups was or was not assumed, respectively.

4.4 Results and Discussion

Antimicrobial Effects of GL13K Coatings on Titanium Surfaces

The antimicrobial effects of peptide coatings were assessed by the activity of *Streptococcus gordonii* on the tested surfaces. The commensal species *S. gordonii* is a primary colonizer in oral biofilms that, significantly, constitutes an attachment substrate for the secondary colonization and biofilm accretion by the potential pathogen of peri-implantitis, *P. gingivalis*. Adherence of *P. gingivalis* to surfaces in the developed biofilm depends on deposition of *S. gordonii* cells on the salivary pellicle at the colonized surface [149]. If *S.gordonii* is not present in the biofilm, only a few *P.gingivalis* cells are able to attach on the surface and as a result they are easier to detach and remove from the compromised surface [150]. Therefore, strategies that prevent *S.gordonii* adhesion on the surface compromise the biofilm formation, and therefore minimize the risk of developing peri-implantitis. The Colony Formation Unit (CFU) assay was used to test the amount of viable bacteria and the Adenosine Triphosphate (ATP) assay was used to investigate the metabolic activity of the bacteria. The combined results showed statistically significant

reduced *S.gordonii* activity after overnight culture on cov-GL13K surfaces in comparison with non-coated control eTi surfaces and surfaces coated with control peptides, cov-GL13KR1 or cov-GK7NH2 (Figure 4.1A). Chitosan (a known highly-cationic antimicrobial agent) was immobilized on titanium surface and tested as positive control group for this experiment. Results showed that cov-GL13K surfaces had higher antimicrobial effect than the chitosan coated surfaces, although differences were not statistically significant.

Live and dead cell staining assay showed the sustained antimicrobial effect of GL13K coatings after 2, 4, 6 hours, and overnight culture with *S.gordonii* (Figure 4.1B). The controls gradually accumulated bacteria as incubation time increased, and thick biofilms were grown after overnight culture. GL13K-coated surface presented significantly reduced bacterial adhesion at each time point. Growth of the *S.gordonii* biofilm was inhibited throughout the experiment on GL13K-peptide coatings, and the scarce bacteria visualized on the GL13K coatings were predominantly dead bacteria. Thus, the GL13K coatings on titanium surfaces showed "killing by contact" effect on bacteria.

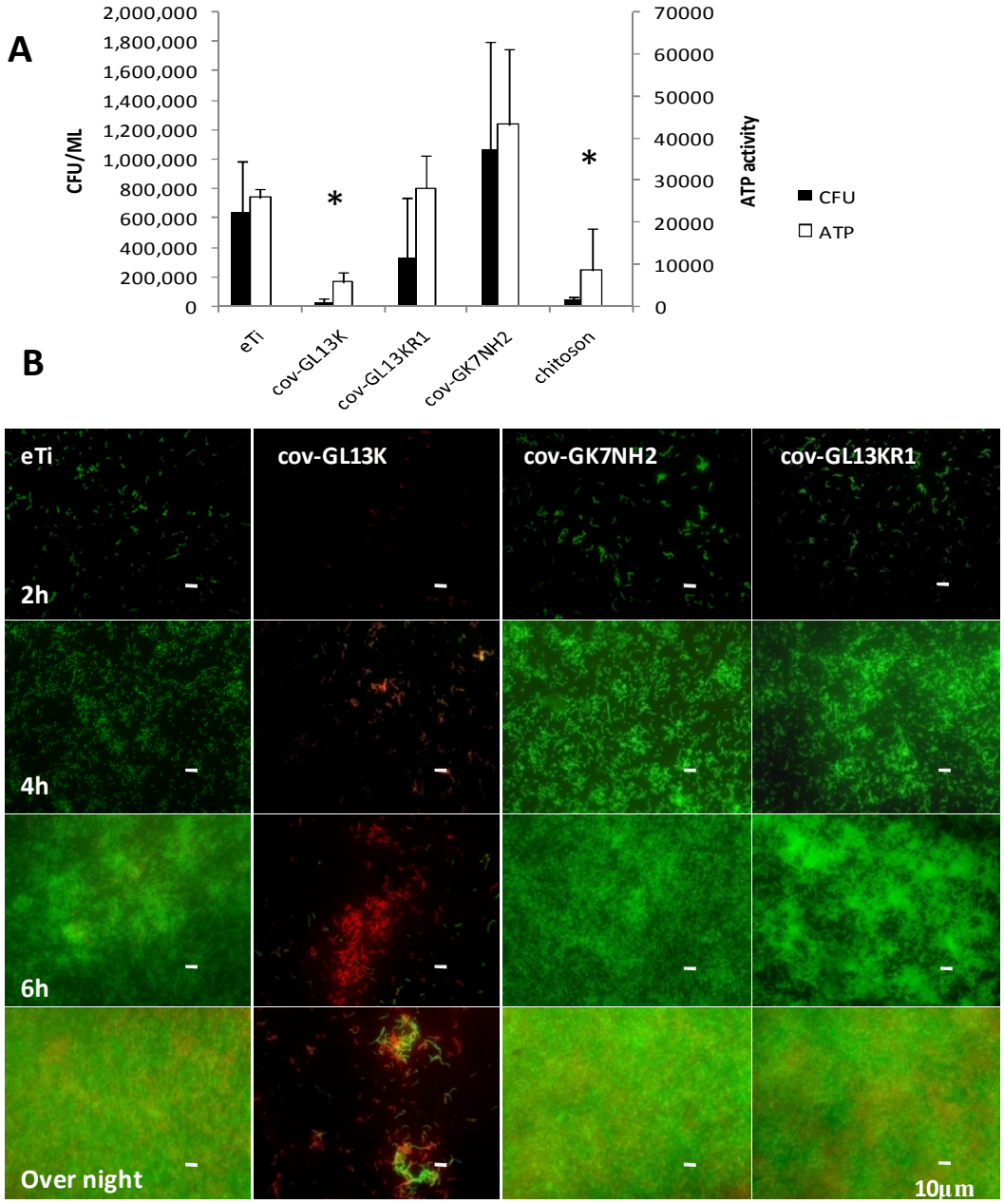

Figure 4.1 Antimicrobial effects of coatings were tested by A) CFU and ATP activity assays and B) Live/dead cell fluorescence staining. A) GL13K-coated surface showed a statistically significant reduction of CFU and ATP activity in comparison to all negative controls. Error bars are the standard deviation of at least three samples in each group. B) Live and dead cell staining showed the sustained antimicrobial effect of GL13K-peptide coatings after 2,4,6 hours and overnight culture with *S.gordonii*. GL13K surface had reduced bacterial adhesion at each time point and "killing by contact" effect to the bacteria.

Scanning Electron Microscopy (SEM) showed the morphological change of *S.gordonii* after overnight culture on the different tested surfaces (Figure 4.2A). Low magnification pictures confirmed results obtained for the live/dead experiment; that is, GL13K-peptide coatings inhibited biofilm formation. The majority of bacteria visualized by SEM on the GL13K-coated surface were isolated cells with bead-like morphology. In contrast, most of the bacteria in the biofilm grown on control surfaces were mature cells with rod-like and/or chain-like morphologies. High magnification images demonstrated that the bead-like cells on cov-GL13K surfaces had morphology of *S.gordonii* which is typical of its planktonic state (Figure 4.2A, lower row). This suggested that GL13K coating stopped the *S.gordonii* developmental process at an early stage; thus, preventing biofilm growth.

We then discerned the viability of bacteria with planktonic morphology and hence their potential to grow and further develop biofilm. We matched fields of images obtained with both SEM and fluorescence microscope after live/dead cell staining (Figure 4.2B). Most of the bacteria on cov-GL13K surfaces, including those that showed planktonic morphologies in SEM images (dashed arrows) were dead bacteria. Only a few bacteria with chain-like morphology were alive (solid arrow). Given that bacterial biofilms grown on medical devices are up to 1000-fold more antibiotic resistant than bacteria in planktonic state [151, 152], the occasional remaining bacteria that are alive or transitory alive on the cov-GL13K surfaces would be more vulnerable to additional antibiotic treatment after implantation as well as more easily cleaned by the immune system.

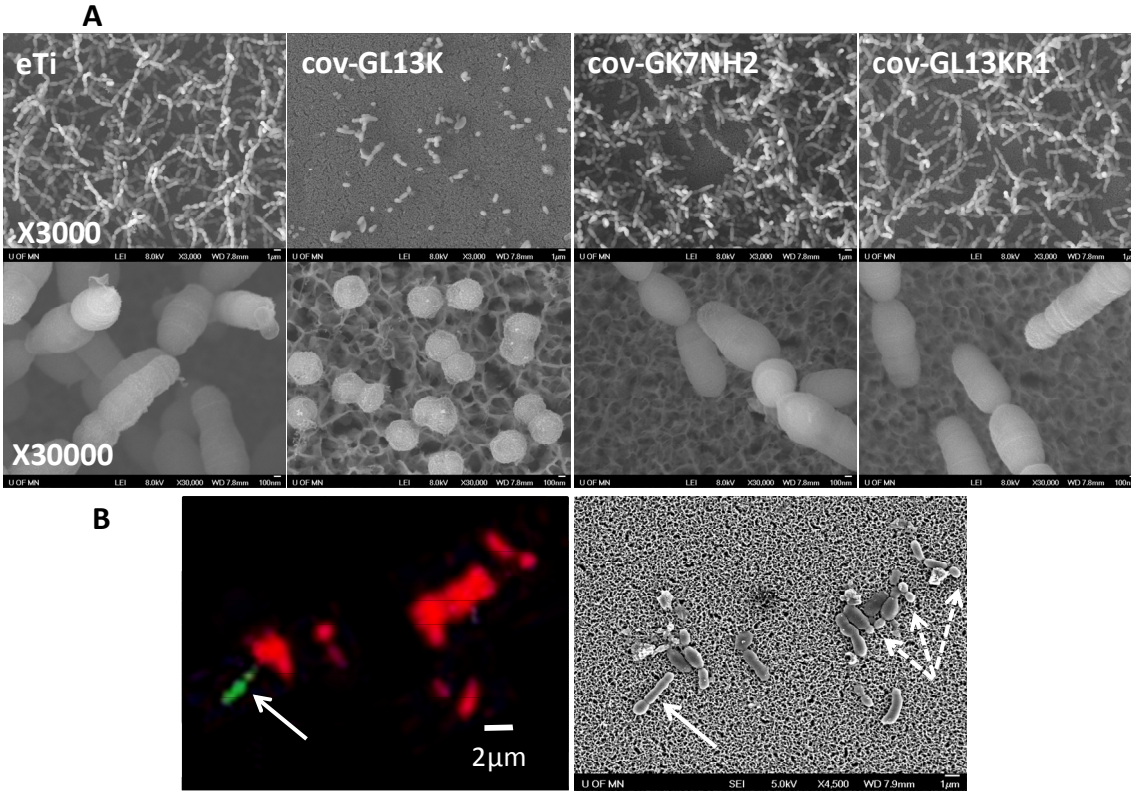

Figure 4.2 SEM images showed the morphology of *S.gordonii* after overnight culture. A) cov-GL13K surfaces prevented biofilm formation and growth. Bacteria on GL13K-coated surfaces showed planktonic morphology, whereas well-established biofilms on control surfaces showed mature cells with chain-like morphology, typical of established biofilms. B) Matched image fields obtained by SEM (right) and live/dead cell fluorescence staining (left) revealed that most of the bacteria on GL13K-coated surfaces, including bacteria with planktonic morphologies (dashed arrows) were dead. Only a few mature bacteria with chain-like morphology were still alive on the antimicrobial surfaces after overnight culture (solid arrow).

It is worth noting that GL13K and GL13KR1 sequences that shared the same amino acids but in different ordered sequence showed notable different antimicrobial activity. Further investigation to discern the key properties contributing to the effective antimicrobial

activity of the GL13K-peptide coatings constitutes the rest of the study discussed in this chapter.

Key Factors for the Antimicrobial Activity of GL13K

It is well accepted that hydrophobicity and charge greatly contribute to the antimicrobial effect of antimicrobial peptides [153]. However, as previously introduced, we hypothesized that the secondary structure of the peptides in the coating is also a key factor affecting its antimicrobial effect. By optimally distributing (location and density) the hydrophobic and charged domains, the secondary structure of the peptides can mediate specific interactions between structural components of the bacteria membrane and the peptides in the coatings. Others have investigated the effect of the secondary structure of the antimicrobial peptides on their efficacy as an isolated factor with also controversial conclusions [154, 155]. Here, we explored the three factors that we anticipate are key for the bioactivity of the antimicrobial peptides and coatings made of them. Thus we analyzed and compared surface hydrophobicity, surface charge and the secondary structure of the antimicrobial GL13K-petide coating and the non-antimicrobial control GL13KR1-peptide coating.

Surface Hydrophobicity

Surface hydrophobicity was tested by water contact angle using the sessile drop method (Figure 3.1 A). Both GL13K and GL13KR1 coatings had very high hydrophobicity, but

with no statistically significant difference. This indicated that surface hydrophobicity alone was not the key factor determining the activity of the GL13K-peptide coatings.

Surface Charge

Surface charge of GL13K and GL13KR1 coatings determined by surface ζ potential also showed only minor differences between these two surfaces (Figure 4.3). At pH 7.4, etched Ti, CPTES silanized Ti and cov-GK7NH2 surfaces were markedly electronegative with zeta potential at -30.4±4.8, -38.3±4.6, and -34.8±3.8 mV, respectively. This was due to the anionic potential of the surface created by the hydroxyl groups formed after NaOH etching. Adding to that, the chloride groups in the CPTES-silanized surfaces added more negative charges to the eTi-Sil surfaces. Cov-GL13K and cov-GL13KR1 groups showed significantly increased (less negative) surface charge due to the abundant cationic amino acids contained in these two immobilized peptide sequences. This greatly minimized the overall negative charge of the coated surfaces with -10.1±4.8 and -14.0±3.3 mV for the GL13K and Gl13KR1 coatings, respectively. The difference in the average surface charge between cov-Gl13K and cov-GL13KR1 surfaces was not significantly different. This further indicated that neither surface hydrophobicity nor surface charge were the determinant(s) for the activity of the GL13K-peptide coatings.

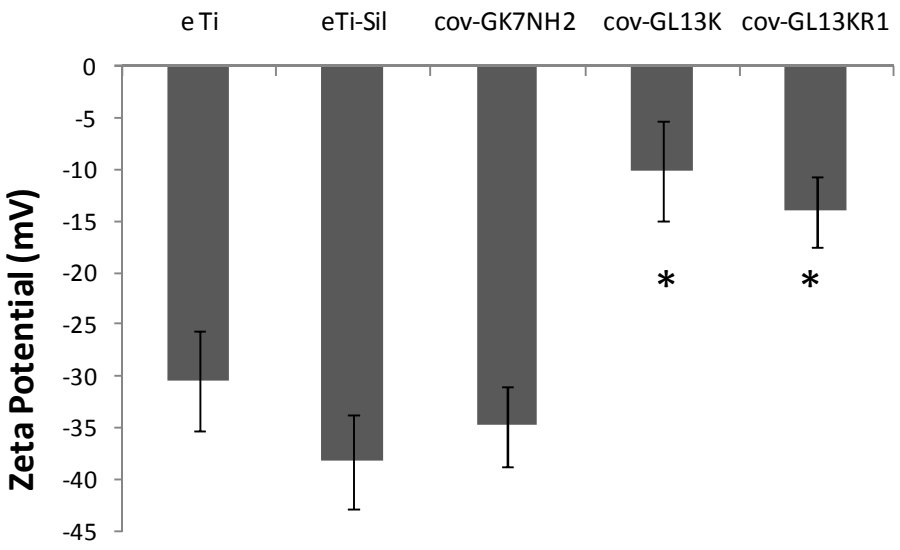

Figure 4.3 Zeta (ζ) potential values of the different surfaces were tested. Etched Ti, silanized Ti and cov-GK7NH2 surfaces were highly negatively-charged at pH 7.4. GL13K and GL13KR1 coated surfaces showed significant reduction of the overall negative charge due to the highly cationic nature of these two peptides. Error bars are the standard deviation of three samples in each group.

Secondary Structure of the Peptides and Peptide Coatings

We also investigated the difference between secondary structures of the GL13K and Gl13KR1 peptides both in solution and covalently-anchored to a surface using silane chemistry. Computer prediction of the secondary structure was conducted by using the web server PSIPRED (http://bioinf.cs.ucl.ac.uk/psipred/; last access 04/16/2014) from the Department of Computer Science at UCL-University College London, UK. GL13K is predicted to have β-sheet structure at the **KIIKLKA** domain, with the two terminal sides predicted to form random coil structures. However, GL13KR1 is predicted to form an α-helix structure through almost the entirety of the aminoacid sequence, **GIKLLKSKLKA,** with only the C- and N-terminal aminoacids having random coil conformations (Figure

4.4). To verify the computer prediction, the secondary structures of the two peptides were tested by CD Spectroscopy.

Figure 4.4 Computer prediction of the secondary structure of A) GL13K and B) GL13KR1

Firstly, we investigated the conformation of GL13K and GL13KR1 peptides in buffered solution. Both GL13K and GL13KR1 showed dominant random coil structures at pH 7.4 (Figure 4.5 A). The spectra consisted of a minimum at ~200nm, which is a characteristic CD spectroscopic signal given by random coil structures. This was consistent with results from V. Balhara [156]. However, when we dissolved the peptides in buffer at pH 10.5, which is the buffer we used for covalently bonding the peptides on the silanized titanium

surfaces, the two peptides changed their conformations and the conformations reached by each of the peptides were significantly different. The secondary structures attained by the two peptides in solution at pH10.5 were those of the computer prediction. On one hand, the CD spectra for GL13K peptides consisted of a maximum at ~195 nm, and a broad minimum at ~215nm, which revealed a conformational state with combined β sheet, α helix and random coil structures, but with a notable prevalence for the β sheet structure. On the other hand, the CD spectra for GL13KR1 peptides showed a maximum at ~190 nm and a broad minimum at ~207nm, indicating a mixture of α helix and random coil structures, with α helix dominance and almost absence of β sheet structure (Figure 4.5 B). Thus, we observed that a pH shift towards more basic conditions triggered folding of the two peptides from a prevalent random coil conformation at pH 7.4 into their predicted structures. These conformational changes are most likely triggered by neutralization of the cationic side chains in the peptides [157]. This leads to decreasing molecular repulsion between peptide molecules and thus, formation of hydrogen bonds and hydrophobic interactions between the molecules is favored. To verify this, we prepared a series of sodium borate buffers at pH 8.5; 9; 9.2; 9.4; 9.6; 9.8; 10; 10.2; 10.4; 10.6. With the gradual pH increase from 8.5 to 10.6, both GL13K (Figure 4.5 C) and GL13KR1 (Figure 4.5 D) peptides progressively modified their structures from prevalent random coil conformations to either β sheet (Figure 4.5 C) or α helix (Figure 4.5 D) structures, respectively. These results suggested that basic solutions triggered and stabilized peptide self-assembly to form their respective favored structural conformations.

Thus the prevalence of the β sheet structural domains formed by GL13K peptides in comparison to the prevalence of α helix structural domains formed by GL13KR1 peptides is a distinctive factor between the two peptides investigated here.

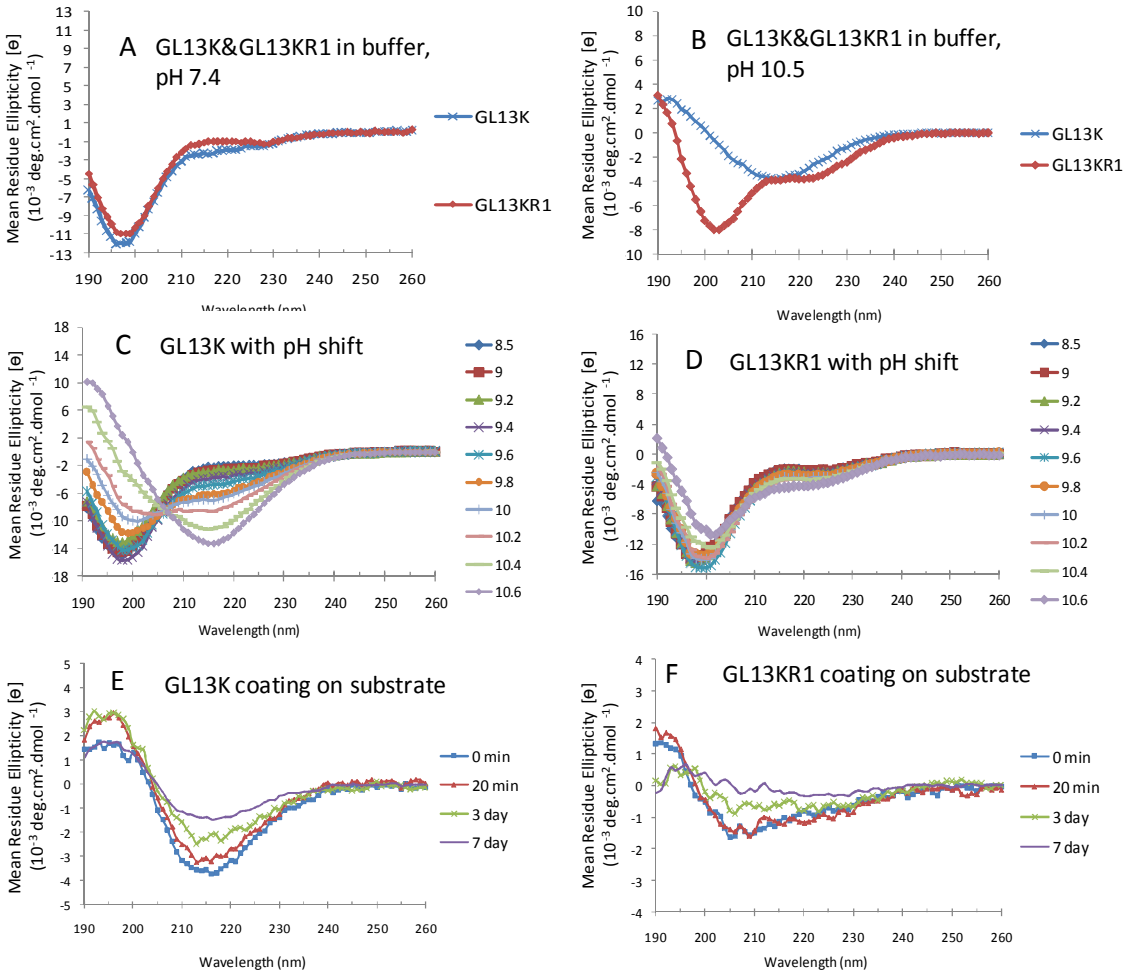

Figure 4.5 Circular Dichroism (CD) spectra. A) GL13K and GL13KR1 in pH 7.4 buffer; B) GL13K and GL13KR1 in pH 10.5 buffer; C) GL13K and D) GL13KR1 in buffers from pH 8.5 to pH 10.6; E) GL13K-peptide coating and F) GL13KR1-peptide coating after different times of immersion in PBS (pH 7.4) up to 7days.

V. Balhara et al investigated the antimicrobial mechanism of GL13K peptides in solution [156]. They found that GL13K peptides had random coil structures in a biological

solution at pH 7.4. However, upon binding with model cellular membranes (1, 2-dioleoylphosphatidylglycerol (DOPG)); (that is, when interaction of the peptides with bacteria membranes is simulated in vitro), GL13K peptides changed their conformation into β-sheet. The authors suggested that the peptides optimize their interaction with the model amphiphilic bi-layer membrane, which in turn disrupts the integrity of the membrane.

Our results and those by Balhara et al indicate that the formation of β sheet structures with the GL13K peptide either in basic solutions or when recruited to the bacteria membrane is key for their effective antimicrobial activity. Therefore, retention and stabilization in the peptides coatings of the β sheet structures by GL13K peptides should be also key for the antimicrobial activity of these coatings.

To validate this, we assessed the effective retention of β sheet and α helix structures on GL13K and GL13KR1 coatings, after covalent-bonding on the surfaces from basic solutions. In fact, we selected a basic buffer (pH 10.5) for the peptide covalent-bonding to the silanized surfaces because it favors the nucleophilic substitution reaction between the silanes and the peptides. Then, the use of this buffer not only improves bonding efficacy of the peptides on the surface, but it also triggers the molecular assembly to form the distinctive secondary structures for each of the peptides. CD spectra of GL13K and GL13KR1 coatings which immobilized on quartz slides using the same CPTES-silanization method to coat Ti surfaces are shown in Figure 4.5 E and Figure 4.5 F, respectively. In the dry state (0 min), GL13K peptides in the coatings conformed a

prevalent β sheet structure, whereas GL13KR1 coatings displayed dominance of the α helix conformation. Thus, both peptides retained in the coatings the same conformational structures they had in solution at pH 10.5. The relative structure content of β sheet, α helix and random coil calculated by CD pro is shown in Figure 4.6.

Finally, the stabilization after retention of the secondary structures of the peptides in the coatings is a crucial property for the effectiveness of the coatings both in vitro and in vivo. Dental implants, after surgery, are surrounded by biological fluids with neutral pH. Therefore, if the β sheet structure of GL13K peptides in the coatings is not stable and the peptides re-conform back to the random coil structures at neutral pH solutions, its antimicrobial effect will be compromised. To investigate this, GL13K and GL13KR1 coatings on the quartz slides were immersed in PBS (pH7.4) for up to 7 days at 37^{o}C. Samples were tested by CD after 20 min, 3d and 7d, in PBS. Secondary structures of the peptides in the coating did not change as incubation time increased (Figure 4.5 E and F). This result demonstrated that the originally retained molecular conformations were stable after exposure to a simulated biological environment. The mean ellipticity was gradually attenuated from time 0 to 7 d, which suggests that some of the peptides were released from the surface during this period.

Overall, these results demonstrate that the secondary structure of the peptides in the coatings is a distinctive key factor that determines their antimicrobial efficiency. Moreover, GL13K-peptide coating displayed its remarkable antimicrobial effect against *S. gordonii* because the coating not only is highly cationic and amphiphilic but also

retains and stabilizes the β sheet structure of the peptides initially formed in a basic solution.

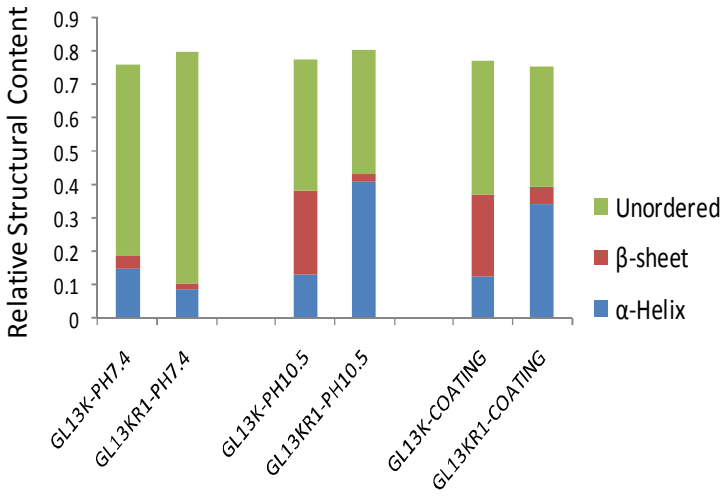

Figure 4.6 Relative structural components (β sheet, α helix and random coil) of the GL13K and GL13KR1 peptides in solution at pH 7.4 (left), and pH 10.5 (center) as well as in the coatings (right).

Interestingly, the MIC value for GL13K against *S. gordonii* was 256 μg/ml, which reveals a limited efficiency of the antimicrobial activity of GL13K peptides in solution. This effect of the peptides in solution differed from the high efficiency of the GL13K-peptide coatings tested here. The concentration of GL13K peptides on the titanium surfaces after covalent-bonding (54.4±34.4 μg/cm^2) is much higher than the concentration of GL13K peptides used in solution against *S. gordonii* (100μg/ml) [134]. The high peptide concentrations on the surface may prevent bacteria mechanisms for resealing and self-repairing their phospholipid membrane bilayer, which have been observed when bacteria are exposed to GL13K peptides in solution after initial damage of their membrane [156]. G. Gao et al also reported that in contrast to peptides that are free

standing in solution, where membrane interaction and perturbation are diffusion limited, the high concentrations of peptides that are achieved when they are tethered on surfaces produced more extended damage to the membrane permeability barrier of the bacteria [158]. Additionally, we propose that the high efficiency of the antimicrobial GL13K-peptide coatings is favored by the strong stabilization of the β-sheet structures of the peptides before and during their interaction with the bacteria membrane.

Figure 4.7 is a schematic representation of the conformational changes of GL13K and GL13KR1 peptides and their consequential effects on interactions with bacteria. Both GL13K and GL13KR1 peptides show random coil structure in buffer at pH 7.4. In the immobilization solution at pH 10.5, GL13K and GL13KR1 peptides preferentially change their conformation to β sheet and α helix structures, respectively. When peptides are immobilized on the surfaces the conformational states of the two peptides are retained on the obtained coatings. Those secondary structures of the peptides in the coatings are stabilized and no notable reverse conformational changes occur when exposed to solutions at neutral pH**.** The stabilized β sheet structure of GL13K peptides in the coating assists membrane disruption; however, the α helix structure of GL13KR1 peptides in the coating does not favors membrane disruption.

Membrane disruption is the well accepted mechanism responsible for the antimicrobial effects of antimicrobial peptides [159, 160]. We did not observe any specific pattern of membrane damage to the surface membranes, but *S. gordonii* have a thick and stiff peptidoglycan wall that prevents them from collapsing or bursting.

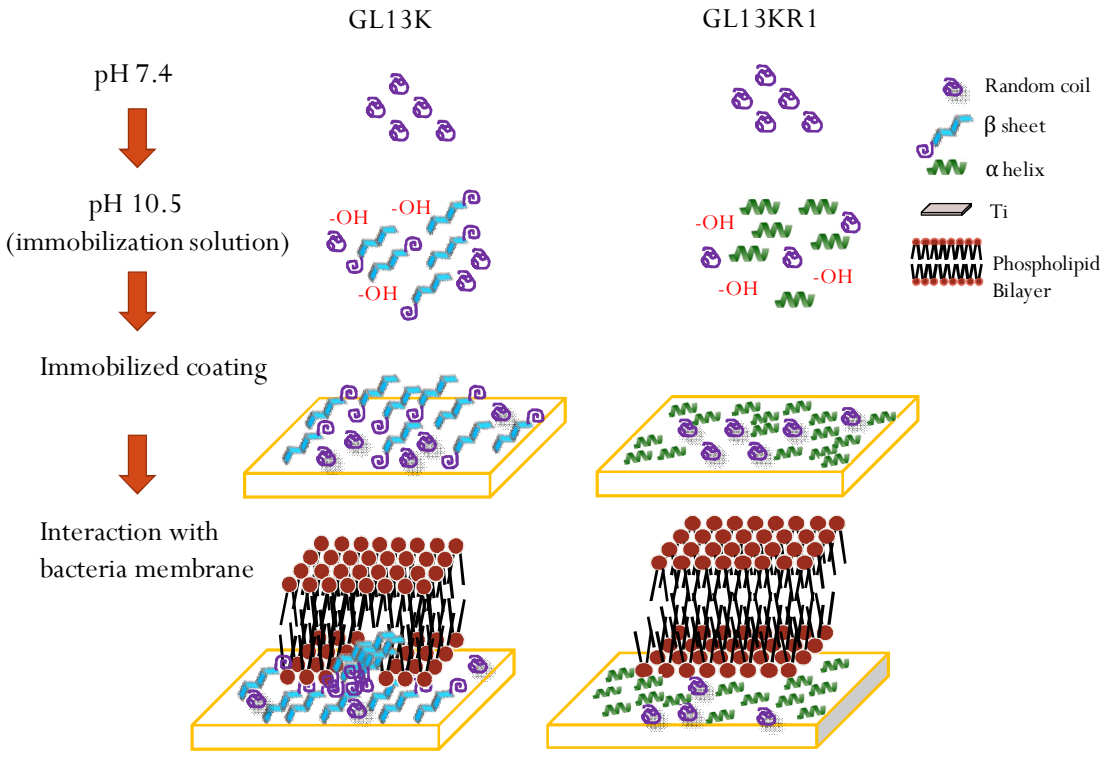

Figure 4.7 Schematics of the conformational changes of GL13K and GL13KR1 peptides in solution and after being immobilized on the coatings. The consequential antimicrobial activity of the peptide coatings is also displayed.

4.5 Conclusions

GL13K-peptide coatings killed *S.gordonii* at their planktonic or early growth stage, preventing the maturity of the bacteria and biofilm formation and growth.

The antimicrobial GL13K and the non-antimicrobial control GL13KR1 coatings had similar hydrophobicity and surface charge, but the two peptides acquired different conformations both in basic solutions and once immobilized in the coatings. GL13K peptides conformed to preferential β-sheet structure, whereas GL13KR1 peptides conformed to α-helix structure. The distinctive conformational changes were triggered by

the high pH of the solution used for immobilizing the peptides on the surface, and it is retained and stabilized in the coatings. Thus, GL13K-peptide coating displayed its remarkable antimicrobial effect against *S. gordonii* because the coating not only is highly cationic and amphiphilic but also retains and stabilizes the β sheet structure of the peptides initially formed in a basic solution.

The stabilized β-sheet structure of GL13K coatings may contribute to the long term in vivo antimicrobial effects of the GL13K coating.

Chapter 5

Cell Wall Damage of Gram Positive Bacteria by GL13K Coating in a Drip Flow Bioreactor

5.1 Objective

The chapter aims to examine the antimicrobial effects of GL13K coating on *S. gordonii* in a drip flow bioreactor. The culturing conditions in a drip flow bioreactor simulate more reliably the biological environment in the oral cavity; i.e., comparable shear forces to the ones exerted by saliva in contact with surfaces and biofilm and a sustained nutrition supply for the microflora. The antimicrobial effects and the prevention of biofilm growth on GL13K-peptides coatings under these simulated bacterial culture condition will be investigated.

5.2 Introduction

Infection is one of the most prevalent causes for implant failure. Antimicrobial peptides are promising alternatives to currently used antimicrobial agents. In our previous work, we tethered the antimicrobial peptide GL13K (a sequence derived from the parotid secretory protein), onto a Ti surface for obtaining coatings with notable antimicrobial effect against *Porphyromonas gingivalis* bacteria [135]; that is, a pathogen species that are closely associated with the development of biofilms and dental peri-implantitis. In addition, the GL13K-peptides coating was cyto-compatible to osteoblasts and human gingival fibroblasts.

In chapter 4, we presented the antimicrobial effects of GL13K against *Streptococcus gordonii*, a primary colonizer on the surface that provides attachment for the biofilm accretion by *P. gingivalis* [149]. However, our previous work and most in the literature

was performed to assess the bioactive effects of the antimicrobial coatings on the targeted bacteria under static or mildly shaking culture conditions. Those culture conditions do not simulate the conditions of biofilm formation and growth in the oral cavity. In the mouth the salivary flow over the coating is persistent and applied continuous shear force and supplies sustained nutrition to bacteria. This may accelerate bacteria metabolism and biofilm formation and growth. SN Sawant et al showed that the formation and growth of E.coli biofilm on surfaces in a drip flow bioreactor was twice more than that in a shaker [161]. Both CFU amount (from live bacteria) as well as carbohydrate and protein concentration (from live and dead bacteria) showed higher values on surfaces in a drip flow bioreactor than that in a shaker. This indicates that the drip flow bioreactor system will generate a greater challenge to the antimicrobial peptide coatings than the one under regular culture conditions.

Here we tested the antimicrobial effects of our GL13K coating against *Streptococcus gordonii* by using the drip flow biofilm reactor system. In this system, media was pumped onto the coating surface with a flow rate simulating the salivary flow rate.

5.3 Material and Methods

Immobilization of Peptide Coatings on Ti Surfaces

See chapter 3.3. In addition, Polymyxin was used as a positive control. CPTES silanized Ti discs were immersed in 0.1mM polymyxin in 0.5mg/ml Na_2CO_3 solution overnight

(cov-polymyxin). The successful immobilization of polymyxin on surfaces was confirmed by water contact angle test.

Bacteria Culture in the Drip Flow Bioreactor

Streptococcus gordonii ML-5 was inoculated in 2ml Bacto Todd-Hewitt broth (BD Biosciences, US) overnight. Titanium discs were UV sterilized for 10min then placed into sample holders in the four channels of the drip flow biofilm reactor (BioSurface Technologies Corp., USA) (Figure 5.1A). Four groups: eTi, cov-polymyxin, cov-GL13K and cov-GL13KR1 were placed into the four channels respectively. Three discs were used each group. The bacteria culture was conducted in 2 phases. The first phase, static phase, consisted in an overnight culture under static conditions to stabilize the biofilm (Figure 5.1B) and the second phase, dynamic phase, consisted of 48h of culturing under continuous flowing conditions (Figure 5.1C). During the static phase, 20ml of 10^7 cfu/ml *Streptococcus gordonii* dilution were loaded in each channel and the bioreactor was positioned parallel to hood floor. The bioreactor was heated with a hotplate (Corning, USA). A highly conducting metal plate made of aluminum was positioned between the hotplate and the bioreactor to evenly distribute the heat among the different channels and positions in each channel. The temperature inside the channels was adjusted to 35^0C in the inlet and monitored with a digital temperature controller (BriskHeat Corporation,USA). After the overnight static culture, the effluent tubing was unclamped and a 10^o inclined base was added underneath the bioreactor to aid the flow of the media throughout the channels during the dynamic culturing phase. A peristaltic pump (Cole

Parmer, USA) was used to force the Todd-Hewitt broth media from an Erlenmeyer flask into the bioreactor channels at a flow rate of 0.3ml/min. The flow rate was selected from the range of un-stimulated salivary flow rate--- 0.1-2 ml/min [162]. The low end of the range was selected in this experiment because the salivary flow rate surround the dental implants; i.e. in gingival sulcus is expected to be much lower than the average flow rate in the mouth. The temperature inside the channels was 29^0C in the dynamic stage. Samples were collected at the end of second phase and rinsed gently with 0.9% NaCl before characterizing biofilms formed on the different tested surfaces.

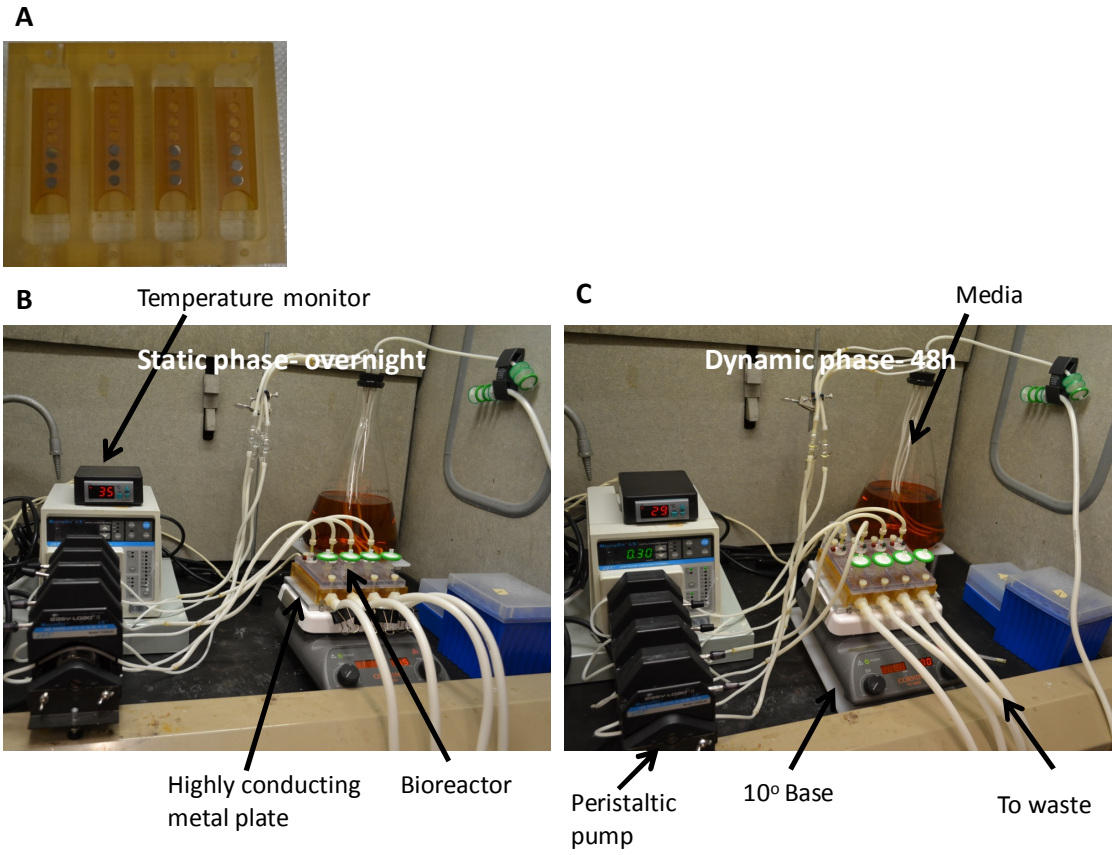

Figure 5.1 Drip flow biofilm reactor system. A) Ti samples with or without coatings were loaded in each of the four channels of the bioreactor. B) *S.gordonii* were cultured overnight under static conditions followed by C) 48h cultured with a continuous media flow rate.

Bacteria Culture in Regular Conditions

Streptococcus gordonii ML-5 was inoculated in 2ml Bacto Todd-Hewitt broth (BD Biosciences, US) overnight. Ti discs were UV sterilized for 10min then transferred into a 48-well plate. 1ml of 10^7 cfu/ml *Streptococcus gordonii* was loaded in each well. The plate was incubated in 35^0C incubator on a shaker (stovall life science, USA) with mild shake (60rpm) for the same time period as the samples in the bioreactor. Samples were collected at the end of the culture period and rinsed with 0.9% NaCl gently before characterizing biofilms formed on the different tested surfaces.

CFU and ATP Activity Assay

Samples were sonicated in 300µl 0.9% NaCl for 10 min to release bacteria adhered to the surface into solution. 100µl of the collected solution was mixed with 100µl of the BacTiter-Glo™ Microbial Cell Viability kit (Promega, US) and the luminescence was measured by microplate luminometer (BioTek, US). Another 100µl of the collected solution was used for CFU test. Briefly, 100µl of the obtained solution was diluted serially in 10, 100, 1000 and 10000 folds. 10µl of each concentration were plated on Todd-Hewitt Agar plates and incubated overnight at 35^0C. The number of CFU was counted after the incubation period.

Live and Dead Cell Staining

LIVE/DEAD® BacLight™ Bacterial Viability Kits (Invitrogen, US) was used for live and dead cell staining. Briefly, Equal volumes of green and red dyes in the kit were mixed

and diluted to concentration 0.3% in H_2O. 10µl of diluted dye was dropped and spread on each test-surface and incubated in the dark for 15 minutes. Samples were transferred to fluorescence microscope for visualization.

Scanning Electron Microscopy

The morphologies of bacteria and structural visualization of the grown biofilms on the tested surfaces were analyzed using field-emission scanning electron microscopy (JEOL 6500 FE-SEM, Japan) at 5 kV. The bacteria were primarily fixed with 2% glutaraldehyde and 0.15% alcian blue in 0.1M sodium cacodylate buffer (pH 7.4) for 1h. Then the samples were washed with 0.1M sodium cacodylate buffer for 5 min. They were secondarily fixed with 1% OsO_4 in 0.1M sodium cacodylate buffer for 1 h and washed with sodium cacodylate buffer. After fixation, samples were dehydrated with ethanol solutions at increasing concentrations (50%, 70%, 80%, 95% and 100%, 5 min each). All samples were critical-point dried (Tousimis Samdi-780, USA). They were mounted on aluminum stubs with double-sided copper tape and sputter coated with 5 nm Pt.

Statistical Analysis

Statistically significant differences among groups were assessed using one-way ANOVA Tables with LSD post-hoc tests ($p<0.05$).

5.4 Results and Discussion

Bactericidal Effect of GL13K-peptide Coatings

The bactericidal effect of the antimicrobial peptide coatings were assessed by evaluating the activity of *S.gordonii* on the tested surfaces. The commensal species *S. gordonii* was selected because it provides an attachment substrate for colonization and biofilm formation by *P. gingivalis*. Adherence of *P. gingivalis* to a surface depends on the deposition of *S. gordonii* cells on the salivary pellicle that form on the surfaces at the oral cavity [149]. CFU assay was used to test the amount of viable bacteria and Adenosine Triphosphate (ATP) assay was used to investigate the metabolic activity of bacteria.

After culture in the bioreactor the combined results showed statistically significant reduced *S.gordonii* viability and metabolic activity on cov-GL13K surfaces than on control surfaces; that is, non-coated eTi and coated with the control peptide GL13KR1 (Figure 5.2A). Coatings of immobilized polymyxin, a well-known strong antimicrobial peptide, were used as the positive control group. The cov-GL13K surfaces had significantly higher antimicrobial effects than the positive control.

Live and dead cell staining assays revealed that after 3 d of culture in the bioreactor, very thick *S. gordonii* biofilms grew on top of all the negative control surfaces (Figure 5.2B). However, the GL13K-peptide coatings significantly reduced bacterial adhesion and prevented the biofilm formation and growth. The dominance of dead bacteria on the cov-GL13K surfaces indicated the effective bactericidal effect of the antimicrobial peptides in

the coating. The bioactivity of the GL13K coating against *S.gordonii* was previously described in our work (chapter 4) in overnight culture under standard culturing conditions in an orbital shaker (60RPM). Our results here demonstrated that the GL13K-peptide coatings preserved their remarkable antimicrobial effect when tested using the simulated and more challenging culturing conditions applied with the bioreactor system. This suggests that the cov-GL13K surfaces are preferential candidates to sustain the peri-prosthetic infectious challenges if they are translated to clinical applications.

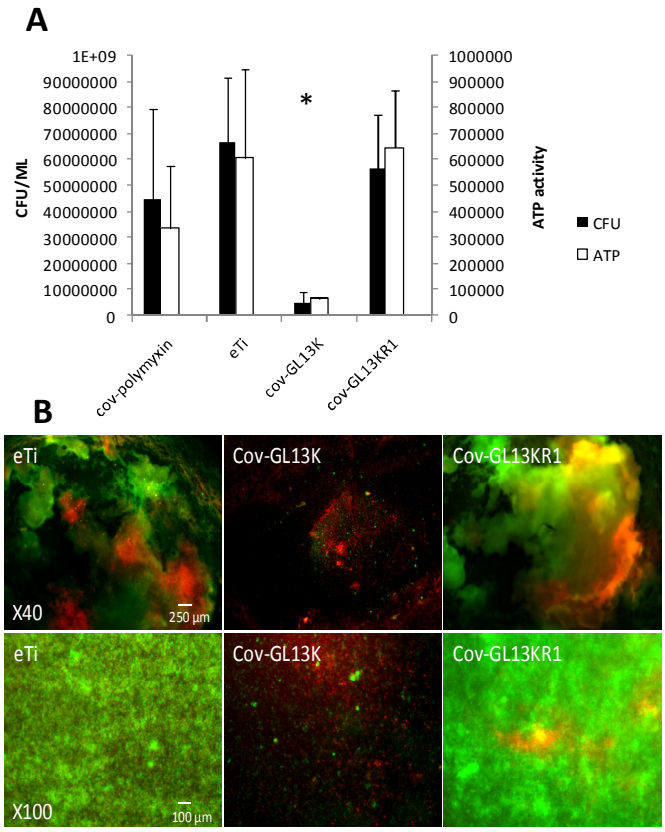

Figure 5.2 Antimicrobial effects on *S.gordonii* of tested surfaces after 3d incubation in a drip flow bioreactor A) CFU and ATP activity; and B) Live/dead cell fluorescence staining. Error bars are the standard deviation of at least three samples in each group.

Cell Wall Damage by GL13K-Peptide Coatings

SEM visualization of the *S. gordonii* biofilms formed in the bioreactor revealed the morphology, surface topography, integrity, and structure of bacteria and biofilms grown on the different tested surfaces. Low resolution SEM images confirmed the live/dead test result as very thick biofilms were detected on the control surfaces; whereas the GL13K-coated surfaces had very low numbers of bacteria adhered and biofilms did not form on them (Figure 5.3, 1st row).

Most notably, high resolution SEM pictures of the bacteria that attached to GL13K-peptide coatings in the bioreactor revealed that a number of cells had a disrupted cell wall (Figure 5.3, 2nd row). They displayed an open-shell morphology (arrow). None of the bacteria in biofilms grown in the bioreactor on the control surfaces (eTi and cov-GL13KR1) exhibited such cell wall damage. These experiments were triplicated with consistent results.

We further investigated the unique occurrence of the observed cell wall rupture by running new experiments with the same surface groups and periods of incubation (up to three days), but under mild shaking (60rpm) conditions. Under these culturing conditions, again the GL13K-peptide coatings prevented biofilm formation whereas dense biofilm was grown on all control surfaces (Figure 5.3, 3rd row). However, damage to the cell wall of the bacteria was not observed in any of the tested cov-GL13K surfaces (Figure 5.3, 4th row). Figure 5.4 showed that the cell wall rupture was already produced at the initial stages (after 6h) of initiating the dynamic phase in the drip-flow bioreactor.

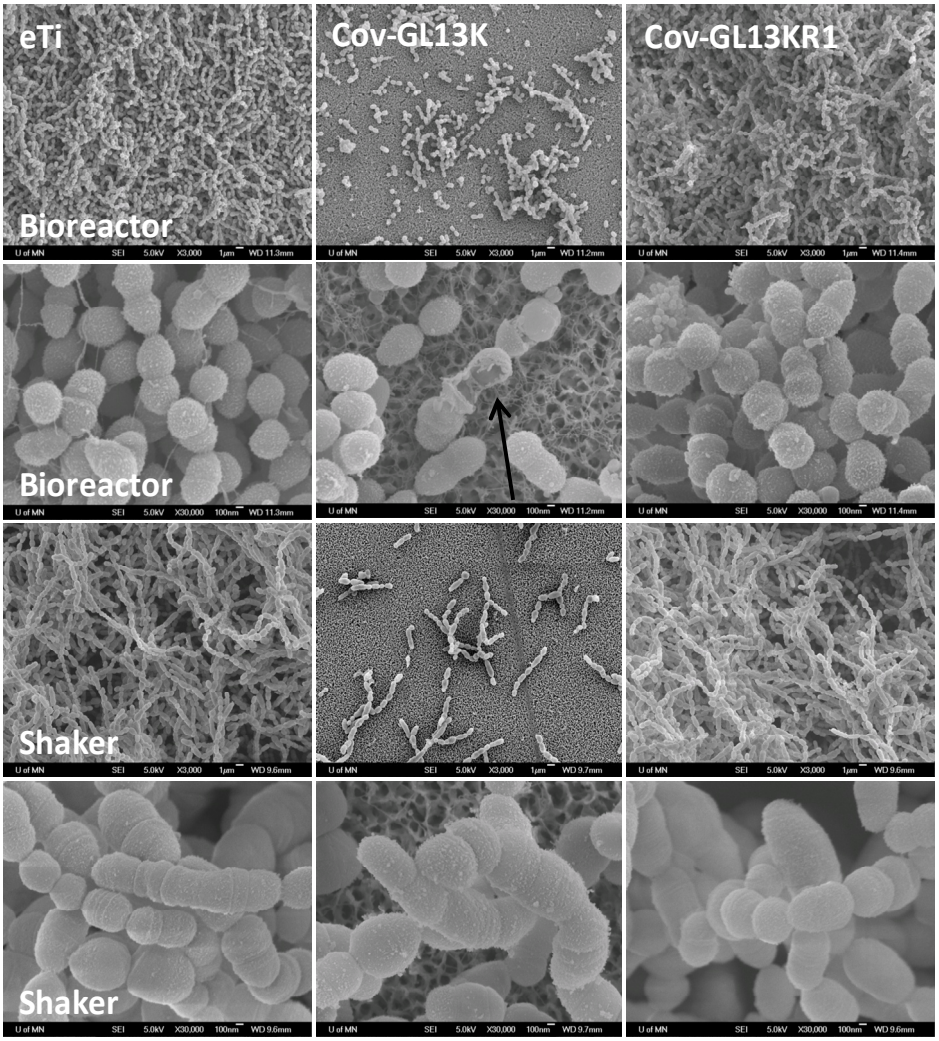

Figure 5.3 SEM images of biofilms grown on the tested surfaces, Low (1st and 3rd rows) and high magnification (2nd and 4th rows) images of surfaces tested in the drip flow bioreactor (1st and 2nd rows) and the orbital shaker (3rd and 4th rows).

All of the evidence demonstrated that the presence of the GL13K-peptide coating alone had bactericidal activity and prevented *S. gordonii* biofilm formation and growth; which has been related to its ability to interact and disrupt the bacteria membrane [156]. However, only when in combination with other specific biological factors of the

simulated oral conditions in the bioreactor system, the GL13K-peptide coating produces disruption of the cell wall in this Gram positive bacteria. In comparison with the limited supply of nutrients in the orbital shaker the sustained supply of media in the bioreactor increases the metabolic activity of the bacteria. In fact, biofilms grown on control surfaces in the bioreactor showed much thicker biofilms with smaller and more actively divided bacteria than the ones grown in the orbital shaker (Figure 5.3). Thus, an increased autolysin enzymatic activity is expected in the bioreactor which can assist the damage produced by the GL13K peptides to disrupt the cell wall. Further studies will aim to test this hypothesis.

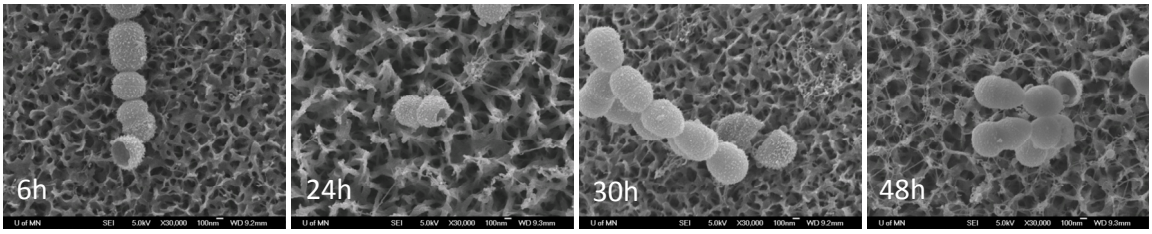

Figure 5.4 SEM showed cell wall damage on the GL13K surface after 6,24,30 and 48 hr of continuous flow culture. Cell wall rupture was formed at the very beginning of flow in stage (6h).

A more detailed look at the morphological features of the disrupted bacteria supports this hypothesis. Figure 5.5 presents high resolution SEM images of multiple bacteria on GL13K coatings with a disrupted wall. Bacteria with two general types of disrupted-wall morphologies were identified: Rupture of the bacteria cell wall with (dashed arrow) or without (solid arrow) the protoplast (Figure 5.5A). Figure 5.5B, D, E showed bacteria with burst cell walls that did not retain their protoplast. This left empty shell-like wall structures of bacteria. Figure 5.5F and G showed splitting of the cell wall that led to

exposed bacteria protoplast. The cracking of the cells commonly occurred in their septum and/or polar area (Figure 5.5C and E, arrow), which are the areas where enzymatic activity is enhanced to initiate the process of severing the cell during the active phases of bacterial division [163]. After enzymatic digestion of the cell wall, the protoplast can be stabilized in an osmotic condition in which cell lysis does not occur. We collected our samples in isotonic solution (0.9% NaCl) so that the morphology of the protoplast was maintained. However, it is noteworthy that the cell membrane in bacteria visualized in Figure 5.5.F and Figure 5.5.G showed localized morphological disturbances (arrows) that may indicate their compromised function.

It is well accepted that antimicrobial peptides base their activity on inducing pore formation on the bacteria membrane through different proposed mechanisms [96]. Our collaborators also concluded that the GL13K peptides in solution can optimally interact with an amphiphilic model bi-layer membrane and hence compromise its integrity [164]. However, Gram positive bacteria possess a thick peptidoglycan cell wall, which protects the cell and provides shape and rigidity to the cell. It has been assessed that the wall of the Gram positive bacteria delays the action of the antimicrobial peptides by trapping them inside the cell wall and thus retarding their interactions with the phospholipid membrane [165]. Here we have shown for the first time that under specific conditions an

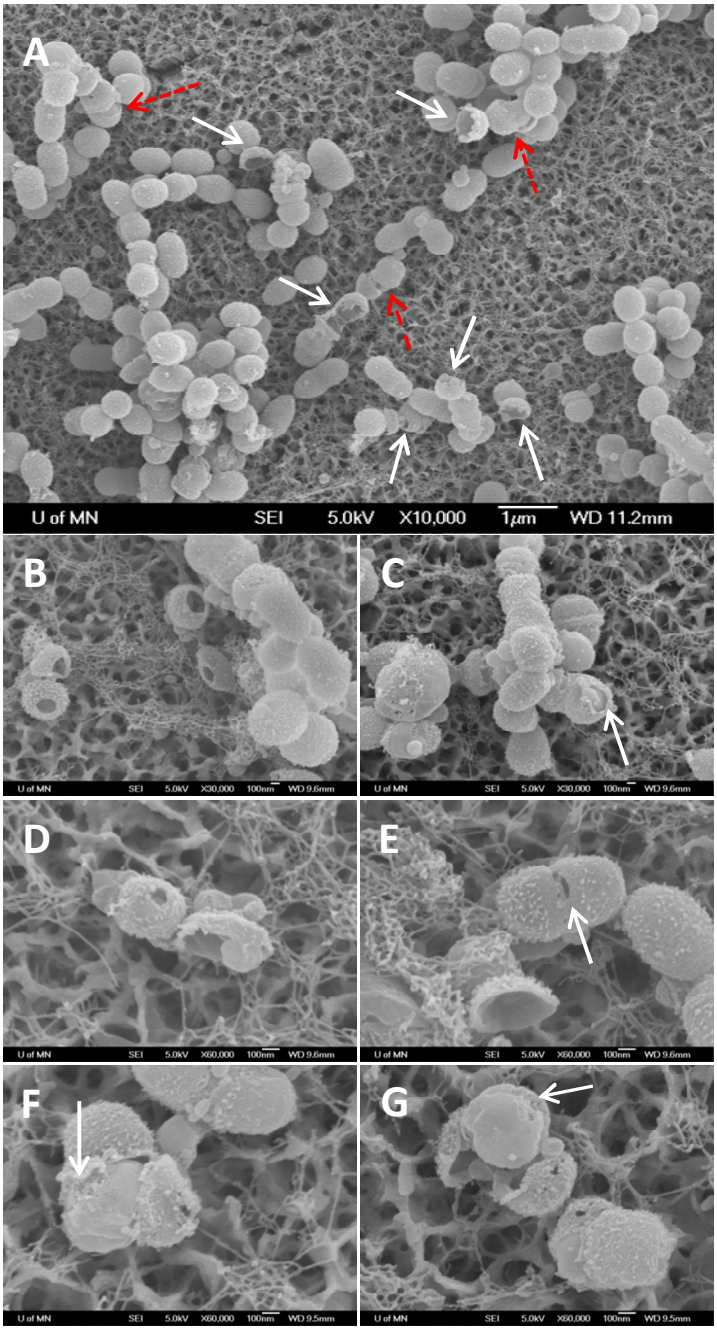

Figure 5.5 SEM pictures show the disruption of *Streptococcus gordonii* cell wall on GL13K surface after a 3d bioreactor culture. A) displayed a number of ruptured cell walls with (dashed arrow) or without (solid arrow) protoplast. B)--E) were the high magnification of the rupture of cell wall; F) and G) showed the cracking of cell wall with the popping out protoplast.

antimicrobial coating made of GL13K-peptides damaged the cell wall of Gram positive bacteria assisting to its disruption and hence suggesting an enhanced and faster exposure of the cell membrane to the peptides in these antimicrobial coatings. One of the possible literature explanations for antimicrobial peptides inducing cell wall damage is that the cell wall disruption is induced by the molecular interaction between GL13K and the wall teichoic acid (WTA). WTA has a molecular structure that is covalently linked to peptidoglycans. WTA contains repeating units of ribitol or glycerol phosphate that can be modified by glyosyl substituents or D-alanine esters. WTA obtains strong affinity for antimicrobial peptides due to their highly anionic properties [166]. Koprivnjak T el al showed that in the absence of WTA, *S.aureus* is 100-fold more resistant to antimicrobial peptides [167]. Moreover, WTA plays an active role in the regulation of the autolytic activity of Gram positive bacteria [166, 168, 169]. Biswas R et al demonstrated the mechanism by which WTA regulates cell wall autolysis activity of the cell [170]. The autolysin activity is known to decline at lower pH. Then, WTA participates in the regulation of the autolysin activity as it has a substantial contribution to the proton-binding capacity of the cell wall. Under normal conditions, the negatively charged WTA phosphate groups trap protons in the cell wall, creating an acidic environment that keeps autolysin activity at a low level (Figure 5.6A). The cationic antimicrobial peptides can strongly interact with the phosphate groups of the WTA leading to the release of protons. The resulting increased local pH activates autolysin, which would weaken the cell wall by breaking down glycosidic bonds and peptide crosslinks (Figure 5.6B). The weakening

of the cell wall through this mechanism would further lead to cell wall rupture when assisted by other factors in the bioreactor system as discussed earlier.

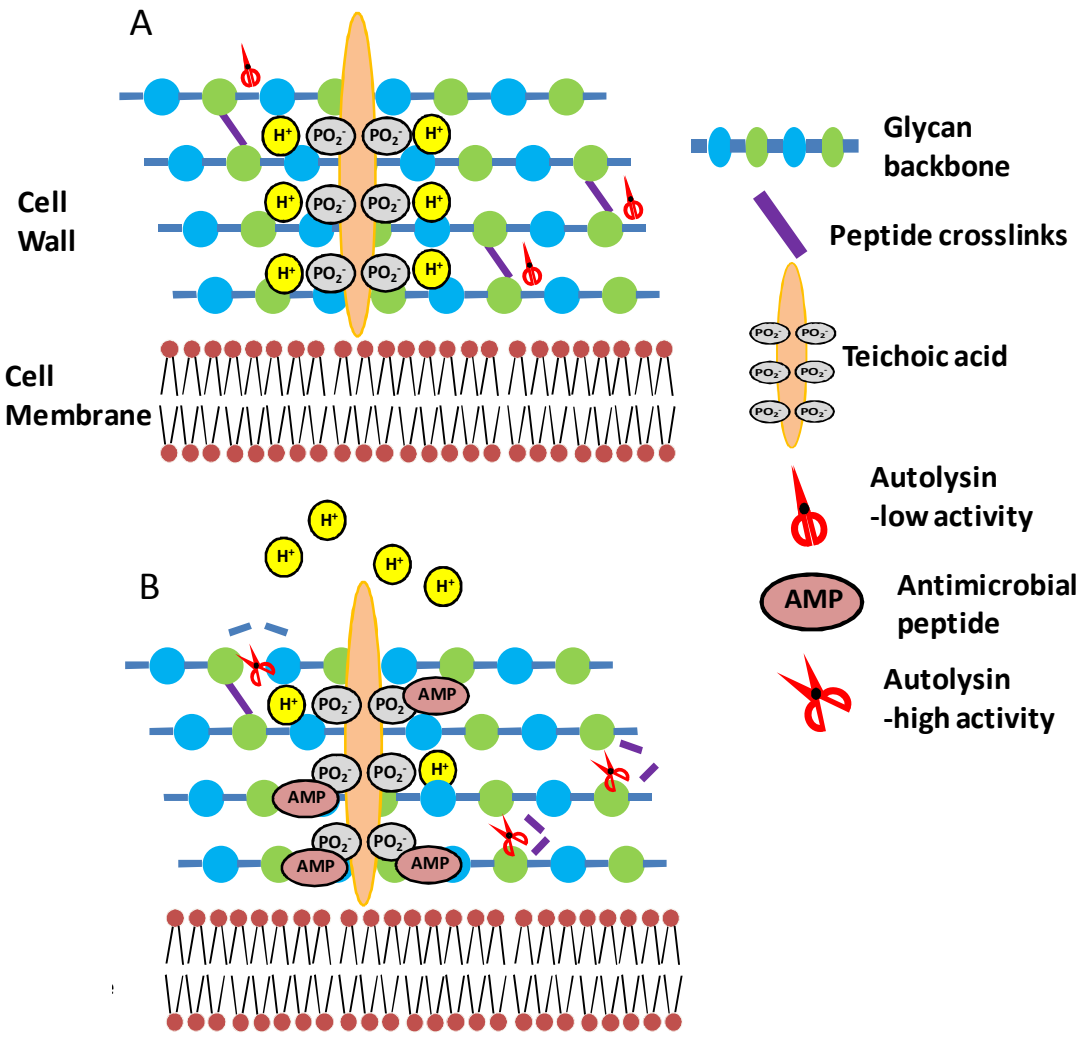

Figure 5.6 Schematics of the hypothesized mechanism by which antimicrobial peptides weaken the bacteria wall via electrostatic bonding to teichoic acid molecules.

It is worth noting that GL13KR1 sequences which share the same charge with GL13K did not present cell wall damage, indicating the molecular interaction between WTA and antimicrobial peptides relies on more than just charge attraction. Our previous work showed that GL13K and GL13KR1 on the coatings had different secondary structures,

which influenced their antimicrobial activity. Here we further speculate that the preferential β-sheet structure in the GL13K peptides optimizes its interaction with WTA, leading to a maximum occupation of the phosphate groups of the WTA. Further experiments are needed to validate this hypothesis.

Conflicting recent unpublished results from the lab of our collaborator, Professor Sven Gorr, with D-GL13K peptides --D-peptide version of GL13K, showed that D-GL13K peptides formed β-sheet structures at lower pH than L-GL13K. This implies that D-GL13K, which has the mirror structural image of GL13K, has an even higher tendency to form this favourable structure for killing bacteria than GL13K. However, D-GL13K peptides rescue the autolysis of *S. gordonii* induced by triton instead of enhancing bacteria autolysis. Therefore, further experiments are needed to validate the functionality of the interactions between teichoic acid and GL13K peptides in the coatings to induce cell wall damage.

5.5 Conclusion

The antimicrobial peptide coating made of immobilized GL13K peptides had excellent antimicrobial activity when exposed to *S. gordonii* cultures in a drip flow biofilm reactor system. These culturing conditions in combination with the activity of the GL13K-peptide coatings result in the cell wall damage.

Chapter 6

Conclusions

We have successfully developed a simple route to covalently co-immobilize two different oligopeptides on Ti surfaces. The obtained peptide coatings showed strong mechanical stability as well as enhanced osteoblast adhesion.

We also successfully covalently bonded antimicrobial peptide GL13K coatings on Ti surface. The obtained coatings are resistant to simulated mechanical, hydrolytic, and proteolytic clinical challenges with sustained bioactivity after cycles of body fluid incubation and autoclaving.

The antimicrobial peptide GL13K coating prevented biofilm formation by killing *S.gordonii* at their early developmental stage and the antimicrobial effect of GL13K-peptides coating depended on the prevalent β sheet secondary structures formed by the tethered GL13K peptides.

Cell wall damage of *S.gordonii* was observed on GL13K-coated surface when cultured under dynamic conditions in a drip flow bioreactor. The effect of the GL13K peptides assisted by the enhanced autolytic activity of *S.gordonii* when cultured under this dynamic condition may be responsible for the damage of the cell wall and its final disruption, which might be mediated by the molecular interactions between GL13K peptides in the coating and teichoic acid molecules in the cell wall.

Future works include investigating the antimicrobial mechanism of GL13K-peptide coating, assessing the interactions between the peptides and teichoic acid molecules resulting in enhanced autolysis activity of the bacteria, evaluating the in vivo

antimicrobial effect of GL13K coating, and developing a multifunctional coating with both bone-regenerative and antimicrobial bioactivities.

Bibliography

[1] Brunski JB. Classes of materials used in medicine. Metals. In: Rutner B, Hoffman A, Schoen F, Lemons J, editors. Biomaterials science, an introduction to materials in medicine. San Diego: Academic Press; 1996.
[2] Ratner BD. A perspective on titanium biocompatibility. In: Brunette DM, Tengvall P, Textor M, Thomsen P, editors. Titanium in medicine: Material science, surface science, engineering, biological responses and medical applications. Berlin Heidelberg: Springer-Verlag; 2001. p. 1-12.
[3] Dabdoub SM, Tsigarida AA, Kumar PS. Patient-specific Analysis of Periodontal and Peri-implant Microbiomes. J Dent Res. 2013;92:168s-75s.
[4] Group MR. Annual Industry Report. Implant dentistry. 2000;9:192-4.
[5] Lindquist LW, Carlsson GE, Jemt T. A prospective 15-year follow-up study of mandibular fixed prostheses supported by osseointegrated implants - Clinical results and marginal bone loss. Clin Oral Implan Res. 1996;7:329-36.
[6] Schwartz-Arad D, Kidron N, Dolev E. A long-term study of implants supporting overdentures as a model for implant success. J Periodontol. 2005;76:1431-5.
[7] Raikar GN, Gregory JC, Ong JL, Lucas LC, Lemons JE, Kawahara D, et al. Surface Characterization of Titanium Implants. J Vac Sci Technol A. 1995;13:2633-7.
[8] Williams DF. Titanium for medical applications. In: Brunette DM, Tengvall P, Textor M, Thomsen P, editors. Titanium in medicine: Material science, surface science, engineering, biological responses and medical applications Berlin Heidelberg: Springer-Verlag; 2001. p. 13-24.
[9] Kasemo B. Biological surface science. Surf Sci. 2002;500:656-77.
[10] Castner DG, Ratner BD. Biomedical surface science: Foundations to frontiers. Surf Sci. 2002;500:28-60.
[11] Elmengaard B, Bechtold JE, Soballe K. In vivo study of the effect of RGD treatment on bone ongrowth on press-fit titanium alloy implants. Biomaterials. 2005;26:3521-6.
[12] Wang HL, Ormianer Z, Palti A, Perel ML, Trisi P, Sammartino G. Consensus conference on immediate loading: the single tooth and partial edentulous areas. Implant dentistry. 2006;15:324-33.
[13] Puleo DA, Nanci A. Understanding and controlling the bone-implant interface. Biomaterials. 1999;20:2311-21.
[14] Zitzmann NU, Berglundh T. Definition and prevalence of peri-implant diseases. Journal of clinical periodontology. 2008;35:286-91.
[15] Gristina AG. Biomaterial-Centered Infection - Microbial Adhesion Versus Tissue Integration. Science. 1987;237:1588-95.
[16] Neoh KG, Hu X, Zheng D, Kang ET. Balancing osteoblast functions and bacterial adhesion on functionalized titanium surfaces. Biomaterials. 2012;33:2813-22.
[17] Hetrick EM, Schoenfisch MH. Reducing implant-related infections: active release strategies. Chem Soc Rev. 2006;35:780-9.

[18] Hori K, Matsumoto S. Bacterial adhesion: From mechanism to control. Biochem Eng J. 2010;48:424-34.
[19] Katsikogianni M, Missirlis YF. Concise review of mechanisms of bacterial adhesion to biomaterials and of techniques used in estimating bacteria-material interactions. Eur Cell Mater. 2004;8:37-57.
[20] Miorner H, Myhre E, Bjorck L, Kronvall G. Effect of specific binding of human albumin, fibrinogen, and immunoglobulin G on surface characteristics of bacterial strains as revealed by partition experiments in polymer phase systems. Infect Immun. 1980;29:879-85.
[21] Xiao SJ, Textor M, Spencer ND, Wieland M, Keller B, Sigrist H. Immobilization of the cell-adhesive peptide Arg-Gly-Asp-Cys (RGDC) on titanium surfaces by covalent chemical attachment. J Mater Sci-Mater M. 1997;8:867-72.
[22] Ahmad N, Saad N. Effects of antibiotics on dental implants: a review. Journal of clinical medicine research. 2012;4:1-6.
[23] Schliephake H, Scharnweber D. Chemical and biological functionalization of titanium for dental implants. J Mater Chem. 2008;18:2404-14.
[24] Le Guehennec L, Soueidan A, Layrolle P, Amouriq Y. Surface treatments of titanium dental implants for rapid osseointegration. Dent Mater. 2007;23:844-54.
[25] Klokkevold PR, Johnson P, Dadgostari S, Caputo A, Davies JE, Nishimura RD. Early endosseous integration enhanced by dual acid etching of titanium: a torque removal study in the rabbit. Clin Oral Implan Res. 2001;12:350-7.
[26] Ivanoff CJ, Hallgren C, Widmark G, Sennerby L, Wennerberg A. Histologic evaluation of the bone integration of TiO2 blasted and turned titanium microimplants in humans. Clin Oral Implan Res. 2001;12:128-34.
[27] Sutter F, Schroeder A, Buser DA. The new concept of ITI hollowcylinder and hollowscrew implants. Part 1. Engineering and design. Int J Oral Maxillofac Implants. 1988:161–72.
[28] Sul YT, Johansson CB, Petronis S, Krozer A, Jeong Y, Wennerberg A, et al. Characteristics of the surface oxides on turned and electrochemically oxidized pure titanium implants up to dielectric breakdown: the oxide thickness, micropore configurations, surface roughness, crystal structure and chemical composition. Biomaterials. 2002;23:491-501.
[29] Buser D, Nydegger T, Hirt HP, Cochran DL, Nolte LP. Removal torque values of titanium implants in the maxilla of miniature pigs. The International journal of oral & maxillofacial implants. 1998;13:611-9.
[30] Borsari V, Fini M, Giavaresi G, Rimondini L, Consolo U, Chiusoli L, et al. Osteointegration of titanium and hydroxyapatite rough surfaces in healthy and compromised cortical and trabecular bone: In vivo comparative study on young, aged, and estrogen-deficient sheep. J Orthop Res. 2007;25:1250-60.
[31] Ronold HJ, Lyngstadaas SP, Ellingsen JE. Analysing the optimal value for titanium implant roughness in bone attachment using a tensile test. Biomaterials. 2003;24:4559-64.

[32] Aparicio C, Padros A, Gil FJ. In vivo evaluation of micro-rough and bioactive titanium dental implants using histometry and pull-out tests. Journal of the mechanical behavior of biomedical materials. 2011;4:1672-82.
[33] Roessler S, Born R, Scharnweber D, Worch H, Sewing A, Dard M. Biomimetic coatings functionalized with adhesion peptides for dental implants. J Mater Sci-Mater M. 2001;12:871-7.
[34] Jahoda D, Nyc O, Pokorny D, Landor I, Sosna A. [Antibiotic treatment for prevention of infectious complications in joint replacement]. Acta chirurgiae orthopaedicae et traumatologiae Cechoslovaca. 2006;73:108-14.
[35] Kazemzadeh-Narbat M, Kindrachuk J, Duan K, Jenssen H, Hancock REW, Wang RZ. Antimicrobial peptides on calcium phosphate-coated titanium for the prevention of implant-associated infections. Biomaterials. 2010;31:9519-26.
[36] García AJ. Surface modification of biomaterials In: Atala A, Lanza R, Thomson JA, Nerem R, editors. Principles of Regenerative Medicine (Second Edition) San Diego: Elsevier/Academic Press; 2011. p. 663-73.
[37] Hall J, Sorensen RG, Wozney JM, Wikesjo UM. Bone formation at rhBMP-2-coated titanium implants in the rat ectopic model. Journal of clinical periodontology. 2007;34:444-51.
[38] Bekos EJ, Ranieri JP, Aebischer P, Gardella JA, Bright FV. Structural-Changes of Bovine Serum-Albumin Upon Adsorption to Modified Fluoropolymer Substrates Used for Neural Cell Attachment Studies. Langmuir. 1995;11:984-9.
[39] Tebbe D, Thull R, Gbureck U. Influence of spacer length on heparin coupling efficiency and fibrinogen adsorption of modified titanium surfaces. Biomed Eng Online. 2007;6:-.
[40] Nanci A, Wuest JD, Peru L, Brunet P, Sharma V, Zalzal S, et al. Chemical modification of titanium surfaces for covalent attachment of biological molecules. J Biomed Mater Res. 1998;40:324-35.
[41] Nadkarni VD, Pervin A, Linhardt RJ. Directional Immobilization of Heparin onto Beaded Supports. Anal Biochem. 1994;222:59-67.
[42] Puleo DA, Kissling RA, Sheu MS. A technique to immobilize bioactive proteins, including bone morphogenetic protein-4 (BMP-4), on titanium alloy. Biomaterials. 2002;23:2079-87.
[43] Rezania A, Johnson R, Lefkow AR, Healy KE. Bioactivation of metal oxide surfaces. 1. Surface characterization and cell response. Langmuir. 1999;15:6931-9.
[44] Kim SE, Song SH, Yun YP, Choi BJ, Kwon IK, Bae MS, et al. The effect of immobilization of heparin and bone morphogenic protein-2 (BMP-2) to titanium surfaces on inflammation and osteoblast function. Biomaterials. 2011;32:366-73.
[45] Tan GX, Zhang L, Ning CY, Liu XJ, Liao JW. Preparation and characterization of APTES films on modification titanium by SAMs. Thin Solid Films. 2011;519:4997-5001.
[46] Lloyd-Williams P, Albericio F, Giralt E. Chemical approaches to the synthesis of peptides and proteins (new directions in organic & biological chemistry). CRC-Press. 1997.

[47] Puleo DA. Biochemical surface modification of Co-Cr-Mo. Biomaterials. 1996;17:217-22.
[48] Bierbaum S, Hempel U, Geissler U, Hanke T, Scharnweber D, Wenzel KW, et al. Modification of Ti6Al4V surfaces using collagen I, III, and fibronectin. II. Influence on osteoblast responses. J Biomed Mater Res A. 2003;67A:431-8.
[49] Ku Y, Chung CP, Jang JH. The effect of the surface modification of titanium using a recombinant fragment of fibronectin and vitronectin on cell behavior. Biomaterials. 2005;26:5153-7.
[50] Steele JG, Johnson G, Mcfarland C, Dalton BA, Gengenbach TR, Chatelier RC, et al. Roles of Serum Vitronectin and Fibronectin in Initial Attachment of Human Vein Endothelial-Cells and Dermal Fibroblasts on Oxygen-Containing and Nitrogen-Containing Surfaces Made by Radiofrequency Plasmas. J Biomat Sci-Polym E. 1994;6:511-32.
[51] Carson AE, Barker TH. Emerging concepts in engineering extracellular matrix variants for directing cell phenotype. Regen Med. 2009;4:593-600.
[52] Ruoslahti E. RGD and other recognition sequences for integrins. Annu Rev Cell Dev Bi. 1996;12:697-715.
[53] Pierschbacher MD, Ruoslahti E. Cell Attachment Activity of Fibronectin Can Be Duplicated by Small Synthetic Fragments of the Molecule. Nature. 1984;309:30-3.
[54] de Jonge LT, Leeuwenburgh SCG, Wolke JGC, Jansen JA. Organic-inorganic surface modifications for titanium implant surfaces. Pharm Res-Dordr. 2008;25:2357-69.
[55] Morra M, Cassinelli C, Cascardo G, Cahalan P, Cahalan L, Fini M, et al. Surface engineering of titanium by collagen immobilization. Surface characterization and in vitro and in vivo studies. Biomaterials. 2003;24:4639-54.
[56] Wen HB, DeWijn JR, Liu Q, DeGroot K, Cui FZ. A simple method to prepare calcium phosphate coatings on Ti6Al4V. J Mater Sci-Mater M. 1997;8:765-70.
[57] Pegueroles M, Aguirre A, Engel E, Pavon G, Gil FJ, Planell JA, et al. Effect of blasting treatment and Fn coating on MG63 adhesion and differentiation on titanium: a gene expression study using real-time RT-PCR. J Mater Sci-Mater M. 2011;22:617-27.
[58] Seol YJ, Park YJ, Lee SC, Kim KH, Lee JY, Kim TI, et al. Enhanced osteogenic promotion around dental implants with synthetic binding motif mimicking bone morphogenetic protein (BMP)-2. J Biomed Mater Res A. 2006;77A:599-607.
[59] Collier JH, Segura T. Evolving the use of peptides as components of biomaterials. Biomaterials. 2011;32:4198-204.
[60] Coin I, Beyermann M, Bienert M. Solid-phase peptide synthesis: from standard procedures to the synthesis of difficult sequences. Nat Protoc. 2007;2:3247-56.
[61] Itoh D, Yoneda S, Kuroda S, Kondo H, Umezawa A, Ohya K, et al. Enhancement of osteogenesis on hydroxyapatite surface coated with synthetic peptide (EEEEEEEPRGDT) in vitro. J Biomed Mater Res. 2002;62:292-8.
[62] Grzesik WJ, Robey PG. Bone-Matrix Rgd Glycoproteins - Immunolocalization and Interaction with Human Primary Osteoblastic Bone-Cells in-Vitro. J Bone Miner Res. 1994;9:487-96.

[63] Kao WJ, Lee D, Schense JC, Hubbell TA. Fibronectin modulates macrophage adhesion and FBGC formation: The pole of RGD, PHSRN, and PRRARV domains. J Biomed Mater Res. 2001;55:79-88.
[64] Feng YZ, Mrksich M. The synergy peptide PHSRN and the adhesion peptide RGD mediate cell adhesion through a common mechanism. Biochemistry-Us. 2004;43:15811-21.
[65] Benoit DSW, Anseth KS. The effect on osteoblast function of colocalized RGD and PHSRN epitopes on PEG surfaces. Biomaterials. 2005;26:5209-20.
[66] Kokkoli E, Ochsenhirt SE, Tirrell M. Collective and single-molecule interactions of alpha(5)beta(1) integrins. Langmuir. 2004;20:2397-404.
[67] Mardilovich A, Kokkoli E. Biomimetic peptide-amphiphiles for functional biomaterials: The role of GRGDSP and PHSRN. Biomacromolecules. 2004;5:950-7.
[68] Aucoin L, Griffith CM, Pleizier G, Deslandes Y, Sheardown H. Interactions of corneal epithelial cells and surfaces modified with cell adhesion peptide combinations. J Biomat Sci-Polym E. 2002;13:447-62.
[69] Popat KC, Eltgroth M, LaTempa TJ, Grimes CA, Desai TA. Decreased Staphylococcus epidermis adhesion and increased osteoblast functionality on antibiotic-loaded titania nanotubes. Biomaterials. 2007;28:4880-8.
[70] Lucke M, Schmidmaier G, Sadoni S, Wildemann B, Schiller R, Haas NP, et al. Gentamicin coating of metallic implants reduces implant-related osteomyelitis in rats. Bone. 2003;32:521-31.
[71] Alt V, Bitschnau A, Osterling J, Sewing A, Meyer C, Kraus R, et al. The effects of combined gentamicin-hydroxyapatite coating for cementless joint prostheses on the reduction of infection rates in a rabbit infection prophylaxis model. Biomaterials. 2006;27:4627-34.
[72] Radin S, Campbell JT, Ducheyne P, Cuckler JM. Calcium phosphate ceramic coatings as carriers of vancomycin. Biomaterials. 1997;18:777-82.
[73] Yamamura K, Iwata H, Yotsuyanagi T. Synthesis of Antibiotic-Loaded Hydroxyapatite Beads and Invitro Drug Release Testing. J Biomed Mater Res. 1992;26:1053-64.
[74] Kim WH, Lee SB, Oh KT, Moon SK, Kim KM, Kim KN. The release behavior of CHX from polymer-coated titanium surfaces. Surf Interface Anal. 2008;40:202-4.
[75] Chen W, Liu Y, Courtney HS, Bettenga M, Agrawal CM, Bumgardner JD, et al. In vitro anti-bacterial and biological properties of magnetron co-sputtered silver-containing hydroxyapatite coating. Biomaterials. 2006;27:5512-7.
[76] Harris LG, Tosatti S, Wieland M, Textor M, Richards RG. Staphylococcus aureus adhesion to titanium oxide surfaces coated with non-functionalized and peptide-functionalized poly(L-lysine)-grafted-poly(ethylene glycol) copolymers. Biomaterials. 2004;25:4135-48.
[77] Chua PH, Neoh KG, Kang ET, Wang W. Surface functionalization of titanium with hyaluronic acid/chitosan polyelectrolyte multilayers and RGD for promoting osteoblast functions and inhibiting bacterial adhesion. Biomaterials. 2008;29:1412-21.
[78] Antoci V, Jr., Adams CS, Parvizi J, Davidson HM, Composto RJ, Freeman TA, et al. The inhibition of Staphylococcus epidermidis biofilm formation by vancomycin-modified

titanium alloy and implications for the treatment of periprosthetic infection. Biomaterials. 2008;29:4684-90.
[79] Antoci V, Adams CS, Hickok NJ, Shapiro IM, Parvizi J. Vancomycin bound to Ti rods reduces periprosthetic infection - Preliminary study. Clin Orthop Relat R. 2007:88-95.
[80] Antoci V, Adams CS, Parvizi J, Ducheyne P, Shapiro IM, Hickok NJ. Covalently attached vancomycin provides a nanoscale antibacterial surface. Clin Orthop Relat R. 2007:81-7.
[81] Antoci V, King SB, Jose B, Parvizi J, Zeiger AR, Wickstrom E, et al. Vancomycin covalently bonded to titanium alloy prevents bacterial colonization. J Orthop Res. 2007;25:858-66.
[82] Weber FA, Lautenbach EEG. Revision of Infected Total Hip-Arthroplasty. Clin Orthop Relat R. 1986:108-15.
[83] Tunney MM, Ramage G, Patrick S, Nixon JR, Murphy PG, Gorman SP. Antimicrobial susceptibility of bacteria isolated from orthopedic implants following revision hip surgery. Antimicrob Agents Ch. 1998;42:3002-5.
[84] Antoci V, Adams CS, Hickok NJ, Shapiro IM, Parvizi J. Antibiotics for local delivery systems cause skeletal cell toxicity in vitro. Clin Orthop Relat R. 2007:200-6.
[85] Ince A, Schutze N, Hendrich C, Jakob F, Eulert J, Lohr JF. Effect of polyhexanide and gentamycin on human osteoblasts and endothelial cells. Swiss medical weekly. 2007;137:139-45.
[86] Ince A, Schutze N, Hendrich C, Thull R, Eulert J, Lohr JF. In vitro investigation of orthopedic titanium-coated and brushite-coated surfaces using human osteoblasts in the presence of gentamycin. The Journal of arthroplasty. 2008;23:762-71.
[87] Naal FD, Salzmann GM, von Knoch F, Tuebel J, Diehl P, Gradinger R, et al. The effects of clindamycin on human osteoblasts in vitro. Archives of orthopaedic and trauma surgery. 2008;128:317-23.
[88] Salzmann GM, Naal FD, von Knoch F, Tuebel J, Gradinger R, Imhoff AB, et al. Effects of cefuroxime on human osteoblasts in vitro. J Biomed Mater Res A. 2007;82:462-8.
[89] Gorr SU, Abdolhosseini M. Antimicrobial peptides and periodontal disease. Journal of clinical periodontology. 2011;38:126-41.
[90] Krisanaprakornkit S, Khongkhunthian S. The Role of Antimicrobial Peptides in Periodontal Disease. Public Health 21st C. 2010:73-103.
[91] Hancock REW, Sahl HG. Antimicrobial and host-defense peptides as new anti-infective therapeutic strategies. Nat Biotechnol. 2006;24:1551-7.
[92] Gao GZ, Lange D, Hilpert K, Kindrachuk J, Zou YQ, Cheng JTJ, et al. The biocompatibility and biofilm resistance of implant coatings based on hydrophilic polymer brushes conjugated with antimicrobial peptides. Biomaterials. 2011;32:3899-909.
[93] Holmberg KV, Abdolhosseini M, Chen X, Li Y, Gorr S-U, Aparicio C. Bio-inspired stable antimicrobial peptide coatings for dental applications. Acta biomaterialia. 2013;accepted.
[94] Kazemzadeh-Narbat M, Lai BFL, Ding CF, Kizhakkedathu JN, Hancock REW, Wang RZ. Multilayered coating on titanium for controlled release of antimicrobial

peptides for the prevention of implant-associated infections. Biomaterials. 2013;34:5969-77.
[95] Bumgardner JD, Adatrow P, Haggard WO, Norowski PA. Emerging Antibacterial Biomaterial Strategies for the Prevention of Pen-implant Inflammatory Diseases. Int J Oral Max Impl. 2011;26:553-60.
[96] Brogden KA. Antimicrobial peptides: Pore formers or metabolic inhibitors in bacteria? Nat Rev Microbiol. 2005;3:238-50.
[97] Puleo DA, Nanci A. Understanding and controlling the bone-implant interface. Biomaterials. 1999;20:2311-21.
[98] Campoccia D, Montanaro L, Arciola CR. The significance of infection related to orthopedic devices and issues of antibiotic resistance. Biomaterials. 2006;27:2331-9.
[99] Beutner R, Michael J, Schwenzer B, Scharnweber D. Biological nano-functionalization of titanium-based biomaterial surfaces: a flexible toolbox. J R Soc Interface. 2010;7:S93-S105.
[100] Schmidmaier G, Wildemann B, Cromme F, Kandziora F, Haas NP, Raschke M. Bone morphogenetic protein-2 coating of titanium implants increases biomechanical strength and accelerates bone remodeling in fracture treatment: A biomechanical and histological study in rats. Bone. 2002;30:816-22.
[101] Xiang W, Baolin L, Yan J, Yang X. The Effect of Bone Morphogenetic Protein on Osseointegration of Titanium Implants. J Oral Maxil Surg. 1993;51:647-51.
[102] Sverzut AT, Crippa GE, Morra M, de Oliveira PT, Beloti MM, Rosa AL. Effects of type I collagen coating on titanium osseointegration: histomorphometric, cellular and molecular analyses. Biomed Mater. 2012;7.
[103] Beutner R, Michael J, Forster A, Schwenzer B, Scharnweber D. Immobilization of oligonucleotides on titanium based materials by partial incorporation in anodic oxide layers. Biomaterials. 2009;30:2774-81.
[104] Michael J, Beutner R, Hempel U, Scharnweber D, Worch H, Schwenzer B. Surface modification of titanium-based alloys with bioactive molecules using electrochemically fixed nucleic acids. J Biomed Mater Res B. 2007;80B:146-55.
[105] Rammelt S, Illert T, Bierbaum S, Scharnweber D, Zwipp H, Schneiders W. Coating of titanium implants with collagen, RGD peptide and chondroitin sulfate. Biomaterials. 2006;27:5561-71.
[106] Kroese-Deutman HC, van den Dolder J, Spauwen PH, Jansen JA. Influence of RGD-loaded titanium implants on bone formation in vivo. Tissue engineering. 2005;11:1867-75.
[107] Seo HS, Ko YM, Shim JW, Lim YK, Kook JK, Cho DL, et al. Characterization of bioactive RGD peptide immobilized onto poly(acrylic acid) thin films by plasma polymerization. Applied Surface Science. 2010;257:596-602.
[108] Petrie TA, Raynor JE, Dumbauld DW, Lee TT, Jagtap S, Templeman KL, et al. Multivalent Integrin-Specific Ligands Enhance Tissue Healing and Biomaterial Integration. Science Translational Medicine. 2010;2.
[109] Zhao LZ, Chu PK, Zhang YM, Wu ZF. Antibacterial Coatings on Titanium Implants. J Biomed Mater Res B. 2009;91B:470-80.

[110] Chen X, Li Y, Aparicio C. Biofunctional Coatings for Dental Implants. In: Nazarpour S, Chaker M, editors. Thin Films and Coatings in Biology Biological and Medical Physics -Biomedical Engineering Series: Springer-Verlag; 2013.
[111] Lee DW, Yun YP, Park K, Kim SE. Gentamicin and bone morphogenic protein-2 (BMP-2)-delivering heparinized-titanium implant with enhanced antibacterial activity and osteointegration. Bone. 2012;50:974-82.
[112] Mani G, Johnson DM, Marton D, Dougherty VL, Feldman MD, Patel D, et al. Stability of self-assembled monolayers on titanium and gold. Langmuir. 2008;24:6774-84.
[113] Auernheimer J, Zukowski D, Dahmen C, Kantlehner M, Enderle A, Goodman SL, et al. Titanium implant materials with improved riocompatibility through coating with phosphonate-anchored cyclic RGD peptides. Chembiochem. 2005;6:2034-40.
[114] Ochsenhirt SE, Kokkoli E, McCarthy JB, Tirrell M. Effect of RGD secondary structure and the synergy site PHSRN on cell adhesion, spreading and specific integrin engagement. Biomaterials. 2006;27:3863-74.
[115] Schmidt DR, Kao WJ. Monocyte activation in response to polyethylene glycol hydrogels grafted with RGD and PHSRN separated by interpositional spacers of various lengths. J Biomed Mater Res A. 2007;83A:617-25.
[116] Petrie TA, Capadona JR, Reyes CD, Garcia AJ. Integrin specificity and enhanced cellular activities associated with surfaces presenting a recombinant fibronectin fragment compared to RGD supports. Biomaterials. 2006;27:5459-70.
[117] Benoit DS, Anseth KS. The effect on osteoblast function of colocalized RGD and PHSRN epitopes on PEG surfaces. Biomaterials. 2005;26:5209-20.
[118] Hopp TP, Woods KR. Prediction of Protein Antigenic Determinants from Amino-Acid-Sequences. P Natl Acad Sci-Biol. 1981;78:3824-8.
[119] Shi ZL, Neoh KG, Kang ET, Poh C, Wang W. Titanium with Surface-Grafted Dextran and Immobilized Bone Morphogenetic Protein-2 for Inhibition of Bacterial Adhesion and Enhancement of Osteoblast Functions. Tissue Eng Pt A. 2009;15:417-26.
[120] Zhang F, Zhang ZB, Zhu XL, Kang ET, Neoh KG. Silk-functionalized titanium surfaces for enhancing osteoblast functions and reducing bacterial adhesion. Biomaterials. 2008;29:4751-9.
[121] Zhang F, Shi ZL, Chua PH, Kang ET, Neoh KG. Functionalization of titanium surfaces via controlled living radical polymerization: From antibacterial surface to surface for osteoblast adhesion. Ind Eng Chem Res. 2007;46:9077-86.
[122] Xiao SJ, Textor M, Spencer ND, Sigrist H. Covalent attachment of cell-adhesive, (Arg-Gly-Asp)-containing peptides to titanium surfaces. Langmuir. 1998;14:5507-16.
[123] Busscher HJ, van der Mei HC, Subbiahdoss G, Jutte PC, van den Dungen JJAM, Zaat SAJ, et al. Biomaterial-Associated Infection: Locating the Finish Line in the Race for the Surface. Science Translational Medicine. 2012;4.
[124] Fowler T, Wann ER, Joh D, Johansson SA, Foster TJ, Hook M. Cellular invasion by Staphylococcus aureus involves a fibronectin bridge between the bacterial fibronectin-binding MSCRAMMs and host cell beta 1 integrins. Eur J Cell Biol. 2000;79:672-9.

[125] Subbiahdoss G, Pidhatika B, Coullerez G, Charnley M, Kuijer R, van der Mei HC, et al. Bacterial biofilm formation versus mammalian cell growth on titanium-based mono- and bi-functional coating. Eur Cell Mater. 2010;19:205-13.
[126] Moy PK, Medina D, Shetty V, Aghaloo TL. Dental implant failure rates and associated risk factors. Int J Oral Max Impl. 2005;20:569-77.
[127] Levin L, Hertzberg R, Har-Nes S, Schwartz-Arad D. Long-Term Marginal Bone Loss Around Single Dental Implants Affected by Current and Past Smoking Habits. Implant dentistry. 2008;17:422-9.
[128] Simonis P, Dufour T, Tenenbaum H. Long-term implant survival and success: a 10-16-year follow-up of non-submerged dental implants. Clin Oral Implan Res. 2010;21:772-7.
[129] Huynh-Ba G. Peri-implantitis: "Tsunami" or Marginal Problem? . The International journal of oral & maxillofacial implants. 2013;28:333-7.
[130] Koldsland OC, Scheie AA, Aass AM. Prevalence of Peri-Implantitis Related to Severity of the Disease With Different Degrees of Bone Loss. J Periodontol. 2010;81:231-8.
[131] Renvert S, Lindahl C, Persson GR. The incidence of peri-implantitis for two different implant systems over a period of thirteen years. Journal of clinical periodontology. 2012;39:1191-7.
[132] Costa FO, Takenaka-Martinez S, Cota LOM, Ferreira SD, Silva GLM, Costa JE. Peri-implant disease in subjects with and without preventive maintenance: a 5-year follow-up. Journal of clinical periodontology. 2012;39:173-81.
[133] Hancock REW, Diamond G. The role of cationic antimicrobial peptides in innate host defences. Trends Microbiol. 2000;8:402-10.
[134] Abdolhosseini M, Nandula SR, Song J, Hirt H, Gorr SU. Lysine substitutions convert a bacterial-agglutinating peptide into a bactericidal peptide that retains anti-lipopolysaccharide activity and low hemolytic activity. Peptides. 2012;35:231-8.
[135] Holmberg KV, Abdolhosseini M, Li Y, Chen X, Gorr SU, Aparicio C. Bio-inspired stable antimicrobial peptide coatings for dental applications. Acta biomaterialia. 2013.
[136] Chen RX, Willcox MDP, Cole N, Ho KKK, Rasul R, Denman JA, et al. Characterization of chemoselective surface attachment of the cationic peptide melimine and its effects on antimicrobial activity. Acta biomaterialia. 2012;8:4371-9.
[137] Bonde M, Pontoppidan H, Pepper DS. Direct Dye Binding - a Quantitative Assay for Solid-Phase Immobilized Protein. Anal Biochem. 1992;200:195-8.
[138] Gulsahi A, Paksoy CS, Ozden S, Kucuk NO, Cebeci AR, Genc Y. Assessment of bone mineral density in the jaws and its relationship to radiomorphometric indices. Dento maxillo facial radiology. 2010;39:284-9.
[139] Witucki G. A Silane Primer: Chemistry and Applications of AIkoxy Silanes. Presented at the 57th Annual Meeting of the Federation of Societies for Coatings Technology. 1992.
[140] Mints D, Elias C, Funkenbusch P, Meirelles L. Integrity of Implant Surface Modifications After Insertion. Int J Oral Max Impl. 2014;29:97-104.

[141] Gibbons RJ, Hay DI, Schlesinger DH. Delineation of a Segment of Adsorbed Salivary Acidic Proline-Rich Proteins Which Promotes Adhesion of Streptococcus-Gordonii to Apatitic Surfaces. Infect Immun. 1991;59:2948-54.
[142] Fernandez ICS, van der Mei HC, Lochhead MJ, Grainger DW, Busscher HJ. The inhibition of the adhesion of clinically isolated bacterial strains on multi-component cross-linked poly(ethylene glycol)-based polymer coatings. Biomaterials. 2007;28:4105-12.
[143] Hsieh MK, Shyu CL, Liao JW, Franje CA, Huang YJ, Chang SK, et al. Correlation analysis of heat stability of veterinary antibiotics by structural degradation, changes in antimicrobial activity and genotoxicity. Vet Med-Czech. 2011;56:274-85.
[144] Zheng D, Neoh KG, Shi Z, Kang ET. Assessment of stability of surface anchors for antibacterial coatings and immobilized growth factors on titanium. J Colloid Interface Sci. 2013;406:238-46.
[145] Boris S, Suarez JE, Barbes C. Characterization of the aggregation promoting factor from Lactobacillus gasseri, a vaginal isolate. J Appl Microbiol. 1997;83:413-20.
[146] Willcox MDP, Hume EBH, Aliwarga Y, Kumar N, Cole N. A novel cationic-peptide coating for the prevention of microbial colonization on contact lenses. J Appl Microbiol. 2008;105:1817-25.
[147] Bagheri M, Beyermann M, Dathe M. Mode of Action of Cationic Antimicrobial Peptides Defines the Tethering Position and the Efficacy of Biocidal Surfaces. Bioconjugate Chem. 2012;23:66-74.
[148] Hilpert K, Elliott M, Jenssen H, Kindrachuk J, Fjell CD, Korner J, et al. Screening and Characterization of Surface-Tethered Cationic Peptides for Antimicrobial Activity. Chem Biol. 2009;16:58-69.
[149] Cook GS, Costerton JW, Lamont RJ. Biofilm formation by Porphyromonas gingivalis and Streptococcus gordonii. J Periodontal Res. 1998;33:323-7.
[150] Lamont RJ, Jenkinson HF. Life below the gum line: Pathogenic mechanisms of Porphyromonas gingivalis. Microbiol Mol Biol R. 1998;62:1244-+.
[151] Costerton JW, Stewart PS, Greenberg EP. Bacterial biofilms: A common cause of persistent infections. Science. 1999;284:1318-22.
[152] Davies D. Understanding biofilm resistance to antibacterial agents. Nat Rev Drug Discov. 2003;2:114-22.
[153] Yin LM, Edwards MA, Li J, Yip CM, Deber CM. Roles of Hydrophobicity and Charge Distribution of Cationic Antimicrobial Peptides in Peptide-Membrane Interactions. J Biol Chem. 2012;287:7738-45.
[154] Zhu X, Dong N, Wang ZY, Ma Z, Zhang LC, Ma QQ, et al. Design of imperfectly amphipathic alpha-helical antimicrobial peptides with enhanced cell selectivity. Acta biomaterialia. 2014;10:244-57.
[155] Ong ZY, Gao SJ, Yang YY. Short Synthetic beta-Sheet Forming Peptide Amphiphiles as Broad Spectrum Antimicrobials with Antibiofilm and Endotoxin Neutralizing Capabilities. Adv Funct Mater. 2013;23:3682-92.
[156] Balhara V, Schmidt R, Gorr SU, Dewolf C. Membrane selectivity and biophysical studies of the antimicrobial peptide GL13K. Biochimica et biophysica acta. 2013;1828:2193-203.

[157] Ghosh A, Haverick M, Stump K, Yang XY, Tweedle MF, Goldberger JE. Fine-Tuning the pH Trigger of Self-Assembly. J Am Chem Soc. 2012;134:3647-50.
[158] Gao G, Cheng JTJ, Kindrachuk J, Hancock REW, Straus SK, Kizhakkedathu JN. Biomembrane Interactions Reveal the Mechanism of Action of Surface-Immobilized Host Defense IDR-1010 Peptide. Chem Biol. 2012;19:199-209.
[159] Hsu BB, Wong SY, Hammond PT, Chen JZ, Klibanov AM. Mechanism of inactivation of influenza viruses by immobilized hydrophobic polycations. P Natl Acad Sci USA. 2011;108:61-6.
[160] Hsu BB, Ouyang J, Wong SY, Hammond PT, Klibanov AM. On structural damage incurred by bacteria upon exposure to hydrophobic polycationic coatings. Biotechnol Lett. 2011;33:411-6.
[161] Sawant SN, Selvaraj V, Prabhawathi V, Doble M. Antibiofilm Properties of Silver and Gold Incorporated PU, PCLm, PC and PMMA Nanocomposites under Two Shear Conditions. Plos One. 2013;8.
[162] Fenoll-Palomares C, Munoz-Montagud JV, Sanchiz V, Herreros B, Hernandez V, Minguez M, et al. Unstimulated salivary flow rate, pH and buffer capacity of saliva in healthy volunteers. Rev Esp Enferm Dig. 2004;96:773-8.
[163] Madigan. M, Martinko. J, Parker. J. Brick biology of microorganisms. New jersey: pearson education, INC.; 2002.
[164] Balhara V, Schmidt R, Gorr SU, DeWolf C. Membrane selectivity and biophysical studies of the antimicrobial peptide GL13K. Bba-Biomembranes. 2013;1828:2193-203.
[165] Saar-Dover R, Bitler A, Nezer R, Shmuel-Galia L, Firon A, Shimoni E, et al. D-Alanylation of Lipoteichoic Acids Confers Resistance to Cationic Peptides in Group B Streptococcus by Increasing the Cell Wall Density. Plos Pathog. 2012;8.
[166] Weidenmaier C, Peschel A. Teichoic acids and related cell-wall glycopolymers in Gram-positive physiology and host interactions. Nat Rev Microbiol. 2008;6:276-87.
[167] Koprivnjak T, Weidenmaier C, Peschel A, Weiss JP. Wall teichoic acid deficiency in Staphylococcus aureus confers selective resistance to mammalian group IIA phospholipase A(2) and human p-defensin 3. Infect Immun. 2008;76:2169-76.
[168] Bizzini A, Majcherczyk P, Beggah-Moller S, Soldo B, Entenza JM, Gaillard M, et al. Effects of alpha-phosphoglucomutase deficiency on cell wall properties and fitness in Streptococcus gordonii. Microbiology. 2007;153:490-8.
[169] Chan KG, Mayer M, Davis EM, Halperin SA, Lin TJ, Lee SF. Role of D-alanylation of Streptococcus gordonii lipoteichoic acid in innate and adaptive immunity. Infect Immun. 2007;75:3033-42.
[170] Biswas R, Martinez RE, Gohring N, Schlag M, Josten M, Xia G, et al. Proton-binding capacity of Staphylococcus aureus wall teichoic acid and its role in controlling autolysin activity. Plos One. 2012;7:e41415.